

Alma Mater Studiorum – Università di Bologna

DOTTORATO DI RICERCA IN

SCIENZE BIOMEDICHE

Ciclo XXVI

Settore Concorsuale di afferenza: 05/ H1

Settore Scientifico disciplinare: BIO/16

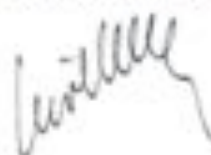
TOWARD A 3D IN VITRO MODEL BASED ON DECELLULARIZED THYMUS
TO MAINTAIN ADULT THYMIC EPITHELIAL CELLS FUNCTIONALITY

Developed under the tenure of the Marco Polo fund of the University of
Bologna at the Tissue Engineering, University Hospital, Basel, Switzerland
Tutor: Prof. Dr. Ivan Martin

Presentata da: Dott.ssa Strusi Valentina

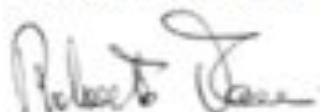
Coordinatore Dottorato

Prof. Lucio Cocco



Relatore

Prof. Roberto Toni



Esame finale anno 2012/2013

The present PhD thesis has been developed on the basis of the following publications by the autor:

1. **Strusi V.**, Piccinini E., Heiler S., Berkemeier C., Wendt D., Barthlott T., Toni R., Hollander G., Martin I. An in vitro 3D model to culture Thymic Epithelial Cells. Abstracts 1th International Conference MiMe-Materials in Medicine, Faenza, ITALY October 8-11, 2013.

2. **Strusi V.**, Zini N., Mastrogiacomo S.,Zamparelli A., Barbaro F., Dallatana D., Parrilli A., Giardino R., Toni R. Identification of putative adult stem cells in the rat thyroid and their use in ex situ bioengineering. *It. J. Anat. Embryol.* 117 n°2 (supplement), 184, 2012.

3. Mastrogiacomo S.,**Strusi V.**, Dallatana D., Barbaro F., Zini N., Zamparelli A., Iafisco M., Parrilli A., Giardino R., Lippi G., Spaletta G., Bassoli E., Gatto A., Sprio S., Sandri M., Tampieri A. Toni R. Poly-L-lactic acid and poly-ε-caprolactone as biomaterials for ex-situ bioengineering of the rat thyroid tissue. *It. J. Anat. Embryol.* 117 n°2 (supplement), 120, 2012.

4. **Strusi V.**, Zini N., Dallatana D., Mastrogiacomo S., Parrilli A., Giardino R., Lippi G., Spaletta G., Bassoli E., Gatto A., Iafisco M., Sandri M., Tampieri A., Toni R. Endocrine bioengineering: reconstruction of a bioartificial thyroid lobe using its three-dimensional (3D) stromal/ vascular matrix as a scaffold. *End. Abst.* 29, P1586, 2012.

5. Toni R., **Strusi V**, Zini N., Dallatana D., Mastrogiacomo S. , Parrilli A., Giardino R., Lippi G., Spaletta G., Bassoli E., Gatto A.,Iafisco M. Sandri

M., Tampieri A. Bioengineering of the thyroid lobe: use of its stromal / vascular matrix as a scaffold for ex situ reconstruction. Abstracts 94th Annual Meeting of the Endocrine Society, Houston, TX, June 23-26, 2012

6. Bassoli E., Denti L., Gatto A., Spaletta G., Paderno A., Zini N., Parrilli A., Giardino R., **Strusi V.**, Dallatana D., Mastrogiacomo S., Zamparelli A., Iafisco M., Toni R. A combined additive layer manufacturing / indirect replication method to prototype 3D vascular-like structures of soft tissue and endocrine organs. *Virt. Phys Prototyp.* 7, 3 -11, 2012

7. Toni R, Tampieri A, Zini N, **Strusi V**, Sandri M, Dallatana D, Spaletta G, Bassoli E, Gatto A, Ferrari A, Martin I. Ex situ bioengineering of bioartificial endocrine glands: a new frontier in regenerative medicine of soft tissue organs. *Ann Anat.* 193; 381-394, 2011.

8. **Strusi V.**, Zini, D. Dallatana, A. Parrilli, R. Giardino, G. Lippi, G. Spaletta, E. Bassoli, A. Gatto, M. Iafisco, M. Sandri, A. Tampieri, R. Toni. Ex situ bioengineering of the rat thyroid using as a scaffold the three-dimensional (3D) decellularized matrix of the glandular lobe: clues to the organomorphic principle. *It. J. Anat. Embryol.* 116 (supplement), 180, 2011.

9. Bassoli E., Denti L. , Paderno A. , **Strusi V.** Additive layer manufacturing for prototyping 3D scaffolds with vascular-like architecture; an experimental perspective. 5th International Conference on Advanced Research and Rapid Prototyping, Leiria, Portugal, September 28 - October 1, 2011

10. Bassoli E., Denti L., Gatto A., Paderno A., Spaletta G., Zini N.,

Strusi V., Dallatana D., Toni R. New approaches to prototype 3D vascular-like structures by additive layer manufacturing. In: P. Bartolo et al. (eds), Innovative Developments in Virtual and Physical Prototyping. London, CRC Press, Taylor & Francis, 35-42, 2011.

11. **Strusi V.**, Mastrogiacomo S., Zini N.,Dallatana D.,Spaletta G., Paderno A.,Bassoli E., Gatto A., Zamparelli A., Iafisco M., Sandri M., Tampieri A., Toni R. Gli organi endocrini bioartificiali: prospettive della ricerca traslazionale applicata alla medicina rigenerativa in endocrinologia. L'Endocrinologo 12, 2011

INDEX

1. INTRODUCTION.....	pag. 7
1.1 Thymus.....	pag. 8
1.1.1 Anatomy of the thymus.....	pag. 10
1.1.2 Development of the thymus.....	pag. 13
1.1.3 Thymic epithelial and dendritic cells in the adult thymus.....	pag. 16
1.1.4 Composition of the thymus microenvironment.....	pag. 19
1.1.5 Physiological function of the thymus.....	pag. 26
1.2 The Natural Scaffold: the extracellular matrix.....	pag. 36
1.2.1 Principles and methods of decellularisation.....	pag. 44
1.2.2 Characterization of the decellularized tissue.....	pag. 54
1.2.3 State of the art of different decellularized scaffolds.....	pag. 58
1.3 Culture of thymic epithelial cells.....	pag. 68
1.3.1 three dimensional culture of thymic epithelial cells.....	pag. 70
2. AIM OF THE THESIS.....	pag. 73
3. MATERIAL AND METHODS.....	pag. 75
3.1 TECs isolation.....	pag.76
3.1.1 TECs extraction.....	pag.76
3.1.2 CD45 depletion.....	pag.78
3.1.3 TECs purity.....	pag.80

3.1.4 Culture medium and supplements.....	pag. 81
3.2 DNA quantification.....	pag. 82
3.3 SEM analysis.....	pag. 84
3.4 Istochemistry.....	pag. 85
3.4.1 Hematoxylin and eosin staining.....	pag. 85
3.4.2 Immunohistochemistry.....	pag. 86
3.5 Reagent for scaffold preparation.....	pag. 91
3.6 MTT assay.....	pag. 91
3.7 Scaffold preparation.....	pag. 92
4. RESULTS AND DISCUSSION.....	pag. 93
4.1 Study of a protocol for thymus decellularization...	pag. 94
4.2 Role of decellularized thymic matrices in regulating the in vitro behaviour of TEC.....	pag. 107
5. CONCLUSION AND PERSPECTIVES.....	pag. 127
6. Aknowledgments.....	pag. 130
7. Bibliography.....	pag. 132

1. INTRODUCTION

1.1 THYMUS

In mammals and man, the thymus is the primary lymphoid organ for T lymphocyte maturation, whereas the bone marrow serves as the primary lymphoid organ for the B lymphocyte compartment, although the gut-associated lymphoid tissue is its phylogenetic ancestor.

The thymus is the first of the lymphoid organs to be formed in all vertebrates, and grows considerably immediately after birth in response to postnatal antigen stimulation and the demand for large numbers of mature T cells. Genetic factors also influence the age of onset, rate and magnitude of thymus dependant immunological function. The thymus reaches maximal size by sexual maturity and then gradually involutes [1].

In humans, the thymus is located in the mediastinum, just anterior to the ascending aorta and inferior to the left brachiocephalic vein. If examined when its growth is most active, it consists of two lateral lobes placed in close contact along the middle line, situated partly in the thorax, partly in the neck, and extending from the fourth costal cartilage upward, as high as the lower border of the thyroid gland. It is covered by the sternum, and by the origins of the Sternohyoidei and Sternothyreoides muscles. Below, it rests upon the pericardium, being separated from the aortic arch and great vessels by a layer of the middle cervical fascia. In the neck it lies on the front and sides of the trachea, behind the Sternohyoidei and Sternothyreoides muscles.

The thymus is of a pinkish-gray color, soft, and lobulated on its surfaces. This superficial arrangement corresponds to a three-dimensional (3D) organization of its parenchyma, specifically to 3D

prismatic structures, histologically constituted by two subcompartments, the cortex and the medulla. Each compartment contains distinct populations of thymic epithelial cells (TEC), as well as mesenchymal cells, endothelial cells and dendritic cells.

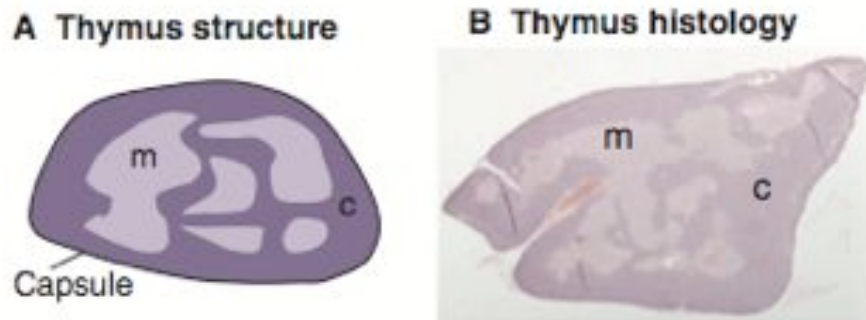


Fig. 1 A: Structure of the mammals thymus. The thymus is a lympho-epithelial organ surrounded by a connective capsule. Each of its constituting units, the thymic lobule can be divided into a central medulla (m) region, which contains medullary thymic epithelial cells (m TECs), and an outer cortex (c), which contains cortical thymic epithelial cells (c TECs). B: Histology of the adult mouse thymus. Hematoxylin and eosin-stained sagittal section highlighting the thymus subcompartments.

The thymus provides a unique microenvironment for the efficient production of a diverse T cell repertoire[2]. However, after puberty it begins to regress. This *involution*, which seems to occur in almost all vertebrates, rodents included, suggesting that this is an evolutionary ancient and conserved process. Age-associated thymic involution includes a decrease in tissue mass and cellularity, together with a loss of tissue organization, leading to a reduction in the cell output. This decline in the T cell output is believed to have a major impact on the properties of the peripheral T cell pool such that with increasing age, these cells exhibit alterations in phenotype and function, loss of diversity, and replicative senescence[3].

1.1.1 Anatomy of the thymus

In mammals and man, the thymus has a bilobed structure, it is classified as a lympho-epithelial organ containing many developing lymphocytes, and is surrounded by a capsule of connective tissue. The two lobes generally differ in size; they are occasionally united, so as to form a single mass; sometimes they are separated by an intermediate lobe. Each lateral lobe is composed of numerous lobules, featured as 3D prismatic structures of prismatic geometry, held together by delicate areolar, stromal tissue; the entire gland being enclosed in an investing capsule of a similar but denser structure. The lobules vary in size and consists of a cortical and a medullary portion. The cortical portion is mainly composed of lymphoid cells, supported by a network of finely branched cells, the cortical thymic epithelial cells (cTECs), which is continuous with a similar network in the medullary portion, formed by medullary TEC (mTECs). A network of reticular TECs forms an adventitia around the blood vessels. In the medullary portion, this reticulum is coarser than in the cortex, the lymphoid cells are relatively fewer in number, and there are found peculiar nest-like bodies, the concentric corpuscles of Hassall, originating from involution of local TECs apposes in concentric layers. These concentric corpuscles are characterized by a central mass, consisting of one or more granular elements, and of a capsule which is formed of epithelioid cells.

Each lobule is surrounded by a vascular plexus, from which vessels pass into the interior, and radiate from the periphery toward the center, forming a second zone just within the margin of the medullary portion. In

the center of the medullary portion there are very few vessels, and they are of minute size.

Arteries supplying the thymus are derived from the internal mammary, and from the superior and inferior thyroids. The veins end in the left innominate vein, and in the thyroid veins. The nerves are exceedingly minute; they are derived from the vagus and sympathetic chain. Branches from the descendens hypoglossus and phrenic nerves reach the investing capsule, but do not penetrate into the substance of the gland. The thymic arteries follow the course of the interlobular connective tissue septae, and enter the thymic parenchyma at the corticomedullary junction. The corticomedullary arterioles ramify into capillaries that extend into the cortex and medulla. In the cortex they form a complex of capillary arcades which together with perivascular lymphocytes, macrophages and peripheral reticular epithelial cells form the blood-thymus barrier[4]. Capillaries in the cortex are rarely fenestrated[5]. This restricts access of circulating antigenic molecules to developing cortical lymphocytes. By contrast, medullary capillaries are fenestrated and freely permeable to circulating antigens. Blood drains into the postcapillary venules, and finally returns to the corticomedullary junction in medullary veins [4].

Prothymocytes are thought to enter the thymic stroma through the large venules at the corticomedullary junction, and re-enter the circulation through the vascular lining of post-capillary venules. These perivascular areas contain accumulations of phenotypically mature T cells that express the marker Mel 14, a receptor involved in the migration of lymphocytes through the lymphoid vasculature [6]. Efferent lymphatics drain into an adjacent pair of lymphnodes. The thymus has no afferent lymphatics. The

rodent thymus has an abundant noradrenergic innervation but some cholinergic innervation has also been demonstrated [7]. Nerves follow the vasculature, within the capsule and septae and the highest concentration of nerve fibres is in the corticomedullary junction.

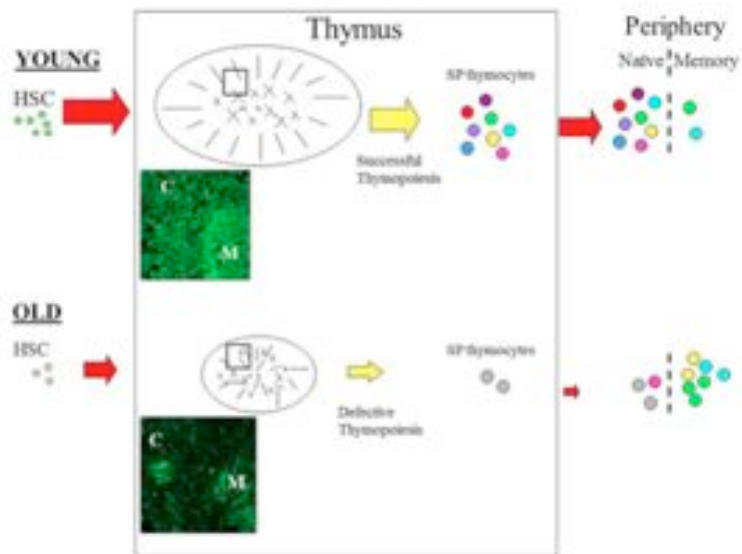


Fig. 2 Schematic diagram outlining the pathway of T cell development. Aging can impact on variety of pathways during the development of T cells.

1.1.2 Development of the thymus

The epithelium of the thymus is derived from the embryonic endodermal layer, with possible contributions from the ectoderm, through a series of differentiating steps, each of which must be completed in order to provide the optimum environment for thymic development and function. The roof of the endodermal yolk sac is folded into the expanding embryo as the foregut (Fig.3). The embryonic pharynx is quite important for the development of many organs, including the thyroid and parathyroid glands as well as the thymus.

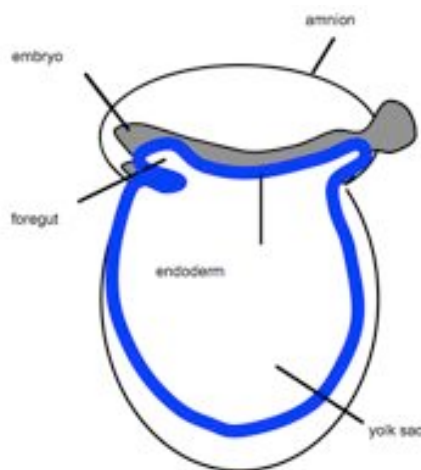


Fig.3 Representation of the foregut formation in the embryo development.

Alongside the thymocytes, at different stages of maturation, the thymic environment is formed by epithelial cells, which form a meshwork to provide mechanical support and stimuli for the proliferation and development of thymocytes and by macrophages, dendritic cells, fibroblast and matrix molecules[8].

The developing pharyngeal region in contact with the ectodermal layer produces inclusions of ectodermal cells into the thymus, a

mechanism possibly explaining the heterogeneity of epithelial cells in the mature thymus. The mass of endodermal cells from the 3rd and 4th pharyngeal pouch give rise to the primordial thymus (and forthcoming parathyroid glands), and attracts lymphoid precursor cells that are brought to this region through the bloodstream. The lymphoid precursor cells leave the blood vessels and migrate through the mesenchyme into the primitive organ bud. This migration starts between 11 and 12 gestation days (GD) [9]. In the rat, the process is less well known and according to the few existing reports, it starts between GD 13 and 15[10]. The earliest phase of organogenesis, culminates in the formation of two primordial buds, one of each antimeres, surrounded by a condensing mesenchymal capsule. By GD 13.5 for mice and 16.5 for rats the parathyroid and thymus are separated into physically distinct organs and soon afterwards they reach their approximate adult positions within the embryo (Fig.4).

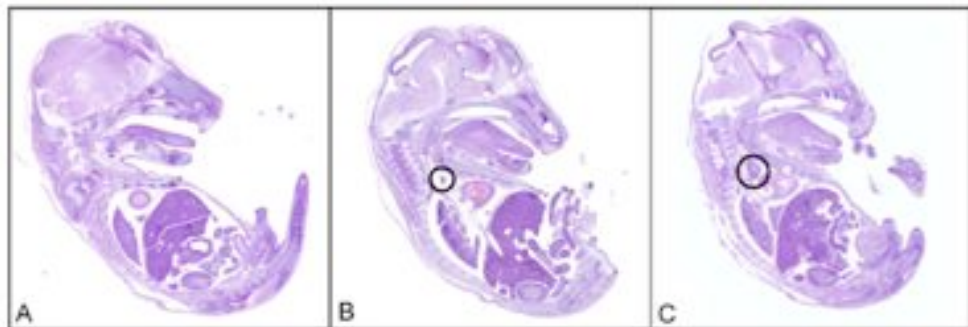


Fig. 4 Photomicrograph showing sagittal sections of the rat embryo. A at 10 GD the thymus is not present; B at 14 GD it is visible as a rudiment of the organ and C at 19 GD the two lobes can be distinguished. Hematoxylin-eosin staining.

In the embryonic thymic cortex, rat lymphocytes, in cortex, show a different antigenic pattern at the 16th day and at the 31th day after the birth. In adult rats, differences in CD4:CD8 cell ratio involve the major histocompatibility complex (MHC) haplotype[11], and peripheral CD4⁺ T cells predominate over CD8⁺ T cells but the origin of these differences

has not yet been elucidated.

Unlike adult thymic precursors, fetal thymic progenitors give rise to reduced numbers of CD4⁺ peripheral T cells in chimeric animals (CD4:CD8 cell ratio <1). This relative under-representation of CD4⁺ peripheral T cells was seen 4–16 weeks after either intrathymic injection of suspensions of foetal CD4⁻CD8⁻ thymocytes into adult thymuses, or transplantation of foetal thymic lobes under the kidney capsule of adult host rats. Then, foetal thymic precursors seem to be responsible for a relative underproduction of CD4⁺ peripheral T cells, regardless of the developmental age of the thymic stromal environment. However, the developmental age of the thymic stromal environment is the key regulatory element involved in the generation of distinct proportions of CD4⁺ and CD8⁺ thymocytes.

1.1.3 Thymic epithelial and dendritic cells in the adult thymus

The bulk of the supporting framework in the thymus is composed of a network of TECs [12]. In the subcapsular region of the thymus, TECs form a layer, 1 or 2 cells deep. In the outer cortex, TECs are thin and sheet like, but elsewhere they assume a stellate appearance.

TECs manifest expression of MHC class I antigens, neuropeptides, neurophysin, oxytocin/vasopressin and neuroendocrine markers. They are responsible for interleukins IL-6 and IL-7 secretion, and for secretion of thymic hormones. Superficial TECs demonstrate common phenotype traits with medullary traits [13]. TECs in the mid and deep cortex also have slender cytoplasmic processes providing a large surface area for cell–cell interactions with developing thymocytes[14].

Morphologically, TECs are characterized by electronlucent vacuoles with a small amount of moderate electrondense material, linked to secretory activity. The cortical TECs are distinguished by expression of both MHC class I and II molecules and protein gene product 9.5 (PGP 9.5). This latter is also a marker of a specific population of cortical TECs, known as thymic nurse cells (TNCs) [13].

In the outer cortex, some TECs appear to completely surround and enclose a large number (about 10–250) of thymocytes[15]. Moreover, TECs have been described in the subcapsular and outer cortical regions of the human [16] and rat thymus[17].

In contrast to cortical TECs, those contain a small number of thymocytes [18]. Scanning electron microscopic images of the mouse

thymus have suggested that thymocytes migrate in or out these lympho-stromal complexes[17]. TECs are thought to provide a specialized microenvironment for T-cell differentiation[19]. Although the epithelium they constitute is thought to be a sessile component of the thymus[20], the subcapsular epithelium in particular may be a dynamic structure, since transitional forms have been observed between sheet-like TECs, basket-like TECs, and TECs depending on the type of cortical lympho- stromal interaction.

Most medullary TECs are closely packed displaying voluminous cytoplasm and short processes. They are commonly subdivided into two subsets, representing different stages of their differentiation[21,13]. Cells of the first subset are defined “undifferentiated” and are around 1% of the total medullary population. They remain unrelatively unknown and are identified on the basis of ultrastructural traits in the outer medulla, as solitary cells or arranged in small groups of cells, which comprise forms of traits intermediate with those of the second subset of medullary TECs. The second type of TECs are polygonal, with a rich cytoplasm, polarized with respect to the position of organelles and having ultrastructural traits of endocrine cells. They express a wide range of peptide hormones and several co-stimulatory molecules including CD40.

In the adult mouse, dendritic cells are present mainly in the medulla; they are voluminous with electronlucent cytoplasm penetrating between surrounding lymphoid cells (Fig.5).

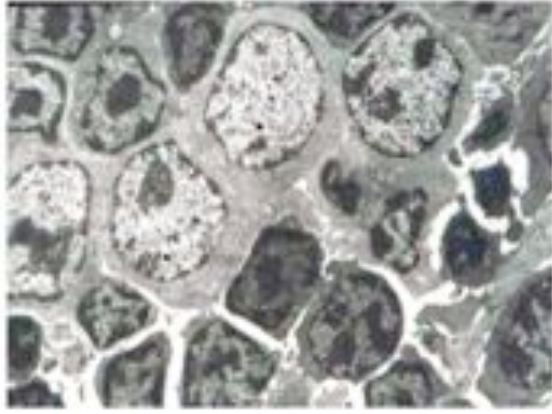


Fig.5 Electron micrograph showing thymic morphology in the rat. Dendritic cells are characterized by electron-lucent cytoplasm.

1.1.4 Composition of the thymus microenvironment

The thymus microenvironment forms a complex network of interaction that comprises non lymphoid cells, extracellular matrix elements (ECM), matrix metalloproteinases, cytokines, chemokines, and other soluble proteins. During their journey inside the thymus, thymocytes interact with stromal cells and extracellular matrix proteins to receive appropriate signals for survival, proliferation and differentiation.

On day 13 of fetal life number of ECM components have been observed in the thymus. Collagen type I expression was restricted to a few cells in the capsule area, whereas laminin was present in the capsule and in some scattered stromal cell clusters. In contrast, a filamentous network observed throughout the organ shows positivity for Collagen type IV and fibronectin[25].

On day 15 of fetal life it is not possible to distinguish cortical and medullary regions by ECM expression patterns, and the entire organ displayed a thin network of laminin, fibronectin and collagen type IV. On day 17 a similar profile is apparent, although all these proteins were additionally detected at basement membranes and intralobular perivascular spaces. At this stage collagen type I expression is similar to that found in young adult animals. The complete adult pattern of thymic ECM distribution was achieved on day 19 of fetal life[25].

The distribution of ECM in the normal thymus does not follow a homogeneous pattern, and glycoproteins such as fibronectin, laminin and collagen type IV are not strictly located at typical basement membrane sites. In the medullary region of the thymic lobules, they form a rather

thick medullary network, whereas very thin ECM fibres are found within the cortex.

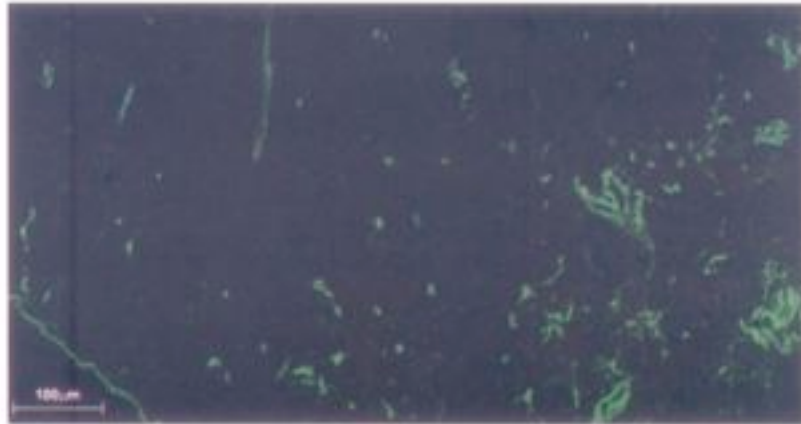


Fig.6 Intrathymic distribution of fibronectin in human thymus, as revealed by confocal microscopy. The fibronectin-containing network is denser in the medulla (right part on the panel) of the thymic lobule, as compared to the cortex (left part of the panel). Additionally, Fibronectin is seen around vessels.

The distribution of collagen type I is limited to the capsule, intraseptal and perivascular spaces[22].

The fibronectin is located throughout the all thymic parenchyma and outlines the cortico-medullary junction of the thymic lobules[23]. Different isoform of the laminin could be found into the thymus. Laminin 2 is restricted to cortical epithelial cells whereas laminin 5 is located surrounding small blood vessels[24]. Laminin 1 and 2 can modulate thymocyte migration within TNCs complexes. In the human thymus a large number of fibers in the interior of the connective tissue septae are made of collagen type I whereas only some fibers are labelled with collagen type IV. Instead the basement membrane bordering these septae contained large amount of collagen type IV. The interior of interlobular septae contain laminin and fibronectin; in contrast the connective fibres situated at the corticomedullary junction are made up of collagen type IV, type I

and fibronectin.

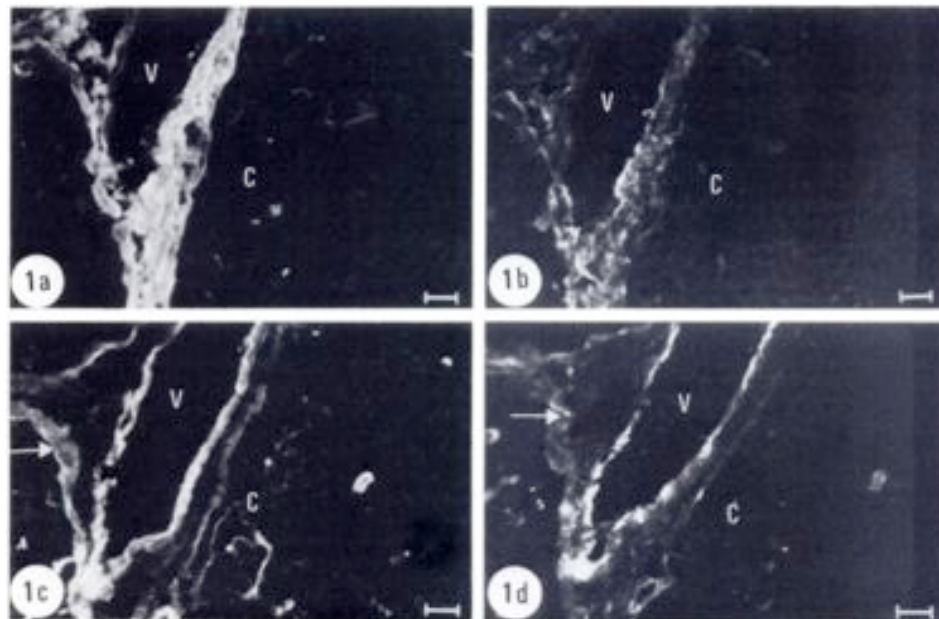


Fig.7 Frozen section of adult mouse thymus showing the distribution pattern of a collagen type I, b type III and C type IV and D fibronectin. A part of cortex (C) of a thymic lobule , as well as septum containing a blood vessel(V) could be seen. Bar 50 μ m

The extracellular localization of the laminin is mainly medullary and also medullary TECs contain and produce this ECM protein.

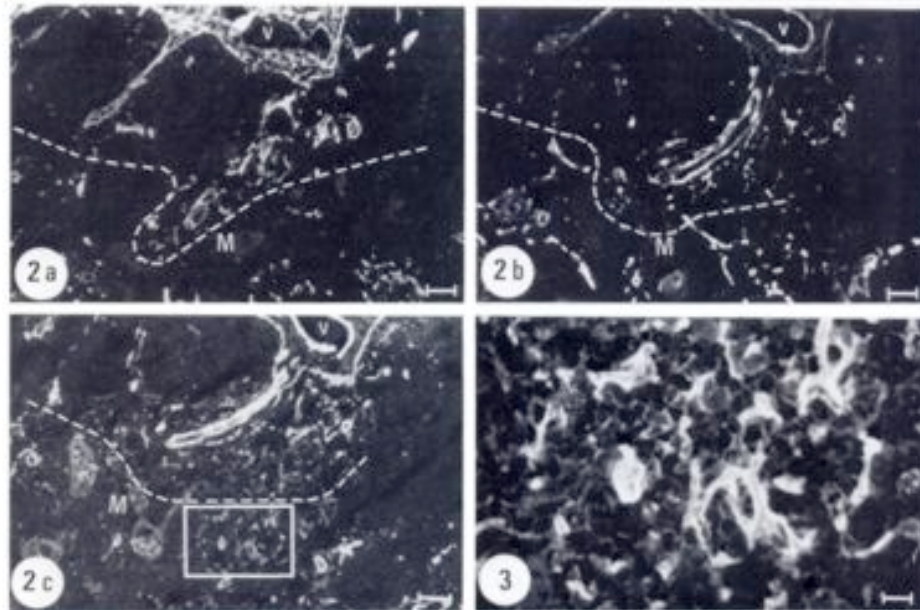


Fig.8 Frozen section of adult mouse thymus showing the distribution pattern of fibronectin within the thymic lobules. (B) Higher magnification of the fibronectin-positive network occurring in the medullary region. Bars: a- 50 μ m b-20 μ m

In the mouse fibronectin and laminin are strongly detected at the basement membranes, not only in the connective tissue septa but also in the interlobular perivascular spaces. In addition, filaments containing fibronectin, laminin and few collagen type IV have been found within the thymic medulla.

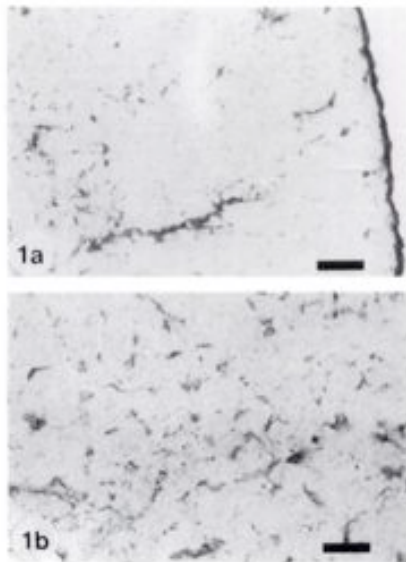


Fig.9 Frozen section of adult mouse thymus showing the distribution pattern of fibronectin within the thymic lobules. (B) Higher magnification of the fibronectin-positive network occurring in the medullary region. Bars: a- 50 μ m b-20 μ m

In normal young adult animals , the distribution patterns of both interstitial and basement membrane proteins were similar to those previously described for the infant human thymus[22].

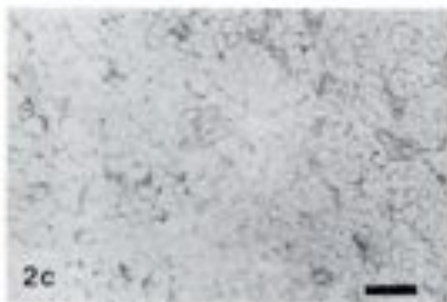


Fig. 10 Extracellular matrix labelling in the fetal thymus. a) fibronectin and b) laminin labeling patterns in a 13- day fetal thymus. c) the fibronectin network observed in a 15.day fetal thymus. Bar-20 μ m

All ECM components are produced by thymic microenvironmental cells, which also drive thymocyte differentiation. Signals triggered by ECM are conveyed into thymocytes or microenvironmental cells through specific membrane receptors, and most of them belong to the type, such

as the VLA-3, VLA-4, VLA-5 and VLA-6. In vitro studies revealed that adhesion of thymocytes to thymic integrin microenvironmental cells is mediated by extracellular matrix. Such an adhesion is preferentially done by immature thymocytes[26].

Cultured TECs produce laminin, fibronectin and type IV collagen, fibroblasts and major histocompatibility complex (MHC) class II⁺ phagocytic cells of the thymic reticulum also produce these ECM components[27,28,29].

Fibronectin, recognized by VLA-5 (very late antigen-5) through its RGD motif, is located throughout the thymic parenchyma, whereas the isoform derived from alternative splicing of fibronectin mRNA (being recognized by VLA-4 through the LEDV motif) seems to be restricted to the medulla[30].

In addition, there are some isoforms of laminin. Laminin-5, formed from the $\alpha 3\beta 3\gamma 2$ heterotrimer, was detected also in the human thymus, being produced by medullary TECs and able to trigger outside-in signals to thymocytes[31]. In the mouse system, anti-laminin-5 monoclonal antibodies significantly blocked thymocyte expansion, as well as double negative(DN) \rightarrow double positive (DP) differentiation[32].

In the human thymus, laminin-1 seems to be distributed widely within lobules and septae, whereas laminin-2 is restricted to cortical TECs.

Laminin-1 and laminin-2 can modulate thymocyte migration within TNC complexes and in addition to the DN \rightarrow DP progression, the migration of DP thymocytes is also influenced by laminin(s).

Cells of the thymic microenvironment express fibronectin receptor

(VLA-4 and VLA-5), as well as laminin receptors (VLA-3 and VLA-6) [33]. These receptors are also expressed by differentiating thymocytes. ECM proteins form molecular bridges between thymocytes and microenvironmental cells, a biological event that potentially provides signals to both cell types.

Thymocyte adhesion to cultured TECs is enhanced in the presence of ECM components, such as fibronectin and/or laminin, whereas antibodies against these adhesive molecules promote an opposite effect.

Thymocyte release from TNCs is enhanced by fibronectin and laminin and diminished by corresponding anti-ECM or anti-ECM receptor antibodies.

ECM-mediated epithelial–thymocyte interactions play a role in the traffic of thymocytes within TNCs, affecting both the entrance and exit of lymphocytes in this particular microenvironmental niche.

The expression of thymic ECM molecules in aging normal mice (50 week-old) is more intense than that observed in young animals.

In addition to a higher expression of basement membrane components in the medullary region, there is a formation of a cortical network of fibronectin, laminin and collagen type IV.

1.1.5 Physiological function of the Thymus

The thymus supports the differentiation and selection of T cells. The thymic development of T cells consists of several processes that require the dynamic relocation of developing lymphocytes into, within and out of the multiple environments of the thymus through distinct cell-cell and cell-matrix interactions. These processes include: 1) the entry of lymphoid progenitor cells into the thymus; 2) the generation of CD4⁺CD8⁺ double-positive (DP) thymocytes at the outer cortex of the thymus; 3) the positive and negative selection of DP thymocytes in the cortex; fourth, the interaction of positively selected thymocytes with medullary thymic epithelial cells (mTECs) to complete thymocyte development and ensure central tolerance; 4) the export of mature T cells from the thymus [34-39] (FIG.11).

Chemokines might act in concert with extracellular matrix (ECM), resulting in the migration of a given cell subset, either within the thymus or at the entrance into and/or exit from the organ [40].

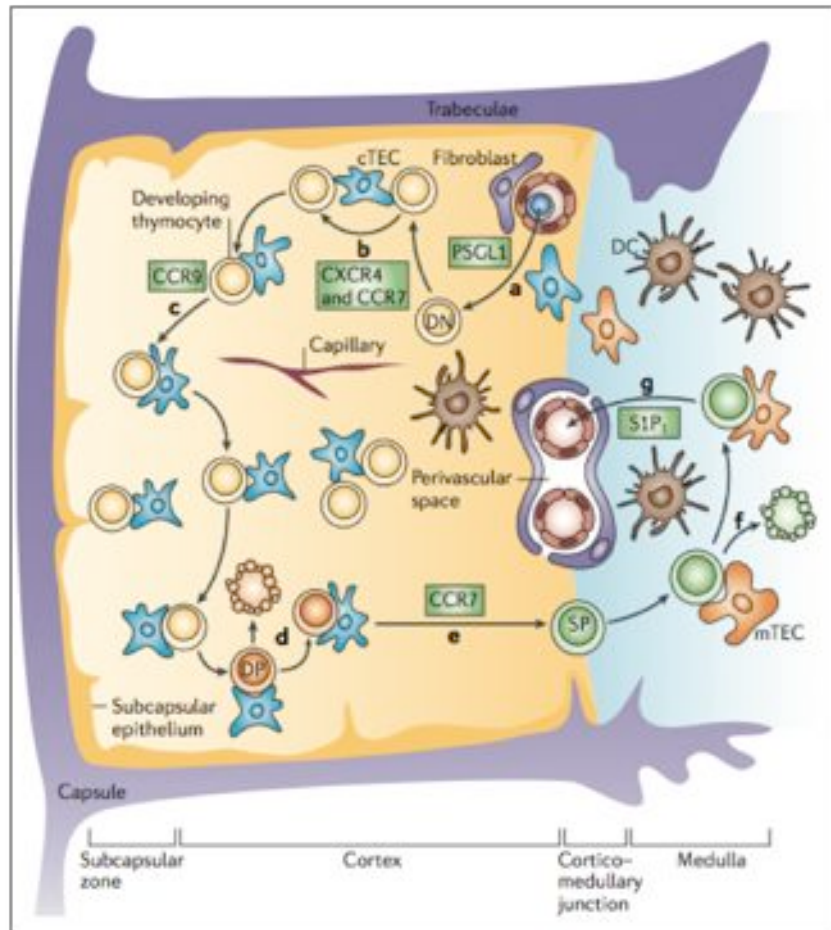


Fig. 11 Traffic of thymocytes for T-cell development and selection. **a** | In the postnatal thymus, circulating T-lymphoid progenitor cells migrate into the thymic parenchyma through the vasculatures that are enriched around the cortico-medullary junction. **b** | The outward migration of $CD4^-CD8^-$ double-negative (DN) thymocytes to the capsule is regulated by chemokine signals through CXC- chemokine receptor 4 (CXCR4) and CC-chemokine receptor 7 (CCR7). **c** | Further outward migration of the DN thymocytes to the subcapsular region is mediated by CCR9 signals. **d** | $CD4^+CD8^+$ double-positive (DP) thymocytes generated in the outer cortex are motile, interacting with stromal cells that are localized in the cortex for positive and negative selection. **e** | Positively selected DP thymocytes that gain the capability to survive and differentiate into $CD4$ or $CD8$ single- positive (SP) thymocytes show an increase in the surface expression of CCR7, through which the cells are attracted to the medulla, which expresses CCR7 ligands. **f** | In the medulla, further selection of SP thymocytes includes the deletion of tissue-specific-antigen-reactive T cells and the generation of regulatory T cells. **g** | Mature SP thymocytes express sphingosine-1-phosphate receptor 1 (SP1) through which the cells are attracted back to the circulation that contains a high concentration of sphingosine-1-phosphate. cTEC, cortical thymic epithelial cell; DC, dendritic cell; mTEC, medullary thymic epithelial cell; PSGL1, platelet-selectin glycoprotein ligand 1.

The seeding of the thymus with lymphoid progenitor cells occurs as early as embryonic day 11.5 (E11.5) in mice at the eight week of gestation

in humans [41-42], and is mediated by at least two different pathways: the vasculature-independent pathway, which probably occurs during the early stage of embryonic development before vascularization of the thymus, and the vasculature-dependent pathway, which probably occurs in the late stage of embryogenesis and postnatally after vascularization.

It is thought that vasculature-independent colonization of the fetal thymus is regulated by the chemotactic attraction of lymphoid progenitor cells to the thymic primordium (FIG. 12a). The partial but significant roles of two chemokines, CC-chemokine ligand 21 (CCL21) and CCL25, in this early stage of fetal thymus colonization have been reported. CCL21 and CCL25 are expressed by the fetal thymus primordium, along with several other chemokines[43-44]. Ccl25 and Cxcl12 regulate the hematopoietic precursor homing process [45]and have also chemotactic functions.

CCL21 and CCL25 are partially involved in fetal thymus colonization. CCL25 is expressed by TECs and dendritic cells and attracts immature thymocytes. The CC-chemokine receptor 9 (CCR9) receptor for CCL25 is expressed at various stages of murine thymocytes differentiation, particularly in DP and CD8+ single positive cells[40].

Interestingly, the entry of lymphoid progenitor cells into the thymus is not a continuous event but an intermittent and gated event that occurs in waves during embryogenesis and in adulthood[46-48]. During embryogenesis, distinct waves of thymus-colonized cells give rise to distinct progenies of $\gamma\delta$ T cells with different usages of T-cell receptor (TCR) -V γ and V δ chains, indicating that T-lymphoid progenitor cells that colonize the fetal thymus differ in developmental potential from T-lymphoid progenitor cells that enter the postnatal thymus[48-52].

Following entry into the thymus, lymphoid progenitor cells begin their development into T cells through the developmental pathway that is commonly identified by the expression profiles of CD25 and CD44, until the developmental checkpoint at the CD4⁻CD8⁻ CD25⁺CD44⁻ (double-negative 3, DN3) stage[53-54].

Only the cells that succeed in in-frame rearrangement of the gene encoding the TCR β -chain are selected for further differentiation beyond this DN3 stage. The initial thymocyte development until the DN3 stage is promoted by Notch-mediated signals delivered by binding of Delta ligands [55-56] and is supported by signals delivered by interleukin-7 (IL-7) [57-58]: the signals derived from cortical thymic epithelial cells (cTECs) (FIG. 12c). Along this developmental pathway, immature DN thymocytes promote the differentiation of thymic stromal cells and trigger the formation of the cortical-epithelial environment in the thymus[59-62].

The differentiation of thymocytes from the DN1 stage to the DN3 stage regulates the differentiation of TEC precursor cells into cTECs that form the cortical environment in the thymus (FIG. 12b).

Concomitantly, DN thymocytes relocate outwards from the cortico-medullary junction to the subcapsular region of the thymic cortex [63] (FIG. 11b). Several chemokine receptors, including CXCR4, CCR7 and CCR9, have been suggested to be involved in this movement of immature thymocytes[64-66].

The chemokine-dependent outward localization of the thymus-seeded progenitor cells from the cortico-medullary junction to the outer cortex seems to be essential for optimal initiation of thymocyte development, although the accumulation of DN3 thymocytes in the

subcapsular region might not be required for further thymocyte development.

In the thymic cortex, on their way to the subcapsular region, DN thymocytes begin to rearrange their *Tcrb* locus and the cells that succeed in generating the in-frame *Tcrb* rearrangement begin assembling TCR β and pre-TCR α (pT α) chains to form the cell-surface pre-TCR complex[67-68]. The successful expression of the pre-TCR complex on the cell surface[68-69], along with the Delta–Notch interaction [70], initiates the signals for further development to DP thymocytes that express TCR $\alpha\beta$ antigen receptors. This is the first checkpoint of T-cell development at the DN3 stage which censors the cells that have succeeded in in-frame TCR β rearrangement and allows further development of thymocytes beyond the DN3 stage. It has been shown that the subcapsular region is rich in transforming growth factor- β (TGF β), which retards the cell-cycle progression of pre-DP thymocytes and negatively regulates the generation of DP thymocytes[71], indicating that the migration of pre-DP thymocytes to the subcapsular region might have a role in regulating the rate of production of DP thymocytes (FIG. 11c).

DP thymocytes that are newly generated in the cortex express low levels of the TCR $\alpha\beta$ antigen–receptor complex. The cortical DP-thymocyte population contains the unselected repertoire of T cells, making this population the main target of the most rigorous positive and negative selection[72-73].

Most thymocytes in the cortex of the adult thymus are highly motile and they pause to interact through their TCR with peptide–MHC complexes that are expressed by stromal cells, such as cTECs, and

dendritic cells in the cortex[74]. Following TCR recognition of peptide–MHC ligands at low-avidity interactions, DP thymocytes are induced to receive signals for survival and further differentiation into single-positive (SP) thymocytes.

High-avidity interactions elicit signals that lead to the deletion of thymocytes. Apoptosis is the mechanism of negative selection. The process of negative selection contributes to the deletion of self-reactive T cells, thereby avoiding autoimmunity. In addition to the negatively selected thymocytes, most cortical DP thymocytes fail to receive TCR signals and are also destined to die at this stage. Therefore, only 3–5% of developing thymocytes survive this checkpoint of T-cell development at the cortical DP-thymocyte stage(FIG. 11d; FIG. 12d) [75-76].

Positively selected DP thymocytes then begin relocating from the cortex to the medulla[77]. The expression of the chemokine receptor CCR7 by developing thymocytes is associated with the phenotypic stage of cortex-to-medulla migration during the development of immature DP thymocytes to mature SP thymocytes[78-79]. Following TCR ligation, cortical DP thymocytes show an increase in cell-surface expression of CCR7. By contrast, CCR7 ligands (CCL19 and CCL21) in the postnatal thymus are predominantly produced by mTECs[80]. Therefore, cortical DP thymocytes that have received TCR-mediated signals are attracted to the medulla through CCR7-mediated chemotaxis (FIGS 11e).

However, the migration of developing thymocytes to the medulla cannot be solely mediated by the passive inward flow, present in the postnatal thymus from the capsular and subcapsular areas to the medullary area[81-82].

The positive selection of thymocytes is a prerequisite for both the formation of the medulla and the migration of positively selected thymocytes to the medulla (FIG. 12e).

The signals of the nuclear factor- κ B (NF- κ B)-mediated signal pathway, occurring through lymphotoxin- β receptor, tumour-necrosis-factor-receptor-associated factor 6 (TRAF6), NF- κ B-inducing kinase (NIK) and the NF- κ B subunit RelB are crucial for the development of the thymic medulla[83-86].

Positively selected DP thymocytes are induced to differentiate into SP (that is, CD4⁺CD8⁻ or CD4⁻CD8⁺) thymocytes and relocate to the medulla. The SP thymocytes are assumed to spend approximately 12 days in the medulla before being exported from the thymus[87]. During this period, the SP thymocytes go through a maturation process that is commonly identified by the expression profiles of CD62 ligand (CD62L; also known as lymphocyte (L)-selectin) and CD69, and with the acquisition of functional capability of these cells as mature but naive T cells[88-90]. The newly generated SP thymocytes are CD62L^{low}CD69^{hi} semi-mature cells that are functionally incompetent and susceptible to various apoptotic signals, including dexamethasone, and undergo further maturation to become mature SP thymocytes that are functional, dexamethasone-resistant and CD62L^{hi}CD69^{low}. The process of SP-thymocyte maturation presumably occurs in the medulla and is accompanied by further deletion of self-reactive thymocytes that have escaped negative selection in the cortex (FIGS 11f). Such additional deletion in the medulla seems to be particularly important in establishing central tolerance to tissue-specific antigens, as mTECs express tissue-

specific anti- gens promiscuously[91]. The expression of tissue-specific antigens by mTECs is at least partially dependent on the transcriptional factor autoimmune regulator (AIRE) [92-93].

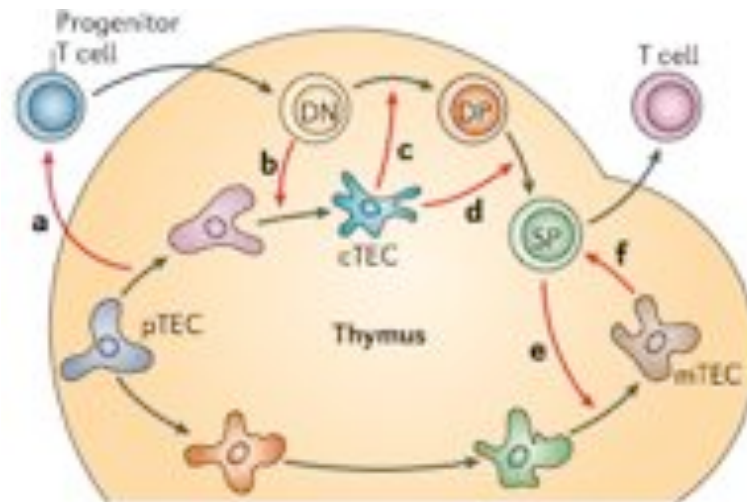


FIG. 12 Crosstalk between thymocytes and thymic stromal cells. Thymic stromal cells, including the common progenitor thymic epithelial cells (pTECs), attract the entry of T-lymphoid progenitor cells to the thymus (signal **a**). The developing double-negative (DN) thymocytes are required for pTECs to generate cortical thymic epithelial cells (cTECs) (signal **b**) that form the cortical environment that is needed to promote the generation of double-positive (DP) thymocytes (signal **c**) and the positive selection of DP thymocytes (signal **d**). The generation of single-positive (SP) thymocytes by the positive selection of DP thymocytes is required for the development of mature medullary thymic epithelial cells (mTECs) (signal **e**) that form the medullary environment to support the maturation, further selection and export of mature SP thymocytes (signal **f**) to supply the peripheral T-cell pool. Red arrows indicate crosstalk signals.

This process of medullary tolerance is shown to occur, at least in part, through the deletion of self-reactive T cells[94-96].

The medulla is thought to be the place for the production of regulatory T cells[97-99]. It has been shown that most forkhead box P3 (FOXP3)- expressing regulatory T cells within the thymus are found in the medulla[98]. Therefore, the period of maturation in the medulla seems to be essential for SP thymocytes to establish central tolerance by ensuring the deletion of T cells that are reactive to tissue-specific antigens and by producing regulatory T cells (FIGS 12f).

Hassall's corpuscles express TSLP, which activates thymic dendritic cells that in turn induce the generation of regulatory T cells[100]. Independent studies have indicated that CCL17 is expressed by dendritic cells that are mostly localized in the medulla[100-101], and CCL22 is expressed by the outer walls of Hassall's corpuscles[102-103], whereas CCR4 (a receptor for CCL22 and CCL17) is expressed by semi-mature SP thymocytes[79,102,103]. These chemokine signals might direct medullary semi-mature SP thymocytes to Hassall's corpuscles and have a role in establishing central tolerance by enhancing the generation of regulatory T cells and/or optimizing negative selection.

In the postnatal thymus, lymphoid progenitor cells that have just entered the thymic parenchyma are found mainly in the area close to the cortico–medullary junction, where the vasculature is well developed, indicating that the lymphoid progenitor cells enter the postnatal thymus by transmigrating from the blood to the thymic parenchyma, mainly through the area around the cortico–medullary junction (FIG. 11a) [63].

Thymus seeding of the adult thymus is regulated by the adhesive interaction between platelet (P)-selectin glycoprotein ligand 1 (PSGL1), which is expressed by circulating lymphoid progenitor cells, and P-selectin, which is expressed by the thymic endothelium[104]. Thymocyte emigration is an active process controlled by signals mediated by G-protein-coupled receptors [105] sphingosine-1-phosphate receptor 1 (of the S1P receptors, is expressed by mature SP thymocytes and that S1P is required for the egress of T cells from the adult thymus[106]. During maturation from DP thymocytes, SP thymocytes acquire the expression of S1P [106-107].

The chemoattraction of mature thymocytes to circulating S1P regulates the exit of mature T cells from the postnatal thymus (FIG. 11g). CCL19-mediated CCR7 signals contribute to thymocyte emigration in newborn mice but not in adult mice [108], indicating that there might be a developmental switch between CCR7-mediated emigration and S1P-mediated emigration during ontogeny. The repulsive movement of SP thymocytes repelled from a high concentration of CXCL12 has a role in the emigration of T cells from artificial thymus organoids [109].

The export of mature thymocytes from the thymic parenchyma to the circulation is thought to occur through the perivascular space, which is channelled to post-capillary venules, arterioles and lymphatics [110-111].

1.2 *The Natural Scaffold: the extracellular matrix*

End-stage organ failure is a key challenge for the medical community because of the ageing population and the severe shortage of suitable donor organs available. It is a serious, growing, and costly issue. Every year in the USA alone, 120 000 people die from chronic lung disease[112], 112 000 die from kidney failure[113], 27 000 die from end-stage liver disease[114], and 425 000 die from coronary heart disease[115]. Equally, injuries to or congenital absence of complex tissues such as the trachea, oesophagus, or skeletal muscle have few therapeutic options.

At present, definitive treatment for end-stage organ failure is allogeneic transplantation. It is a well-established procedure but is a victim of its own success in that there is a growing disparity in numbers between the donor organ pool available for transplantation and the patients eligible for such a procedure, with high mortality rate in those who are on the waiting list[116].

Patients fortunate enough to receive a donor organ endure life-long immunosuppressive therapy with its associated morbidity and also are at risk of acute or chronic organ rejection[117].

Recent advances in tissue engineering, an interdisciplinary field that applies the principles of engineering and life sciences toward the development of functional replacement tissue for clinical use, and regenerative medicine have established a foundation on which the functional replacement of whole organs and complex tissues such as skeletal muscle, trachea, and oesophagus seems possible. Many

developments employ the seeding and cultivation of cells onto acellular scaffolds[116]. These scaffolds can act as an inductive template for functional tissue and organ reconstruction after recellularisation with autologous stem cells or differentiated cells. This approach involves the use of naturally occurring extracellular matrix, obtained by the decellularisation of allogeneic or xenogeneic whole organs or tissues (Figure 13). The ready availability of an off-the-shelf xenogeneic scaffold that could subsequently be recellularised with autologous cells is a potential solution to the donor shortage that exists for allogeneic whole-organ transplantation. In addition, this approach would obviate the need for immunosuppression.

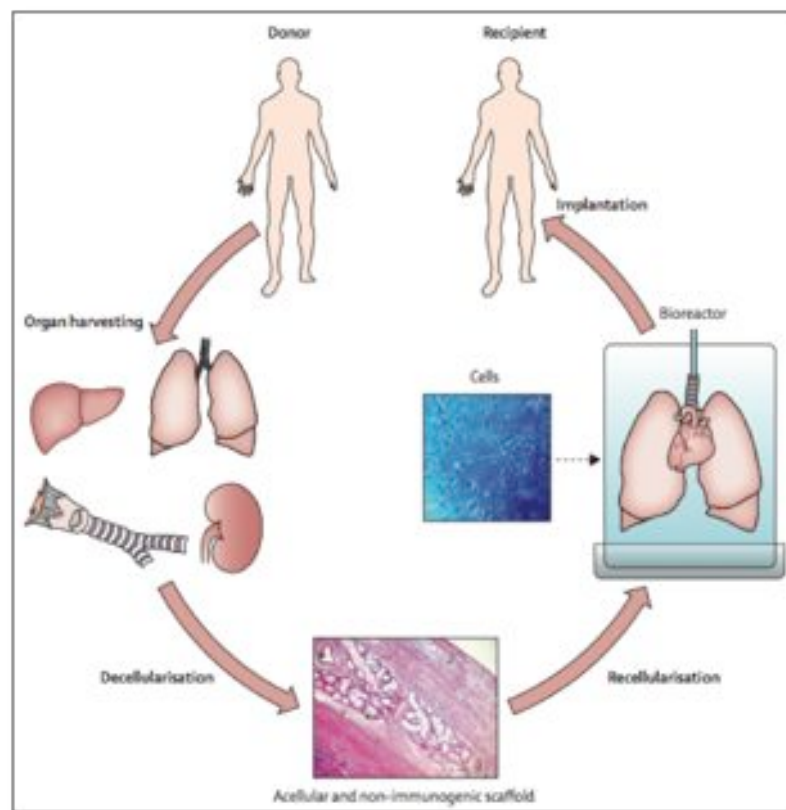


Fig : 13 Organ and tissue Bioengineering

An advantage of utilizing the ECM in its native state as a scaffold for tissue repair is the presence of all of the attendant growth factors (and their inhibitors) in the relative amounts that exist in nature and, perhaps most importantly, in their native three-dimensional ultrastructure. It is reasonable, therefore, to consider ECM scaffolds as temporary controlled-release vehicles for naturally occurring growth factors[118].

Another key advantage of this approach is the ready availability of an intact vascular network in the decellularised organs with appropriately sized inflow and outflow conduits for anastomosis to the recipient circulation and thus perfusion with nutrients and appropriate cues for cell behaviour.

The feasibility of a therapeutic strategy based on cellular repopulation of an intact extracellular matrix has evolved as a result of an improved understanding of cell–matrix interactions[119-120], development of methods for isolation of tissue-specific and organ-specific native extracellular matrix with little change in native structure and composition[121], rapid advancements of stem cell and progenitor cell biology (including the potential use of inducible pluripotent stem cells) [122-123], and the integration of the principles of developmental biology into regenerative medicine[120]. Although notable scientific and ethical challenges remain as this approach advances to clinical use, successful proof of principle for organs such as liver[124-125], heart[126], and lung [127-130]and complex tissues such as the trachea[131], oesophagus[132], and skeletal muscle[133] has been shown. Functional restoration of such tissues and organs with matrices might become a

viable and practical therapeutic approach to meet future demand after organ failure[124-128,131].

Biologic scaffold materials composed of ECM are commonly used to facilitate the constructive remodelling of a variety of tissue both in preclinical animal studies and in human clinical applications[134-137].

The ECM possesses the ideal characteristics of the tissue-engineered scaffold or biomaterial, being biocompatible, a supportive medium for blood vessels, nerves, and lymphatics and for the diffusion of nutrients from the blood, as well as being able to undergo constructive remodeling and degradation within the body's own systems[138-140].

All tissues and organs are made up of cells and associated extracellular matrix (ECM), a secreted product of the resident cells consisting of a unique, tissue-specific three-dimensional environment of structural and functional molecules. It is custom designed and manufactured by the resident cells of each tissue and organ and is in a state of dynamic equilibrium with its surrounding microenvironment[141].

The extracellular matrix is a multicomponent structure, a dynamic protein network that provides cells with positional and environmental information, serving as a tissue-specific structural framework that controls cell function. The composition of ECM is represented by a complex mixture of functional and structural molecules that affect a variety of cell activities[142]. These molecules are arranged in a unique, tissue specific, three-dimensional ultrastructure and are ideally suited to the tissue or organ from which the ECM is harvested. The structure and the composition of the ECM are constantly changing in response to the

current metabolic activity of the resident cell population, the mechanical demands of the tissue, and the prevailing microenvironmental niche conditions. This concept of “dynamic reciprocity” between the ECM and the resident cell population is a major advantage for the use of ECM scaffold materials and emphasize the importance of maintaining as much of the native composition and ultrastructure as possible during the preparation of these three-dimensional scaffolds. Matrix organization and its connection to intracellular pathways are important regulators of cell function, [143]defects in which can have significant pathological consequences [144].

Individual components of the ECM are common throughout most tissues such as collagen, laminin, fibronectin, and hyaluronic acid.

Collagen is the most abundant protein within the ECM. More than 20 distinct types of collagen have been identified and the most prevalent form found in mammalian tissues is type I collagen. Collagen has been well characterized and is ubiquitous across both the animal and plant kingdoms [145]. Collagen has maintained a highly conserved amino acid sequence through the course of evolution and for this reason allogeneic and xenogeneic sources of type I collagen have been long recognized as effective biologic scaffolds for tissue repair with low antigenic potential. Collagen types other than type I exist in the native ECM, although in much lower quantities. These alternative collagen types each provide distinct mechanical and physical properties to the ECM and contribute to the utility of the intact ECM (as opposed to isolated components of the ECM) as a scaffold for tissue repair. By way of examples: type IV collagen is present within the basement membrane of all vascular structures and is an

important ligand for endothelial cells, type VII collagen is the principal component of the anchoring fibrils of keratinocytes to the underlying basement membrane of the epidermis, and type VI collagen functions as a connector of functional proteins and glycosaminoglycans to larger structural proteins such as type I collagen, helping to provide a gel-like consistency to the ECM. Type III collagen exists within selected submucosal ECMs, such as the submucosal ECM of the urinary bladder, where nonrigid structure is demanded for appropriate function. Most collagen types cause differentiation of progenitor cell populations. It is common, therefore, to find little if any collagen in the ECM surrounding ESC populations.

Fibronectin represents an important noncollagenous component of the ECM. Fibronectin exists both in soluble and tissue isoforms and possesses many desirable properties of a tissue repair scaffold, including ligands for adhesion of many cell types[142,146]. In fact, this protein is the first example of a protein recognized to have dual functions, i.e., both structural and functional properties. Fibronectin exists within the ECM of both submucosal structures and basement membrane structures [147,142]. Fibronectin, on the other hand, has been shown to play a central role in the development of vascular structures and can be found at an early stage in developing embryos. Fibronectin has also been found to be critical for the maintenance of hematopoietic stem cell activity *ex vivo*, which is another indication of the important role for this molecule in the support of the stem cell phenotype.

Laminin is a complex adhesion protein found within the ECM, especially within the basement membrane form of ECM[142]. This trimeric

crosslinked polypeptide exists in numerous forms dependent on the particular mixture of peptide chains[148,149]. The prominent role of laminin in the formation and maintenance of vascular structures is particularly noteworthy when considering the ECM as a scaffold for tissue repair[150,151] . Laminin can be found within basement membrane structures and is perhaps the best studied of the ECM protein found in ESC-derived embryoid bodies[152]. Laminin plays a prominent role in the formation and the maintenance of vascular structures and is among the first and most critical of the ECM components in the process of cell and tissue differentiation.

Glycosaminoglycans (GAGs) are important components of ECM and play important roles in the binding and preservation of growth factors and cytokines, water retention, and the gel properties of the ECM. The heparin binding properties of numerous cell surface receptors and of many growth factors (e.g., FGF family, VEGF) make the heparin-rich GAGs extremely desirable components of scaffolds for tissue repair[118].

The composition of the ECM includes a variety of bioactive molecules admixed with the binding molecules such as decorin and biglycan. Although cytokines and growth factors are present within ECM in extremely small quantities, these molecules act as potent modulators of cell behavior.

The ability of the ECM scaffold to facilitate and integrate cellular and external environmental cues is the consequence of its bioinductive properties, allowing the important constructive remodeling of tissue after the in vivo implantation of ECM scaffolds[153-155]. This remodeling cannot be solely attributed to characteristics such as viscoelastic

behavior, biomechanical properties, or host cell attachment through collagen, fibronectin, and laminin ligands within the ECM. Angiogenesis, abundant host cell infiltration, mitogenesis, and deposition and organization of new host ECM are common events during the remodeling of ECM scaffolds. Component growth factors such as vascular endothelial cell growth factor (VEGF), basic fibroblast growth factor (bFGF), and transforming growth factor beta (TGF- β) are released during scaffold degradation and exert their biologic effects as they are dissociated from their binding proteins and activated[156-161]. These growth factors promote angiogenesis, mitogenesis and cellular differentiation during the remodeling process. The rapid degradation of the native ECM scaffold material is mediated by enzymatic and cellular processes and may be considered as a mechanism for controlled release of the ECM constituent molecules. The degradation process itself, which is mediated by enzymatic and cellular processes, may be considered as a mechanism for controlled release of the ECM constituent molecules. Indeed, the process of scaffold degradation and growth factor release continue until the scaffold is completely degraded. Perhaps more importantly, degradation products of the parent molecules that constitute the ECM appear to mediate a subsequent series of remodeling events. Cryptic peptides released by the degradation process initiate and sustain the recruitment of circulating, bone-marrow-derived cells that actively participate in long-term tissue remodeling[162-163].

The phenotype of the resident cells, including their active genetic profile, proteome, and functionality, is influenced by conditions of the microenvironmental niche including factors such as oxygen concentration,

pH, mechanical forces, and biochemical milieu. In turn, resident cells secrete the appropriate molecules in which to survive, function effectively, and communicate with neighbouring cells. Through this reciprocal interaction, the ECM has an essential role in prenatal development and postnatal maintenance of healthy function[119,120,164,165]. In addition to the matrix's role in development and adult homeostasis, it can be used as an inductive scaffold to promote a constructive tissue remodelling response after injury. Mechanisms of this response include release of cryptic peptides that are mitogenic and chemotactic for endogenous stem and progenitor cells[166-167], modulation of the innate immune response[169], and provision of tissue-specific molecular cues that support cell phenotype and function[129,169-171].

1.2.1 Principles and methods of decellularisation

The preparation of a matrix from a large, intact mammalian organ requires several sophisticated processing steps. The selection of decellularization reagents is critically important because these agents can damage the structure and composition of the resultant matrix[172].

Several factors can affect the ability to decellularize tissues/organs which include: (a) the cellular density of a particular tissue or organ, (b) the specific density of the tissue/organ, (c) lipid content, (d) thickness of the tissue/organ and (e) properties of the selected decellularization agent(s) [121]. The most effective agents for decellularization of each tissue and organ will depend upon many factors, including the tissue's cellularity (e.g. liver vs. tendon), density (e.g. dermis vs. adipose tissue), lipid content (e.g. brain vs. urinary bladder), and thickness (e.g. dermis vs.

pericardium). It should be understood that every cell removal agent and method will alter ECM composition and cause some degree of ultrastructure disruption. Minimization of these undesirable effects rather than complete avoidance is the objective of decellularization.

Detergents, enzymes and chemicals used for whole organ decellularization have been used in decellularization for various organs. Since decellularization agents can also negatively impact the native ECM composition and structure during the decellularization process, selection of these agents, along with the development of new protocols, have been considered to be critical steps of the process. To achieve this goal, several different groups of decellularization agents have been explored and such agents include: (a) non-ionic (Triton-X), ionic (sodium dodecyl sulfate: SDS) and zwitterionic detergents, (b) enzymatic agents, (c) physical agents and (d) direct application of force[121] .

- ***Chemical agents***

Acids and bases cause or catalyze hydrolytic degradation of biomolecules. Peracetic acid is a common disinfection agent that doubles as a decellularization agent by removing residual nucleic acids with minimal effect on the ECM composition and structure[173-174] . Acetic acid damages and removes collagens with a corresponding reduction in ECM strength, but it does not affect sulfated glycosaminoglycans (sGAG) [175]. Bases (e.g. calcium hydroxide, sodium sulphide, and sodium hydroxide) are harsh enough and commonly used to remove hair from dermis samples during the early stages of decellularization[176-177] . However, bases can completely eliminate growth factors from the matrix and decrease ECM mechanical properties more significantly than

chemical and enzymatic agents[177] . The primary mechanism by which bases such as sodium hydroxide reduce mechanical properties is the cleavage of collagen fibrils and disruption of collagen crosslinks [178].

Hypertonic saline dissociates DNA from proteins [180]. Hypotonic solutions can readily cause cell lysis by simple osmotic effects with minimal changes in matrix molecules and architecture . For maximum osmotic effect, it is common for the tissues to be immersed alternately in hyper- and hypotonic solutions through several cycles. Hypertonic and hypotonic solutions also help rinse cell residue from within tissue following lysis.

Ionic, non-ionic, and zwitterionic detergents solubilize cell membranes and dissociate DNA from proteins, and they are therefore effective in removing cellular material from tissue [179-181]. However, these agents also disrupt and dissociate proteins in the ECM as evidenced by their use in protein extraction procedures in tissue proteomics [182-183]. The removal of ECM proteins and DNA by detergents increases with exposure time[184-185] and varies with organ subunit, tissue type, and donor age[186-188]. Combining multiple detergents increases ECM protein loss [187] but also allows for more complete detergent removal from ECM after decellularization [188-189]. Triton X-100 can effectively remove cell residues from thick tissues such as valve conduits where enzymatic and osmotic methods are insufficient, with concomitant ECM protein loss accompanied by decreased adverse immune response in vivo[191]. Sodium dodecyl sulfate (SDS) appears more effective than Triton X-100 for removing nuclei from dense tissues while preserving tissue mechanics[186,192]. The addition of a detergent

such as SDS to a decellularization protocol can make the difference between complete and incomplete cell nuclei removal[193] but has the associated drawback of ultrastructure disruption[194-195] and growth factor elimination [177]. The zwitterionic detergent 3-[(3-cholamidopropyl)dimethylammonio]-1-propanesulfonate (CHAPS) is most effective for cell removal from thinner tissues such as lung and may be ineffective for decellularization of thicker tissues, even when used in combination with SDS[197] or alone for relatively acellular tissues[185]. A blinded categorical comparison of detergents for peripheral nerve decellularization showed better preservation of ultrastructure by non-ionic and zwitterionic detergents but better cell removal by ionic detergents[198]. However, the low concentration of cell bodies in peripheral nerve and the size of the tissue may limit the translation of these results to other tissues.

Care must be taken to flush residual chemicals from ECM after decellularization, particularly detergents such as SDS that penetrate into thick or dense tissues. Cytotoxicity is possible even at reduced agent concentrations and will inhibit or completely negate the beneficial properties of a cell-free ECM scaffold[199-200]. Even thin tissues such as valve leaflets require multiple (more than six) agitated washes to completely remove detergents[197].

Alcohols such as glycerol aid in tissue decellularization by dehydrating and lysing cells instead isopropanol, ethanol, and methanol are more effective than lipase in removing lipids from tissue and are capable of rendering adipose tissue lipid-free in a relatively brief period[201-202].

Methanol in combination with chloroform has been used during delipidation of tissues[176].. Caution should be used in treating tissues with alcohols such as ethanol and methanol due to their use as tissue fixatives in histology, their ability to precipitate proteins[203], and the damage they cause to ECM ultrastructure[178-202-203].

Acetone can also be used to remove lipids during decellularization[192]. However, like alcohols, the use of acetone as a tissue fixative [203] and its damage of ECM ultrastructure[204] warrant conservative use, especially for biological scaffolds used in load-bearing clinical applications[178]. In comparison to detergent treatments, acetone crosslinks ECM to produce stiffer scaffolds with mechanical properties further removed from those of native tissue[192].

-Biologic agents

Enzymes reported in tissue decellularization protocols include nucleases, trypsin, collagenase, lipase, dispase, thermolysin, and a-galactosidase. Enzymes can provide high specificity for removal of cell residues or undesirable ECM constituents. However, complete cell removal by enzymatic treatment alone is difficult and enzyme residues may impair recellularization or evoke an adverse immune response.

Nucleases (e.g. DNases and RNases) cleave nucleic acid sequences and can therefore aid in removal of nucleotides after cell lysis in tissues[169,184,193,205]. Endonucleases such as benzonase[169] may be more effective than exonucleases because they cleave nucleotides mid-sequence and thereby more effectively fragment DNA in preparation for its removal. Likewise, non-restriction endonucleases will more effectively fragment DNA compared to their sequence-dependent

counterparts.

Trypsin is a serine protease commonly used as an enzymatic decellularization agent. However, ECM proteins such as collagens have limited resistance to trypsin cleavage[206] and tissue exposure to trypsin should therefore be used with caution. In comparison to detergents, trypsin is more disruptive to elastin and collagen and slower to remove cells but shows better preservation of GAG content[195, 188, 207,208]. Trypsin disruption of ECM can be correlated to changes in mechanical properties[208]. Removal of cells and ECM constituents by trypsin is time-dependent, and complete decellularization by trypsin alone may require lengthy incubation even for thinner tissues such as valve leaflets[209]. Trypsin can be used effectively to disrupt tissue ultrastructure and improve penetration of subsequent decellularization agents; therefore, exposure to trypsin as the initial step in a tissue decellularization protocol may be desirable or even necessary, particularly for complete removal of cell nuclei from dense tissues[184].

Collagenase may be used during decellularization, but only when ultrastructure preservation and maximum collagen retention are not critical to the intended clinical application of the resultant ECM.

Lipase aids in delipidation but is typically insufficient to remove all lipids when used alone[201-202].

Dispase and trypsin can be used successively to improve cell removal from thicker tissues such as dermis if used in combination with detergents, and repeated treatments with dispase may further improve decellularization[210]. Using an enzyme such as dispase or thermolysin as the sole decellularization agent is only effective for removing cells on

the surface of a tissue and is likely to require mechanical abrasion for complete cell removal[211]. With regard to the underlying basement membrane and ECM, thermolysin is less disruptive compared to dispase[211].

Decellularized xenogeneic tissues can be treated with α -galactosidase to reduce the immunogenic cell surface antigen galactose- α - (1,3)-galactose (Gal epitope) [212], although the immunomodulatory effect of Gal epitope does not adversely affect in vivo remodeling of xenogeneic ECM[213].

-Non-enzymatic agents

Chelating agents such as ethylenediaminetetraacetic acid (EDTA) and ethylene glycol tetraacetic acid (EGTA) aid in cell dissociation from ECM proteins by sequestering metal ions[214-215]. It is likely that chelating agents contribute to subtle disruptions in protein-protein interactions by the same mechanism[216]. Chelating agents alone are insufficient for superficial cell removal even with agitation, and they are therefore typically used in combination with enzymes such as trypsin[193, 184,205] or detergents[177,193,196,205]. The combined efficacy of chelating agents and simple hyper- or hypotonic solutions for decellularization is unknown[193,205,217].

Serum associates with nucleic acid fragments to aid in their removal from tissue, but it does not remove some immunogenic constituents such as phospholipids[197]. Additionally, xenogeneic serum has the disadvantage of introducing immunogenic constituents that may associate with the ECM, thus potentiating a downstream adverse host response.

The use of serum in preparing ECM for clinical applications is therefore limited.

Serine protease inhibitors such as phenylmethylsulfonyl fluoride (PMSF) [193,201,217], aprotonin, and leupeptin[218] prevent undesirable damage to ECM that might otherwise result from release of intracellular proteases during cell lysis.

-Physical and miscellaneous agents

Freeze-thaw processing effectively lyses cells within tissues and organs, but the resulting membranous and intracellular contents remain unless removed by subsequent processing. A single freeze- thaw cycle can reduce adverse immune responses such as leukocyte infiltration in vascular ECM scaffolds[217]. Multiple freeze-thaw cycles may be used during decellularization [201-219]and do not significantly increase the loss of ECM proteins from tissue. The effect of freeze- thaw processing on mechanical properties is minimal for load- bearing, mechanically robust tissues[188].

Cells on the surface of a tissue or organ (e.g., urinary bladder, small intestine, skin, amnion) can be effectively removed by mechanical abrasion in combination with enzymes[211], hypertonic saline, or chelating agents, all of which facilitate dissociation of cells from their subjacent basement membrane. However, underlying ultrastructure and basement membrane integrity are invariably damaged by any direct application of mechanical force[211].

Hydrostatic pressure requires relatively little time and can be more effective than detergents or enzymes for removing cells from blood vessel and corneal tissues, although the baric formation of ice crystals may

disrupt ECM ultrastructure. [205] Increased temperature during pressure decellularization prevents ice crystal formation[205] but may disrupt ECM due to the associated increase in entropy, which can be mitigated by colloids such as dextran.

Agent/Technique	Mode of action	Effects on ECM
Chemical Agents		
Acids and bases	Solubilizes cytoplasmic components of cells, disrupts nucleic acids, tend to denature proteins	May damage collagen, GAG, and growth factors
Hypotonic and hypertonic solutions	Cell lysis by osmotic shock, disrupt DNA-protein interactions	Effectively lyses cells, but does not effectively remove cellular residues
Non-ionic detergents	Disrupt DNA-protein interactions, disrupt lipid-lipid and lipid-protein interactions and to a lesser degree protein-protein interactions	
- Triton X-100		Mixed results with efficacy dependent on tissue, more effective cell removal from thin tissues, some disruption of ultrastructure and removal of GAG, less effective than SDS
Ionic detergents	Solubilize cell and nuclear membranes, tend to denature proteins	
- Sodium dodecyl sulfate (SDS)		Effectively removes nuclear remnants and cytoplasmic proteins from dense tissues, tends to disrupt ultrastructure, removes GAG and growth factors and damages collagen
- Sodium deoxycholate		Mixed results with efficacy dependent on tissue thickness, some disruption of ultrastructure and removal of GAG
- Triton X-200		More effectively removes cells from thin tissues but with greater disruption of ultrastructure compared to other detergents
Zwitterionic detergents	Exhibit properties of non-ionic and ionic detergents	
- CHAPS		Effectively removes cells with mild disruption of ultrastructure in thin tissues
- Sulfobetaine-10 and -16 (SB-10, SB-16)		Effectively removes cells with mild disruption of ultrastructure in thin tissues
Solvents		
- Alcohols	Cell lysis by dehydration, solubilize and remove lipids	Effectively removes cells from dense dense tissues and inactivates pyrogens, but crosslinks and precipitates proteins, including collagen
- Acetone	Cell lysis by dehydration, solubilizes and removes lipids	Effectively removes cells from dense dense tissues and inactivates pyrogens, but crosslinks and precipitates proteins, including collagen
- Tributyl phosphate (TBP)	Forms stable complexes with metals, disrupts protein-protein interactions	Mixed results with efficacy dependent on tissue, dense tissues lost collagen but impact on mechanical properties was minimal

Biologic Agents		
Enzymes		
- Nucleases	Catalyse the hydrolysis of ribonucleotide and deoxyribonucleotide chains	Difficult to remove from the tissue, could invoke an immune response
- Trypsin	Cleaves peptide bonds on the C-side of Arg and Lys	Prolonged exposure can disrupt ECM ultrastructure, removes ECM constituents such as collagen, laminin, fibronectin, elastin, and GAG, slower removal of GAG compared to detergents
- Dispace	Cleaves specific peptides, mainly fibronectin and collagen IV	Prolonged exposure can disrupt ECM ultrastructure, removes ECM components such as fibronectin and collagen IV
Chelating Agents (EDTA, EGTA)	Chelating agents bind metallic ions, thereby disrupting cell adhesion to ECM	Typically used with enzymatic methods (e.g. trypsin) but can be used with other agents, ineffective when used alone
Physical and Miscellaneous Agent		
Temperature (freezing and thawing)	Intracellular ice crystals disrupt cell membrane	Ice crystal formation can disrupt or fracture ECM
Direct application of force	Removal of tissue eliminates cells and force can burst remaining cells	Force can directly damage ECM
Pressure	Pressure can burst cells and aid in removal of cellular material	Pressure can disrupt ECM
Electroporation	Pulsed electrical fields disrupt cell membranes	Electrical field oscillation can disrupt ECM

Fig. 14 scheme of the different agents used in the decellularization protocols.

Unlike agitation and diffusion-only techniques used for the decellularization of simple and thin tissues, solid organs require dynamic decellularization techniques in order to efficiently remove cellular components from the entire organ system. In particular, the mechanical forces incorporated with dynamic decellularization techniques are important for efficient decellularization. Such mechanical parameters can be pressure, shear stress and flow rate of decellularization agents. Different levels of mechanical forces need to be applied to decellularization processes depending on the size and types of organs. Antegrade and retrograde perfusion techniques of the decellularization agent(s) through the native vascular system of the organ has been the most commonly used method to produce acellular whole organ scaffolds[169,172,177,184]. In this approach, perfused decellularizing agent(s) are evenly distributed throughout the organ and, in addition, the application of a certain amount of pressures during the perfusion process has shown to effectively achieve tissue permeation from large blood

vessels down to the capillary level. Perfusion of decellularization solution also allows cellular debris to be excreted through the venous system. [172]

1.1.2 Characterization of the decellularized tissue

After the decellularization process, it is necessary to evaluate the resulting scaffolds to determine the extent of decellularization and whether or not the scaffold is damaged. Assays used for this purpose include qualitative and quantitative assays. Qualitative evaluation involves demonstrating that cellular material has in fact been removed from the matrix as well as demonstrating that the main ECM proteins have been retained. This is performed using several different histological and immunofluorescent methods. The removal of cellular components by the decellularization process can be confirmed by observing the lack of visible nuclear material in tissue sections stained with 4, 6-diamidino- 2-phenylindole (DAPI) or hematoxylin & eosin (H&E). The retention of ECM components is visualized by several staining methods, such as Masson's trichrome and Herovici staining for collagens, Alcian blue/PAS staining for glycosaminoglycans (GAGs) and Movat's staining for collagen and elastin fibers. In addition, electron microscopic studies using a scanning electron microscope (SEM) and/or transmission electron microscope (TEM) are often conducted to examine the decellularized scaffolds on a very fine scale to identify ultrastructure within the scaffolds[121].

However, these techniques are not sensitive enough to identify and quantitatively analyze the residual DNA content within the ECM[176]. The presence of DNA is directly correlated to adverse host reactions[188,191].

Hence, interest in the quantification of the residual nucleic material after decellularization has been justified[176]. Based upon findings from in vivo studies in terms of constructive remodeling and adverse host responses using two-dimensional decellularized tissues, the following minimal criteria for acceptable amounts of residual DNA after decellularization have been created[176]: (a) <50 ng double strand DNA per mg dry weight, and (b) <200 bp DNA fragment length[188].

Likewise, the biological activities of ECM components need to be considered in the process of whole organ bioengineering. Following the decellularization of solid organs, the resulting acellular organ scaffolds will be combined with a cellularization technique for further application in in vivo studies, and the biological activities of many matrix proteins are required for the recellularization step to be successful. First, cell adhesion to the acellular organ matrix is a pre-requisite step for the recellularization process. In many cases, natural cell-adhesion domain sequences in the matrix (e.g., RGD) [204] can bind with members of the integrin family, which are expressed on many cell types. This binding is crucial to allow cells to adhere to acellular organ matrices. These types of cell adhesion peptide motifs exist on ECM components such as collagen and fibronectin. Collagen is particularly important because it retains the RGD motif as well as bound growth factors. Fibronectin is a representative glycoprotein in ECM that plays roles in cell adhesion, growth, migration and differentiation[195,203].

The presence of collagen, fibronectin and laminin is crucial for cells seeded onto a decellularized organ to attach to the matrix and begin recellularizing the organ.

Once seeded cells are attached to the ECM components within acellular scaffolds, the behaviors of the cells will be influenced by growth factors and bioactive molecules that confer inherent bioactivity within the matrix. Generally, growth factors easily degrade after secretion from the cells that produce them. However, within the ECM, GAGs are critically important in the protection of free growth factors from proteolytic degradation[196]. Due to the existence of heparan sulfate residues on GAGs and the low isoelectric point (IEP \approx 5) of heparan sulfate, GAGs are able to bind growth factors that have an IEP of \approx 10, such as fibroblast growth factor-2 (FGF-2), vascular endothelial growth factor (VEGF), transforming growth factor- β (TGF- β) and platelet-derived growth factor (PDGF). Such growth factors become anchored to GAGs and can thus be protected from enzymatic degradation. This process allows them to retain biological activity, and they can affect cells that bind the various ECM compounds during the recellularization of a decellularized organ scaffold. Another role of GAGs for the recellularization process is of particular importance in morphogenesis which promotes cellular adhesion permissive cell shape changes and motility as well as the maintenance of original phenotypes of repopulated cells[221]. Hyaluronic acid (HA), one subset of GAGs, is such a molecule. HA is considered to be important for several aspects of cellular behaviors such as the direction of cellular shape changes and the induction of cytoskeletal rearrangements within cells. However, during current decellularization processes, 50 to 90% amounts of GAGs in various organs [222,223] were reported to be removed when compared to that of original organs. The reduction of GAG amounts may cause the inactivation of endogenous growth factors and

also adversely influence the efficient recellularization process due to lack of primary components of GAGs. Further investigations may be needed into the modification of decellularization method for the maintenance of GAG architectures after decellularization.

Just as solid organs have an intricate vascular tree within them, acellular organ scaffolds should maintain continuous and intact vascular structures after the decellularization process. This vascular matrix can be used to reseed the matrix for efficient whole organ bioengineering. This vascular system can be used as a template for cell seeding with organ-specific types of parenchymal cells or it can be directly seeded with endothelial cells. This is especially important because a continuous and functional re-endothelialized vascular system within a recellularized whole organ can reduce thrombosis and blood clots when the organ is integrated with the vasculature of the host during the implantation procedure.

1.2.3 State of the art of the different decellularization scaffolds

Intact three-dimensional extracellular matrix scaffolds from different allogeneic and xenogeneic tissues and organs have been manufactured effectively for regenerative medicine.

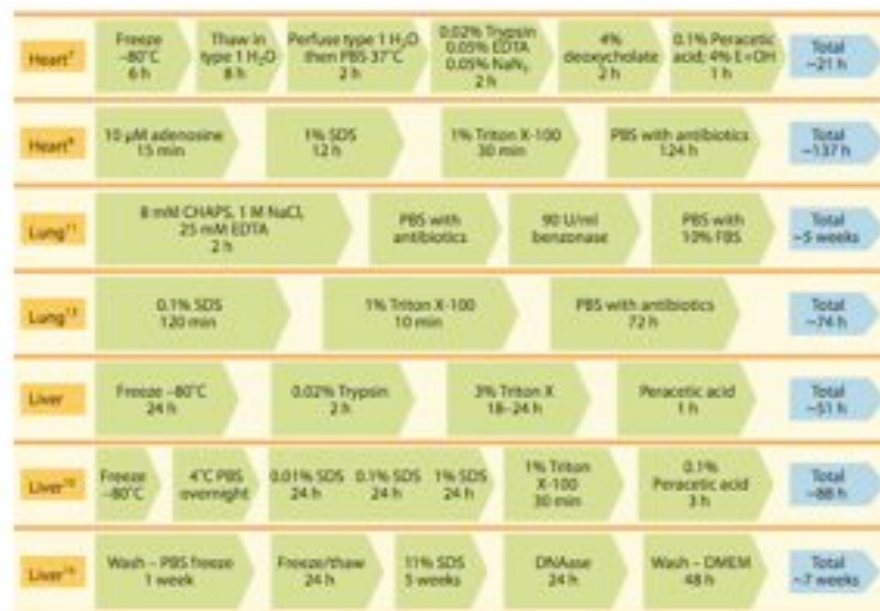


Fig.15 Some reported perfusion protocols for decellularization of heart, liver and lung. Abbreviations: DMEM, Dulbeccos's Modified Eagle's Medium; EDTA, ethylene diamine traacetic acid; FBS, fetal bovine serum; PBS, phosphate buffered saline; SDS, sodium dodecyl sulfate.

The heart

The first report in which whole-organ decellularization was successfully performed was on the heart[222]. The aorta of a rat heart was cannulated to allow retrograde coronary perfusion with heparinized phosphate-buffered saline with adenosine, 1% sodium dodecyl sulfate (SDS), and 1% Triton X-100 in sequence alternating with rinsing with

deionized water between steps. This produced a decellularized scaffold that was structurally similar to the heart, but had a translucent white appearance throughout (Fig. 16). Reimplantation of the acellular heart scaffold onto the aorta demonstrated an intact and patent vascular network .

Recellularization of the heart scaffold with cardiomyocytes under electro- physiological stimulation formed a construct capable of muscular contraction[126].

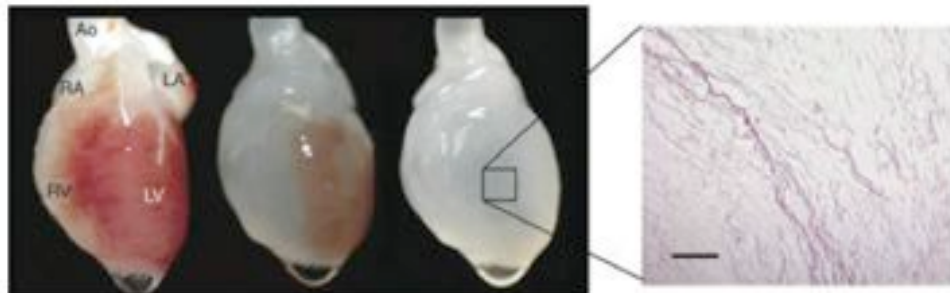


Fig. 16 The heart in stages of increasing decellularization over time with 1% sodium dodecyl sulfate as the decellularizing agent, with the end result of a translucent appearing heart-like scaffold structure. The panel on the right shows histological evidence (H&E staining) of decellularization. Scale bar = 200 μ m.

The lungs

A number of groups have investigated the use of perfusion decellularization in the lungs[128,129,194,223,224], which contain two accessible compartments separated by a short diffusion distance, that is, the vascular and the airway systems, by using varying protocols of vascular perfusion alone[194,224], or in combination with endotracheal instillation[128,223], or perfusion of the airway compartment[129]. The decellularizing agents used were also far more varied from protocol to protocol, from SDS at different concentrations [129,198,224] to 8mM CHAPS[128], to a combination of Triton X-100/deoxycholate/DNAse/bleach[223]. All groups demonstrated preservation of the major components of the ECM and the micro- and macroarchitecture of the lung.

Recellularization was achieved with all the reports, although Petersen et al. mimicked physiological conditions within the bioreactor by ventilation of the airway compartment at negative pressure at 1 breath/min, and maintained pulmonary artery pressure at 20 mmHg or below. Orthotopic implantation of these tissue-engineered lung constructs demonstrated active gas exchange occurring via sampling of pulmonary arterial and venous blood.

However, results in this study and Ott et al. showed vascular leakage and pulmonary edema after a few hours of implantation, indicating damage to the microvasculature from the decellularization process. In a follow-up study to Ott et al., Song et al. demonstrated further optimization of graft preservation and oxygenative function post-implantation for as long as 7 days[224]. Recellularization was performed with mixtures of whole-lung cell isolates in four cases[128,194,223,224],

but one group used a homogeneous mouse embryonic stem cell population[129], which showed that the matrix was capable of promoting site-appropriate differentiation without any other specific differentiation cues.



Fig. 17 Perfusion decellularization of whole rat lungs. (a) Photographs of a cadaveric rat lung, mounted on a decellularization apparatus allowing antegrade pulmonary arterial perfusion. pa, pulmonary artery; pv, pulmonary vein; tr, trachea; RUL, right upper lobe; RML, right middle lobe; LL, left lobe. Freshly isolated lung (left), after 60 min of SDS perfusion (middle), and after 120 min of SDS perfusion (right). The lung becomes more translucent as cellular material is washed out first from apical segments, then from the middle segments and finally from the basal segments.

The liver

Liver decellularization has been performed by antegrade perfusion via the portal vein with SDS and Triton X-100, either alone or in combination [124, 225-227], although another study used trypsin/EGTA[185], and Baptista et al. used Triton X-100 in combination with ammonium hydroxide[177, 228]. Decellularization was demonstrated with histology and evidence of DNA removal, and retention of key ECM constituents with preservation of microvasculature and ECM ultrastructure. Hepatocytes were seeded onto the acellular liver scaffold via portal vein perfusion and were shown to be functional in four studies [177,225,227-228]by showing evidence of synthesis of lactate dehydrogenase, albumin, and urea after heterotopic implantation. In particular, two studies attempt to scale-up this approach to further approximate human- scale engineered organ constructs by use of ferret[177] and porcine[227] livers, and both studies seeded the bioscaffolds with human liver cells, which were shown to be compatible on these xenogeneic scaffolds.

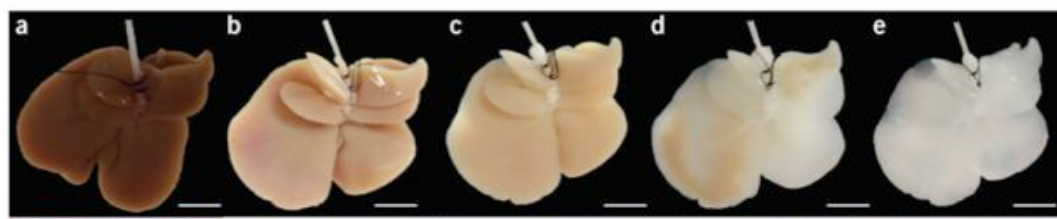


Fig. 18 Decellularization of ischemic rat livers. (a–e) Representative images of ischemic rat livers during decellularization process at 0 h (a), 18 h (b), 48 h (c), 52 h (d) and 72 h (e).

The kidney

Several groups have decellularized whole kidneys by the perfusion method with preservation of the vascular network and complete cell removal[228-230]. Decellularizing agents vary from 1% Triton or SDS[228-229] to 3% Triton with DNase and additional 4% SDS[230]. The preservation and presence of ECM constituents such as laminin and collagen IV were also demonstrated, as well as collagen I, fibronectin, and heparin sulfate in a separate study, which did not employ perfusion[208]. The latter study juxtaposed fetal cells in fresh renal explants with the ECM scaffolds by layering fetal kidney tissue against the ECM, which supported developmental renal phenotypes in these cells after they migrated into the ECM. In the study by Ross et al., decellularized rat kidneys scaffolds were reseeded with murine embryonic stem cells, and the renal ECM was shown to support the renal differentiation of the embryonic stem cells.

The last but not the least Ott et al. decellularized rat, porcine and human kidneys by detergent perfusion, yielding acellular scaffolds with vascular, cortical and medullary architecture, a collecting system and ureters.

To regenerate functional tissue, they seeded rat kidney scaffolds with epithelial and endothelial cells and perfused these cell- seeded constructs in a whole-organ bioreactor. The resulting grafts produced rudimentary urine *in vitro* when perfused through their intrinsic vascular bed. When transplanted in an orthotopic position in rat, the grafts were perfused by the recipient's circulation and produced urine through the ureteral conduit *in vivo*. [231]

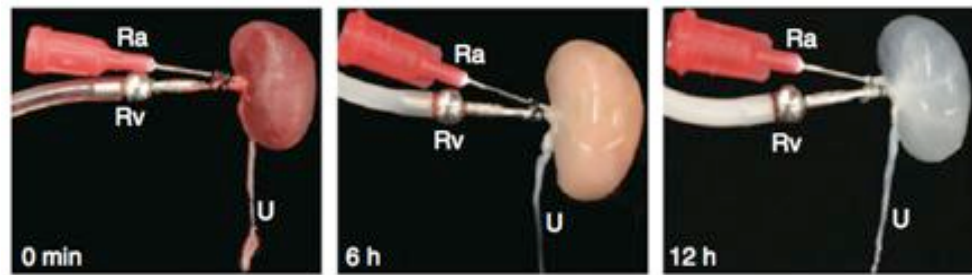


Fig. 19 Perfusion decellularization of whole rat kidneys. (a) Time-lapse photographs of a cadaveric rat kidney undergoing antegrade renal arterial perfusion decellularization. Shown are a freshly isolated kidney (left) and the same kidney after 6 h (middle) and 12 h (right) of SDS perfusion. Ra, renal artery; Rv, renal vein; U, ureter.

Trachea

Macchiarini et al. repopulated a decellularized human windpipe in a bioreactor with cultured autologous respiratory epithelial cells and autologous chondrocytes of bone marrow-derived mesenchymal stromal cell origin, and used the resultant graft to replace a terminally diseased left main bronchus.

For the decellularization technique they used 25 cycles of distilled water for 72 h, then incubated in 4% sodium deoxycholate and 2000 kU deoxyribonuclease I in 1 mmol/L sodium chloride (Sigma Chemicals, Barcelona, Spain). [131]



Fig. 20 The graft obtained after the decellularization process and immediately before the implantation.

SIS (small intestinal mucosa)

Totonelli et al in 2012, using a detergent-enzymatic treatment (DET), optimized in rats a protocol that creates a natural intestinal scaffold, as a base for developing functional intestinal tissue. After 1 cycle of DET, histological examination and SEM and TEM analyses showed removal of cellular elements with preservation of the native architecture and connective tissue components. This DET consists of deionized water at 4 °C for 24 h, 4% sodium deoxycholate (Sigma) at room temperature (RT) for 4 h, and 2000kU DNase-I (Sigma) in 1 M NaCl (Sigma) at RT for 3 h, as previously describe also for trachea. Maintenance of biomechanical, adhesion and angiogenic properties were also demonstrated strengthen the idea that matrices obtained using DET may represent a valid support for intestinal regeneration[131].

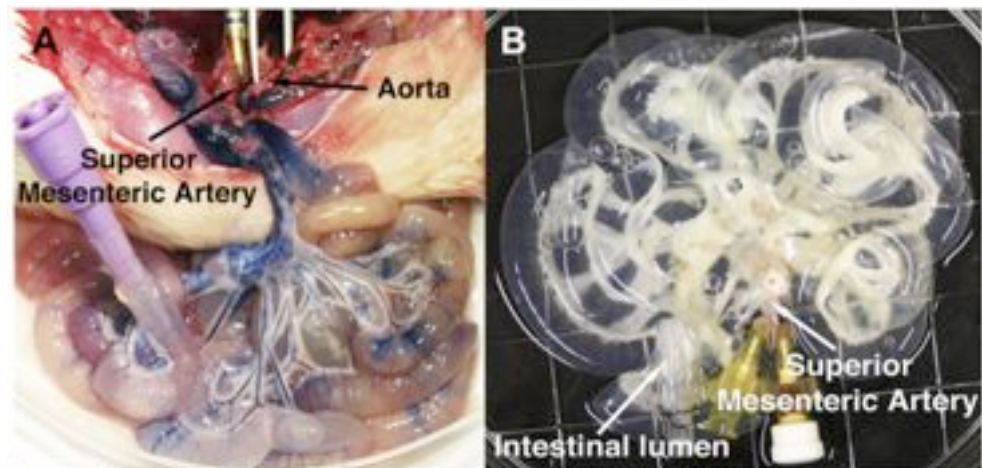


Fig.21 Decellularization of rat small intestine with detergent-enzymatic treatment. Macroscopic pictures prior (A) and following (B) one cycle of decellularization.

Thyroid

Working in the laboratory of Regenerative Morphology and Bioartificial Structures at the S.Bi.BI.T Department of the University of Parma, under the supervision of Prof. Roberto Toni, I have been engaged in developing a protocol for decellularization of the rat thyroid. We settled a protocol based on freeze and thaw, 0.02% of trypsin, 3% of Triton X-100 in PBS, 4% of Sodium deoxycholate in PBS and final sterilization with Peracetic Acid. After tissue process the structure of the matrix remained intact, in terms of 3D-structure, and at the same time the matrix obtained was very well cleaned in DNA.

We also collected preliminary results on the recellularization of this scaffold, using a culture model with cells derived from the same animal source, the rat thyroid. As a result, we observed that after 7 days of culture the thyroid matrix provided attachment of the seeded cells, and maintenance of their differentiation state [233].

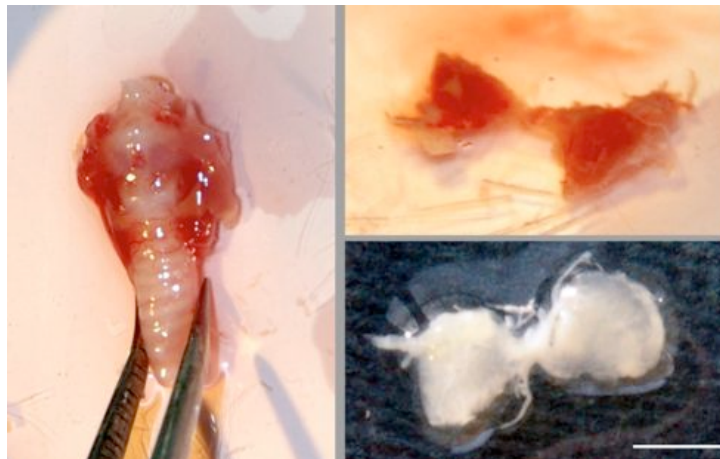


Fig.22 Decellularization of rat thyroid with detergent-enzymatic treatment. Macroscopic pictures prior in situ (A) and ex situ (B) following (C) decellularization protocol.

1.3 Culture of thymic epithelial cells

Culturing thymic epithelial cells in vitro, freshly obtained from the tissue, is a problem of substantial interest.

In vivo, Thymic epithelial cells undergo a rapid expansion during the early stages of thymus development, but as lymphopoiesis progresses, the more mature epithelial cells exit the cell cycle to leave only thymic epithelial stem cell pool.

Monolayer cultures of thymic stromal cells have been used for in vitro assays of stromal cell function. immortalization techniques have been used in conjunction with monolayer culture to generate long term stromal cell lines and it has been shown that monolayer cultures are capable of inducing the maturation of CD4⁻ CD8⁺ CD3⁻ cells from their CD4⁻ CD8⁻ CD3⁻ precursors.

Thymic epithelial cell lines have also been used to induce a limited growth and differentiation of early thymic precursors cells in coculture.

A number of studies have shown that thymic stromal cells cultured as monolayer rapidly lose their ability to support T-cell development, suggesting a change in their normal phenotype.

They change their normal phenotype in a serum free medium, although fetal calf serum or human serum has been used as a necessary constituent of the culture medium but this has several disadvantages such as the addition of unknown factors (hormones, endotoxins, viruses and other macromolecules) [234], which may vary from batch to batch. This creates problems of reproducibility but also makes it difficult to define growth requirements for the cells, and to isolate and figure out the

meaning of biological activities executed by molecules released by the cells into the culture medium [235].

It has been reported that for growing of murine TEC is essential the epidermal growth factor, insulin and hydrocortisone [236] instead, for human TEC, it's important the supplement of selenium, transferrin and insulin to the culture media. [237-238]

There are also some different way to culture thymic epithelial cells using not only a specific media but doing coculture with other cell type that could support TEC.

In 1986, Ehmann at al., cultured TEC, using a tissue culture plastic, were plated together with letally irradiated cells of the LA7 rat mammary tumor line that gave a support for growing. Epithelial cells from the normal mouse thymus could be cultured and subcultured for at least 8 passages in this way. As the irradiated LA7 cells slowly decreased in number TEC proliferated concomitantly to form a confluent monolayer like show in figure 23. [239]

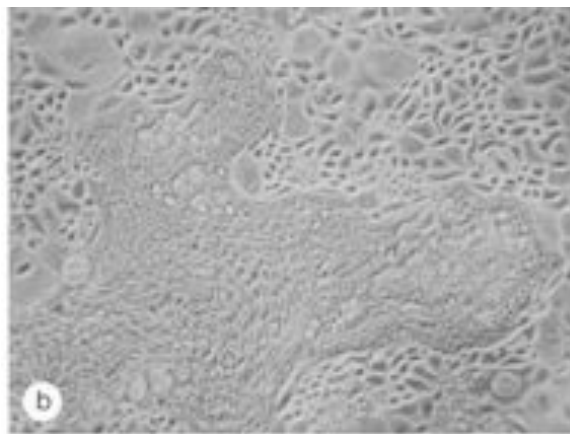


Fig.23 An image of a colony of distinct thymus cells with LA7 cells near the top of the image. Magnification X89 .

1.3.1 Three dimensional culture of thymic epithelial cells

Culturing thymic epithelial cells in vitro preserves the ability of these cells to promote thymocytes maturation so long as they are cultured as 3-dimensional aggregates. The 3-dimensional structure of the thymic epithelial cells is essential to maintain their function within the intact thymus.

The correct 3-dimensional structure therefore appears to be a prerequisite for full epithelial cell function in vitro since the 3D thymic architecture contributes to critical cell-cell interactions.

3D matrices were created by culturing thymic fragments on the surface of disks of CellFoam (Cytomatrix) and this resulted in the colonization with thymic stromal cells reaching 80% of confluency [240].

These matrices were then used with the addition of progenitor cells CD34⁺ or AC133⁺ and a coculture for 14 days demonstrated that these matrices were capable to induce a differentiation in the progenitor cells and they were able to highly proliferate in the presence of interleukin 2 and phytohemagglutinin [241].

There was also some way of doing a coculture in a 3D structure like a three dimensional organotypic coculture model. This was used for the culture of isolated mTECs to mimic a dermal equivalent in vitro. It consisted of dermal fibroblast that were embedded in an inert scaffold constituted by fibrin gel like shown in Fig. mTEC seeded on top of this fibrin gel proliferated and underwent terminal differentiation. This three dimensional model preserves key features of mTECs: proliferation and terminal differentiation of CD80^{lo}, Aire⁻ mTECs into CD80^{lo}, Aire⁺ mTECs,

responsiveness to RANKL and sustained expression of FoxN1, Aire and tissue-restricted genes into CD80^{hi} mTECs [242].

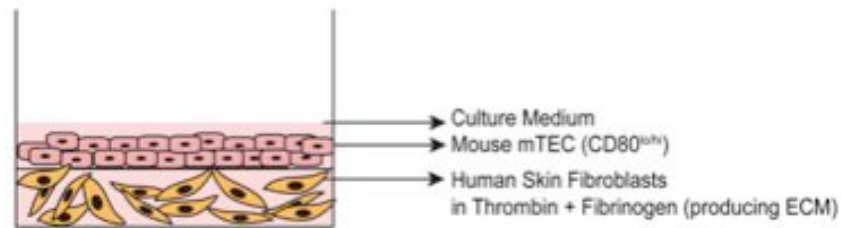


Fig.24 A schematic representation of the 3D organotypic coculture.

Less it has been done for the reconstruction of the thymus, in vitro and then in vivo, since it has been demonstrated that after injection of IL-22 after chemioterapic treatment is enough in the regeneration of thymic epithelium.

IL-22 has been identified as an important player in the thymic regeneration. It appears to be mainly produced by thymic innate lymphoid cells in response to tissue damage, and this process is at least partly regulated by dendritic cells through the production of IL-23. The receptor for IL-22 is expressed on TEC and seems to induce their survival and proliferation[243].

In 2002, Gill et al, identified a population of MT24+ cells, a subpopulation of TEC. These cells contained epithelial progenitor cells that were competent and sufficient to fully reconstitute the complex thymic epithelial microenvironment that supported normal T cell development. This population has been cultured for 24 hours and then, after reaggregation, it has been implanted under the kidney capsule of congenic recipient mice. These reaggregates were able, after 3 weeks, to induce the maturation of pre T-lymphocytes in a comparable situation to

the normal thymic tissue[241].

In 2012, Piccinini et al, developed an in vitro 3D module to culture TEC. They were cultured in different 3D shape with a scaffold made up fibrin and they identified like a best shape a simple drop in which cells are embedded. In this configuration TEC were able to maintain their differentiated state like underlined by the expression of a series of marker that were expressed in a comparable quantity to the in vivo situation. They maintained their phenotype after 14 days in vitro and, after coculture with pre-T lymphocytes, they were able also to induce the maturation of them in a more differentiated phenotype[244].

2.AIM OF THE THESIS

2. AIM

The aim of my experimental work has been to develop an innovative technique to reproduce in vitro the 3D thymic microenvironment, to be eventually used for growth and differentiation of thymocytes, and possible transplantation replacement in conditions of depressed thymic immune regulation. The work has been developed in the laboratory of Tissue Engineering at the University Hospital in Basel, Switzerland, under the tutorship of Prof. Ivan Martin, Director of this research Center.

Since a number of studies have suggested that the 3D structure of the thymic microenvironment might play a key role in regulating the survival and functional competence of thymocytes, I've focused my effort on the isolation and purification of the extracellular matrix of the mouse thymus, chosen as a suitable research model. Specifically, based on the assumption that TEC can favour the differentiation of pre-T lymphocytes, I've developed a specific decellularization protocol to obtain the intact, and DNA-free extracellular matrix of the adult mouse thymus. In this manner, I have tried to prevent the cytotoxic effect of contaminating nucleic acids on seeded TECs, and to provide a functional 3D structure rich in intrinsic proteins for TEC growth and assembly.

This 3D matrix, then, has been used as a natural scaffold for culturing TEC in static conditions. In particular, I have analyzed a number of surface markers indicating TEC capability to maintain their own phenotype, and eventually promote the differentiation of pre-T lymphocytes, similar to what previously demonstrated with other 3D structure like the fibrin gel.

3.MATERIALS AND METHODS

3.1 TECs isolation

3.1.1 Thymi digestion

TECs are isolated from B6 mice, 4-6 weeks old.

Thymus isolation and cleaning is performed on the lab bench, while the digestion is performed in sterile conditions under the hood.

Mice are sacrificed by cutting the head to avoid CO₂ and excessive bleeding in the thymic area.

The mouse is open cutting the peritoneum, cutting the membrane separating the chest from the peritoneum, cutting the ribs and exposing heart and thymus.

The thymus is isolated by pulling it, without cutting, and after it is placed in a Petri dish on ice containing PBS + 2%Fetal Bovine Serum.

After the explant and before the digestion, Thymi are cleaned, under the microscope, by fat and capsule to facilitate enzymes' action in a solution of

The thymi are cleaned under the microscope. First lobes are separated and then each lobe is cleaned from fat and connective tissue. Finally to favor the digestion small holes are done in the capsule.

The digestion is carried out in a water bath at 37°C in an enzymatic solution made of PBS, Liberase (Product Number:05401127001 Roche Diagnostic) and DNase (Product Number:11284932001 Roche Diagnostic).

For 6 thymi the solution is made of:

Liberase: 50mg/20 ml H2O sterile 500 μ l

DNase: 10mg/1 ml H2O sterile 50 μ l

PBS: 5,5 ml

The thymi are left at 37°C for ten minutes. Then the solution with pieces are pipetted up and down with a tip of 1000 μ l ,cut before to favor the digestion. This is done for two times.

The pellet is allowed to sit down, the supernatant with cells is collected and enzymes are inactivated added to them IMDM+ 2%Fetal Bovine Serum.

3ml of the digest solution is added to pellet and left at 37°C for ten minutes. Then the solution with pieces are pipetted up and down with a tip of 1000 μ l ,cut before to favor the digestion. This is done for two times.

After these steps all pieces are digested and enzymes are inactivated added to solution IMDM+ 2%Fetal Bovine Serum.

Two solutions, coming from first and second digestion respectively, are pooled down together at 1500 rpm 5'.

Cells are resuspended in 10ml of PBS + 2%Fetal Bovine Serum and filtered through a 70 μ m strainer.

10 μ l of the solution is used to count cells at the Cell Coulter.



Fig.25 An image of the cell coulter.

For the counting $10\mu\text{l}$ of solution with cells is added to 10ml of PBS and 3 drops of Zap-oglobin.

The result obtained on Cell Coulter is multiplied per 2 and per 10^3 per the ml of the solution.

The solution is adjusted to bring cells to a concentration of 100×10^6 cells.

3.1.2 CD45 depletion

The cells' solution freshly obtained is used for CD45 depletion. CD45 beads (Product Number:130-052-301 Miltenyi Biotec) are added to cells at a concentration of $5\mu\text{l}/10^7$ cells.

The solution is left 15' at 4°C in the dark.

After that cells are washed 2 times with PBS + 2%Fetal Bovine Serum spinning down at 1500rpm 5'.

Cells are filtered through a $70\mu\text{m}$ strainer and then distributed in FACS tubes (2ml each tube) after another filtration through a $45\mu\text{m}$

strainer attached to a 2,5 ml syringe.



Fig.26 A image prior the filtration of the cell suspension.

The enrichment can start with the AutoMACS Pro Separator System(Miltenyi Biotec) using the protocol **Deplet_s + QRinse**.



Fig.27 A image of the AutoMacs used for the CD45 depletion.

Cells of interest will be in the CD45⁻ fraction. These cells are spinned down at 1500rpm 5' and the pellet is resuspended in 1ml of

Iscove's Modified Dulbecco's Medium(IMDM) (Gibco; Invitrogen) containing 10% FCS, β -mercaptoethanol and Kanmycin (Gibco; Invitrogen) and again counted as described above.

3.1.3 TECs purity

75 μ l of total cells obtained are used to check the purity.

The 75 μ l of solution are brought to 1ml with PBS + 2% FBS. To the tube are added directly the two antibodies:

EpCam Alexa 647(1:2000) (Product Number:118211 BioLegend)

CD45 Alexa 700 (1:20) (Product Number:103127 BioLegend)

The solution is incubated 15' a 4°C, then centrifugated and resuspended in 300 μ l of PBS + 2% FBS. A filtration is performed through a 45 μ m strainer attached to a 2,5 ml syringe and then 100 μ l of DAPI (Product Number:422801 BioLegend) are added and all is acquired at FACS Aria.



Fig.28 FACS Aria used for FACS analysis.

TECs purity usually goes from 20% to 30% of total cells obtained.

3.1.4 Culture medium and supplements

TEC were cultured in CnT-57 cell culture medium (CELLnTEC, Bern, Switzerland). CnT-57 is a progenitor cell target liquid culture medium with low calcium concentration (0.07mM) and low concentrated Bovine Pituitary extract (BPE) (6 μ gr/ml). CnT-57 is a protein free medium containing a variety of amino acids, minerals, vitamins and other factors such as Fibroblast Grow Factor (FGF), Epidermal Growth Factor (EGF), and Insulin.

Additionally, the culture medium was supplemented with 10nM dihydrochloride monohydrate, a cell permeable anti-apoptotic selective Rho-associated Kinase (ROCK) Inhibitor (10nM; Calbiochem, Merk) to enhance viability. Kanamycin was supplemented to the medium to reduced potential hazard of contamination.

3.2 DNA Quantification

Samples were dried onto sterile paper and weighted. Samples were then frozen at -20°C.

The day before the analysis, samples were put in a solution of Proteinase K at 56°C, until complete digestion. Usually overnight is enough to digest the entire sample.

This lysis solution contains:

Proteinase K: 1mg/ml in 50mM Tris pH 7.6 (SIGMA-ALDRICH Product Number:P2308)

Pepstatin A: (SIGMA-ALDRICH Product Number:P5318)

EDTA 100mM+Iodoacetamide 100mM (Siegfried)

TRIS: (SIGMA-ALDRICH Product Number:A5456-3)

DMSO: (FLUKA Product Number:41640)

The day after the digestion:

Thaw the CyQUANT® Cell Proliferation Assay Kit (Invitrogen Product Number:C7026)

a. Preparation of the working buffer

- Dilute Component B (20x): 20 ml = 1 ml Component B + 19 ml H₂O

- Add Component A (400x) to the same tube 50 µl / 20ml

The component A is light sensitive so you have to wrap the tube in an aluminum sheet

b. Preparation of DNA working solution

- Bovine DNA: Stock solution 10 µg/ml

- DNA working solution : 1 $\mu\text{g/ml}$ Dilution 1/10

c. Preparation of the standards

For each standard we need: 3 x 200 μl so we prepare 640 μl

d. Preparation of the standard curve: (use the black plates)

Each standard will be done in triplicate: Pipette 200 μl /well for each standard

e. Preparation of the samples

Dilution 1/200: 5 μl sample directly to the well

+ 195 μl working Buffer directly to the well

When all the samples are pipetted, cover the plate with an aluminium paper

f. Reading of the values

Use the Perking Elmer HTS 700 apparatus, and a protocol with a wavelength of 480/520nm.

Results were normalized for the weight, and compared using the bar graph.

3.3 SEM Analysis

Samples were fixed and dehydrated following this sequence:

- Rinse in PBS for 10 min
- Formaldehyde 4% overnight 4 ° C
- 2X rinse in PBS for 10 min
- 3X 20 min 30% Ethanol
- 3X 20 min 50% Ethanol
- 3X 20 min 70% Ethanol
- 3X 20 min 90% Ethanol

Tissues were transferred to 100% ethanol, subjected to Critical Point Drying, and covered with gold particles.

3.4 Istochemistry

3.4.1 Hematoxylin and Eosin Staining

Samples were fixed by immersion with Paraformaldehyde 4% for 12 hours at 4°C, and then put in Sucrose(Sigma Aldrich Product Number:

S7903) 30% in Milli Q water.

After that, samples were put in the embedding machine for the alcohol dehydration and the final step in liquid paraffin at 60°C.

When samples were in liquid paraffin, were embedded and then cut with the microtome in slides of 6µm using polylysinate glasses.

Then slides were dried at 37°C overnight and put in the staining machine.

The staining includes these phases:

- Ultraclear 90s (Biosystem Product Number:41-5213-00)
- Ultraclear 90s
- Ultraclear 90s
- Ethanol 100% 90s
- Ethanol 100% 90s
- Ethanol 96% 90s
- Ethanol 70% 90s
- Ethanol 50% 90s
- H2O distilled 90s
- HE mayer 90s (Biosystem Product Number:38-7010-00)

- HE mayer 90s
- HE mayer 90s
- H2O tap 90s
- HCl -Alcohol 0.2% 90s
- H2O tap + NH4 90s
- Eosin 0.2% 90s (Biosystem Product Number:38-7410-00)
- Eosin 0.2% 90 s
- Eosin 0.2% 90s
- Ethanol 96% 90s
- Ethanol 96% 90s
- Ethanol 100% 90s
- Ultraclear 90s
- Ultraclear 90s
- Ultraclear 90s

Slides were mounted with Mounting medium (Pertex Product Number:41-4012-00), and acquired at different magnification with an Olympus DP80 light microscope.

3.4.2 Immunohistochemistry

The immunoistochemistry it has been used to evaluate the presence of specific proteins in tissues analyzed:

Antibody anti-Collagen type IV (AbCam Product Number:ab6586)

Antibody anti-Fibronectin (AbCam Product Number:ab2413)

- Ultraclear 10m (Biosystem Product Number:41-5213-00)
- Ultraclear 10m
- Ethanol 100% 5m
- Ethanol 95% 1m
- Ethanol 70% 1m
- Ethanol 35% 1m
- Rinse with buffer TBS 1X 1m
- Rinse with buffer TBS 1X 1m
- HEAT MEDIATED ANTIGEN RETRIEVAL
 - Retrieval solution (Dako Product Number:S1700) 10m at 95°C
 - Let it cool down for 10-15m
 - Rinse with buffer TBS 1X 5m
 - Rinse with buffer TBS 1X 5m
- BLOCKING
 - Goat serum (Invitrogen Product Number:16210-064) 10m
 - Rinse with buffer TBS 1X 5m
- Primary antibody diluted in TBS 1%BSA overnight at 4°C
- Rinse with buffer TBS 1X 5m
- Rinse with buffer TBS 1X 5m
- Secondary antibody diluted in TBS 1%BSA 1:200 45m (polyclonal Goat anti Rabbit Immunoglobulins/HRP E0432)
- Rinse with buffer TBS 1X 5m
- Rinse with buffer TBS 1X 5m
- DAB 5 m (1 tablet in 15ml of TBS1X plus 12 µl of 30% H2O2)
(Sigma Aldrich Product Number:D5905)

- Rinse with buffer TBS 1X 5m
- Rinse with buffer TBS 1X 5m
- Rinse with tap water 1m
- Hematoxylin 20s
- Rinse with tap water 1m
- Ethanol 96% 90s
- Ethanol 96% 90s
- Ethanol 100% 90s
- Ultraclear 90s
- Ultraclear 90s
- Ultraclear 90s

Slides were mounted with Mounting medium (Pertex Product Number:41-4012-00), and acquired at different magnification with an Olympus DP80 light microscope.

Antibody anti-Laminin (AbCam Product Number:ab128053)

- Ultraclear 10m (Biosystem Product Number:41-5213-00)
- Ultraclear 10m
- Ethanol 100% 5m
- Ethanol 95% 1m
- Ethanol 70% 1m
- Ethanol 35% 1m
- Rinse with buffer TBS 1X 1m
- Rinse with buffer TBS 1X 1m
- ENZYMATIC DIGESTION

- Trypsin 0,1% in TBS (Gibco Product Number:15090-046)
- BLOCKING
 - Goat serum (Invitrogen Product Number:16210-064) 10m
 - Rinse with buffer TBS 1X 5m
- Primary antibody diluted in TBS 1%BSA overnight at 4°C
- Rinse with buffer TBS 1X 5m
- Rinse with buffer TBS 1X 5m
- Secondary antibody diluted in TBS 1%BSA 1:200 45m (polyclonal Goat anti Rabbit Immunoglobulins/biotinylated E0432)
- Rinse with buffer TBS 1X 5m
- Rinse with buffer TBS 1X 5m
- Vectastain ABC/AP kit (Linaris Product Number:AK-5000) 45 m in a humid chamber
- Rinse with buffer TBS 1X 5m
- Rinse with buffer TBS 1X 5m
- Vector Red AP substrate + Levamisole (Linaris Product Number: SK-5100)
- Rinse with buffer TBS 1X 1m
- Rinse with tap water 1m
- Hematoxylin 20s
- Rinse with tap water 1m
- Ethanol 96% 90s
- Ethanol 96% 90s
- Ethanol 100% 90s
- Ultraclear 90s

- Ultraclear 90s
- Ultraclear 90s

Slides were mounted with Mounting medium (Pertex Product Number:41-4012-00), and acquired at different magnification with an Olympus DP80 light microscope.

3.5 Reagent for the decellularization process

- Triton X-100 (Sigma Aldrich Product Number:T8532)
- Sodium Deoxycholat (Sigma Aldrich Product Number:30970)
- DNase I from Bovine Pancreas (Sigma Aldrich Product Number:D4263)

3.6 MTT assay

The yellow tetrazolium salt (MTT) (Sigma Aldrich Product Number: M5655) is reduced in metabolically active cells to form insoluble purple formazan crystal, which are solubilized by the addition of a detergent.

1. Weight 12.5 mg
2. Dilute it in 25 mL culture medium w/o phenol red.
3. Filter sterilize = *MTT stock solution (0.5mg/ml)*, storage in the freezer
4. Dilute 1/10 of MTT stock solution with culture medium w/o phenol red = *MTT working solution (0.05mg/ml=50ug/ml)*
5. Remove culture medium from your wells
6. Rinse with PBS
7. Add *MTT working solution* (to cover the sample)
8. Keep in incubator for about 2 hours
9. Remove *MTT working solution*
10. Rinse with PBS
11. Look at the distribution of the cells in the scaffold

3.7 Scaffold preparation

- Dry the scaffold on paper to let it dry for the disruption
- The scaffold is put into cryovial with metal beads inside given with the machine itself (Mikro-Dismembrator).
- The vials were freezed in dry ice to let the scaffold hard and more easy to disrupt
- After 10 minutes the vials were transferred into the Mikro-Dismembrator S
- The scaffold were disrupted at 3000 rpm for 1 minute.
- the product of dismembration is a powder that is subsequently dissolved in 200 µl per thymus of MilliQ water
- 50 µl of the solution are distributed for each well of 96 well
- the 96 well is directly freezed at -20°C
- after 2 hours the weel is transferred into the lhyophilizator
- it is set at a pressure of 0.0030mbar and a temperature of -50°C
- the sample are left overnight for drying

4. RESULTS AND DISCUSSION

4.1 STUDY OF A PROTOCOL FOR THYMUS DECELLULARIZATION

To obtain an efficient protocol to decellularized the murine thymus, I started to apply a protocol, previously developed for the rat thyroid. It consists of different steps, detailed in the table below.

Freze and thaw	
Trypsin 0.05%	30 minutes at 37°C
Triton X-100 3%	48 hours
Deoxycholic acid 4%	24 hours
PBS	30 minutes at 4°C
Peracetic acid 0.1 %	3 hours at RT
PBS	48 hours

Table 1. protocol of thyroid decellularization applied to mouse thymus

The obtained matrices were analyzed to determine the extent of decellularization, if the cellular material had been thoroughly removed and wheter or not the scaffold tissue was damaged. For this purpose Haematoxylin and Eosin (H&E) staining and SEM analysis were performed.

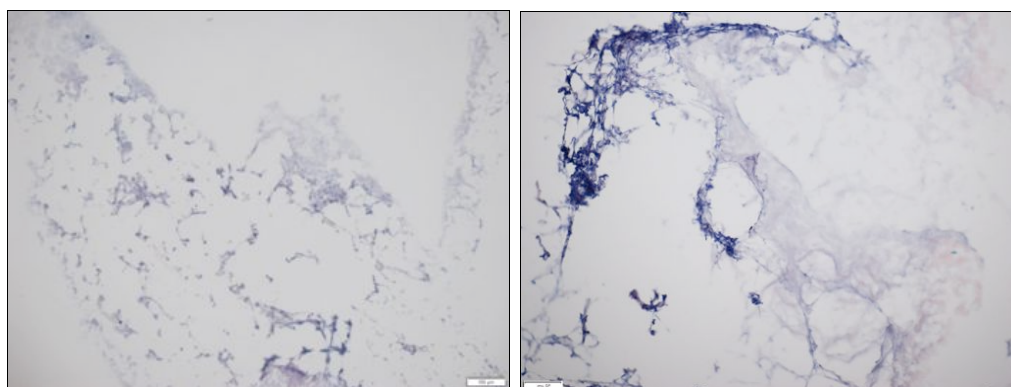


Fig.29 H&E staining of decellularized thymus at 10X and 20X of magnification

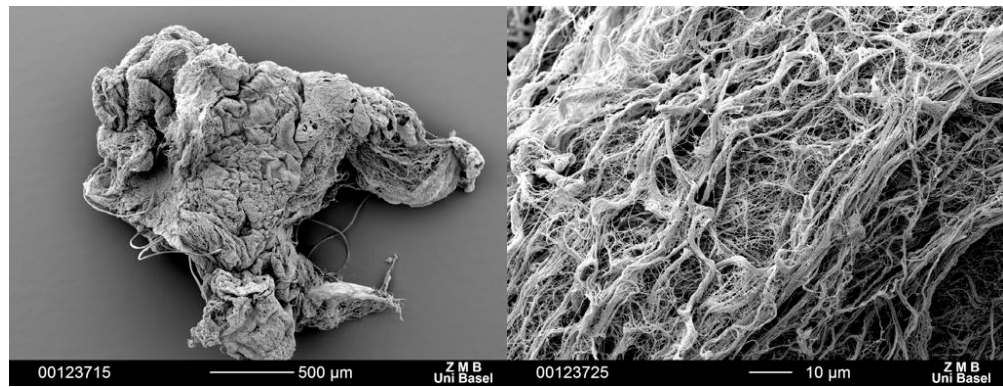


Fig.30 SEM analysis of the matrix obtained at two different magnification

These analysis showed that the protocol initially is too aggressive for the mouse thymus and it damaged the structure and the compositions of its ECM when compared to the native one.

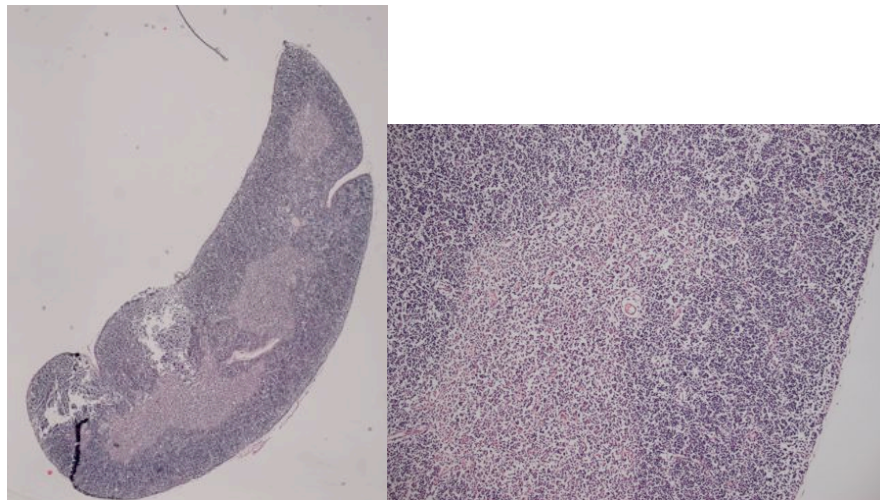


Fig.31 H&E staining of native thymus at 4X and 20X of magnification

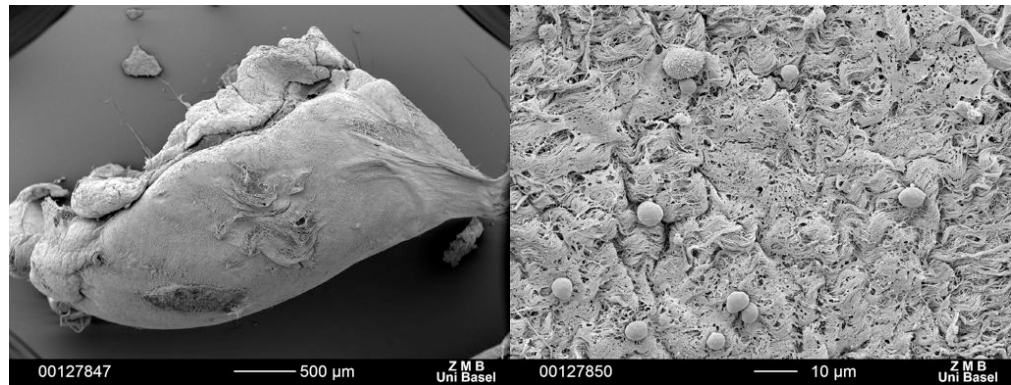


Fig.32 SEM analysis of the native thymus at two different magnification. At higher magnification is possible to see some lymphocytes on the surface of the organ itself.

Starting from this point, I've analyzed the role played by different agents used in the protocol and their activity on the mouse thymus.

Thymic matrices were decellularized using the same protocol but eliminating one by one the different solutions to evaluate the action of the different agents on the ECM.

The different agents evaluated has been: Triton X-100 3%, Deoxycholic Acid 4%, Trypsin 0,05% and 0,01%. The matrix structure was evaluated by H&E staining, SEM and DNA quantification to figure out the influence of these agents on the ECM of the thymus and its 3D structure.

In the following table is described the first modified protocol tested on the mouse thymus to evaluate the action of the Deoxycholic acid on the ECM.

Freze and thaw	
Trypsin 0.05%	30 minutes at 37°C
Deoxycholic acid 4%	24 hours
PBS	30 minutes at 4°C
Peracetic acid 0.1 %	3 hours at RT
PBS	48 hours

Table 2. Protocol of thymus decellularization without the use of Triton X-100

The matrix obtained was evaluated performing Haematoxylin and Eosin (H&E) staining and SEM analysis.

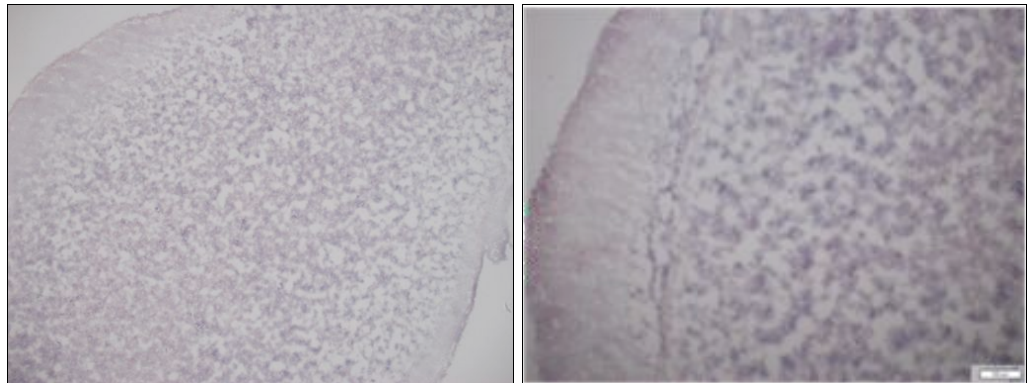


Fig.33 H&E staining of decellularized thymus without the use of the Triton X-100 at 10X and 20X of magnification

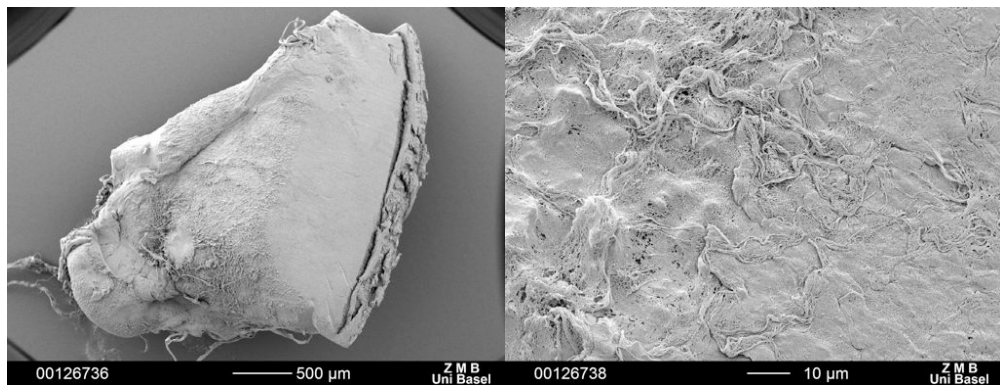


Fig.34 SEM analysis of the matrix obtained without the use of the Triton X-100 at two different magnification

In the following is described table the second modified protocol tested on the mouse thymus to evaluate the action of the Triton X-100 on the ECM.

Freze and thaw	
Trypsin 0.05%	30 minutes at 37°C
Triton X-100 3%	48 hours
PBS	30 minutes at 4°C
Peracetic acid 0.1 %	3 hours at RT
PBS	48 hours

Table 3. Protocol of thymus decellularization without the use of Deoxycholic Acid

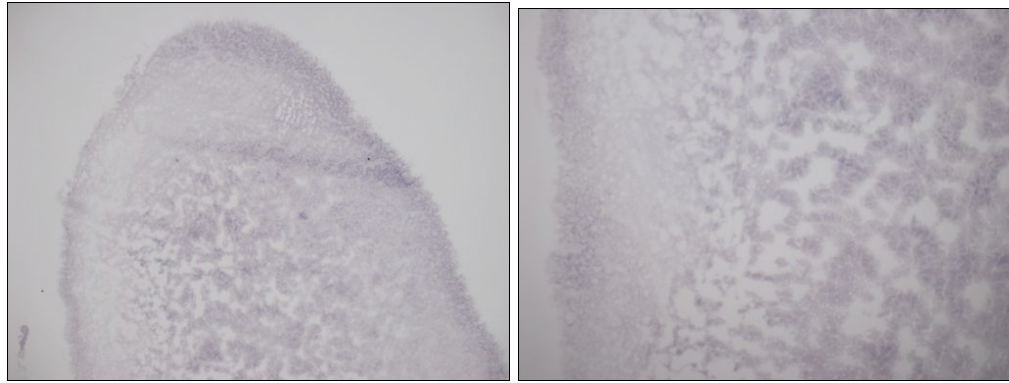


Fig.35 H&E staining of decellularized thymus without the use of the Deoxycholic acid at 10X and 20X of magnification

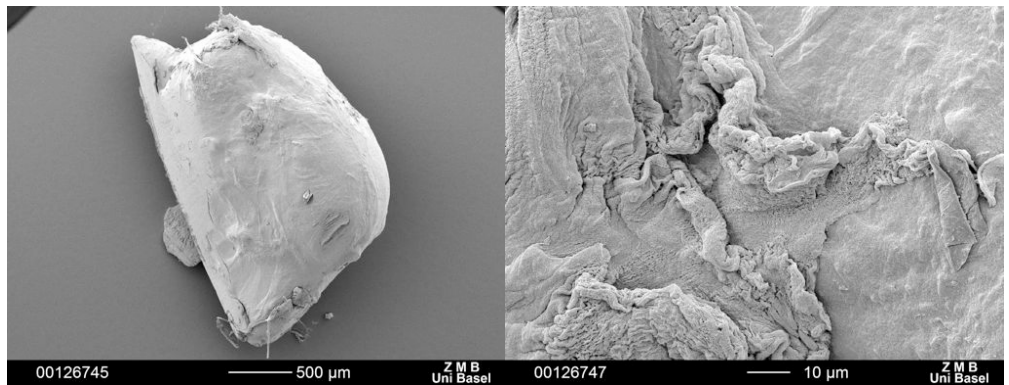


Fig.36 SEM analysis of the matrix obtained without the use of the Deoxycholic acid at two different magnification

In the following table is described the third modified protocol tested on the mouse thymus to evaluate the action of the Deoxycholic acid on the ECM.

Freze and thaw	
Triton X-100 3%	48 hours
Deoxycholic acid 4%	24 hours
PBS	30 minutes at 4°C
Peracetic acid 0.1 %	3 hours at RT
PBS	48 hours

Table 4. Protocol of thymus decellularization without the use of Trypsin

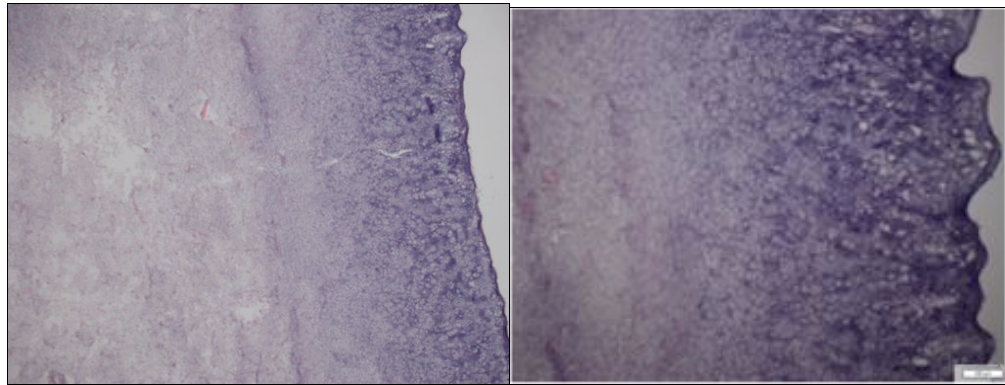


Fig.37 H&E staining of decellularized thymus without the use of the Trypsin at 20X of magnification

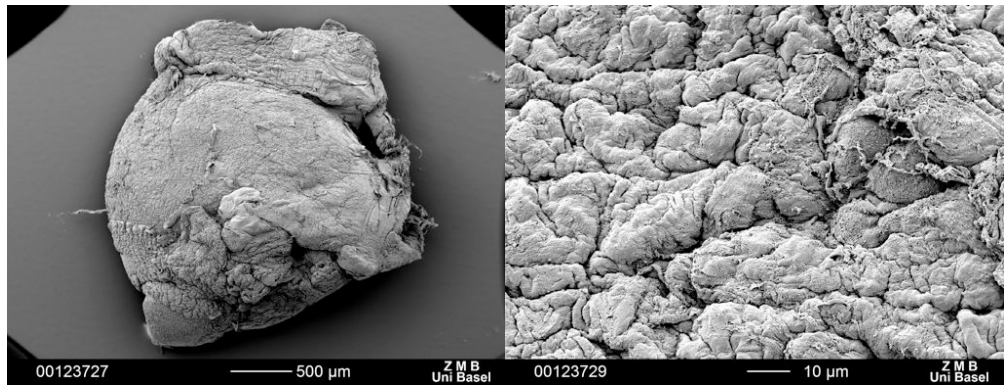


Fig.38 SEM analysis of the matrix obtained without the use of the Trypsin at two different magnification

Freze and thaw	
Trypsin 0.01%	30 minutes at 37°C
Triton X-100 3%	48 hours
Deoxycholic acid 4%	24 hours
PBS	30 minutes at 4°C
Peracetic acid 0.1 %	3 hours at RT
PBS	48 hours

Table 5. Protocol of thymus decellularization with Trypsin diluted at 0,01%

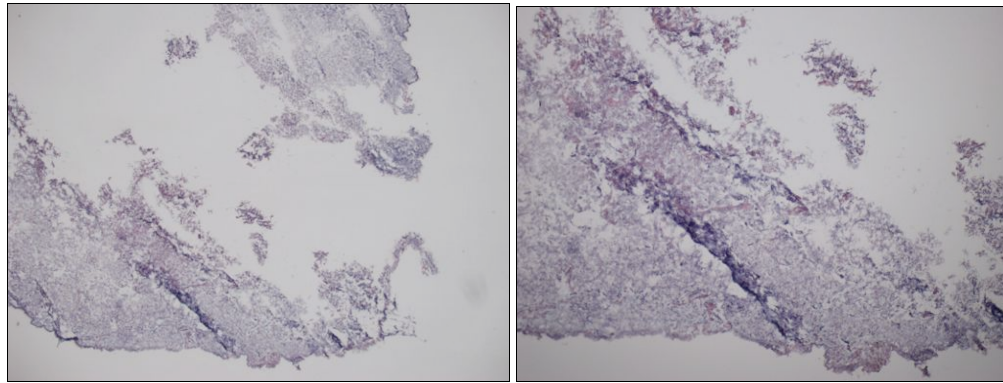


Fig.39 H&E staining of decellularized thymus with the use of the Trypsin 0,01% at 10X and 20X of magnification

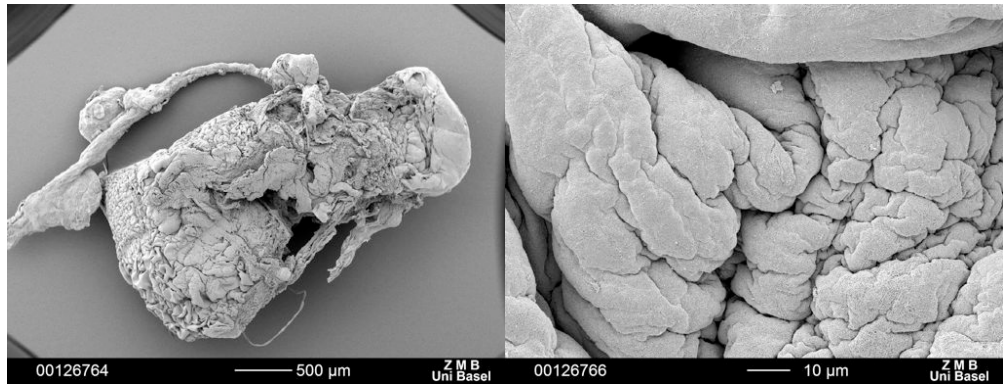


Fig.40 SEM analysis of the matrix obtained with the use of the Trypsin 0,01% at two different magnification

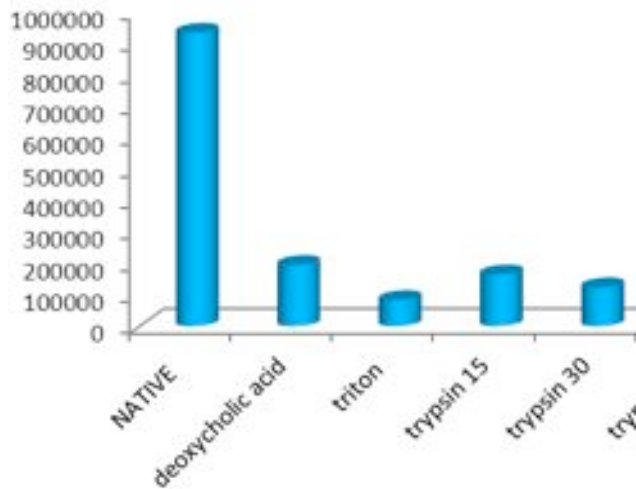


FIG.41 DNA quantification of decellularized thymi in absolute value.

Although the different solutions analyzed proved to be adequate to efficiently decellularize the thymic matrix, nevertheless they resulted too

aggressive for maintenance of its 3D structure, and basic ECM components. In addition, using H&E a violet staining meaning was sometimes detected, indicating presence of cellular debris and nucleic acids, able to bind to the hematoxylin. In particular, trypsin either at 0,05% or 0,01% was able to destroy both the cells and ECM, as a consequence of the low protein amount present in the mouse thymus. In addition, Triton X-100 and Deoxycolic acid resulted inadequate to efficiently clean the ECM from cell fragments and DNA contamination, although delicate enough to reasonably preserve the native structure of the thymus matrix.

I, therefore, proceeded to modify the original protocol by adding MilliQ water and DNase, based on protocols previously established with other organ like trachea [131], with the aim of preserving the ECM structure and, at the same time to improve its cleaning from contaminating cellular residues.

MilliQ water was chosen for its ability to induce an osmotic stress to cells, and to eliminate them as floating fragments, as a result of the shaker movements forcing cellular membranes to pass from the organ into the solution.

DNase was chosen for its ability to degrade DNA. It was used at the end of the decellularization process, to digest the DNA remained into the matrix without damaging the ECM.

The new protocols tested are listed in the table below.

	<i>Protocol A</i>	<i>Protocol B</i>	<i>Protocol C</i>	<i>Protocol D</i>
MilliQ water 72 hours at 4°C	√	√	√	√ x 2 cycles
Triton X-100 3% 12 hours at RT	√	√		
Deoxycholic acid 4% at RT		√ 24 hours	√ 4 hours	√ 4 hours x 2 cycles
DNAse 3hours at RT	√	√	√	√ x 2 cycles

Table 5. Scheme of different protocols used for thymus decellularization

An Haematoxylin and Eosin (H&E) staining and SEM analysis were performed to analyse resulting scaffold tissues obtained. They are showed in pictures below.

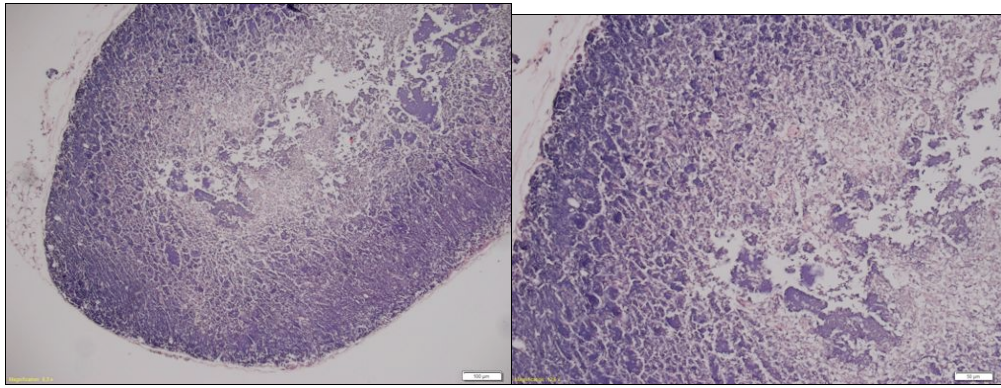


Fig.42 H&E staining of decellularized thymus with the protocol A at 10X and 20X of magnification

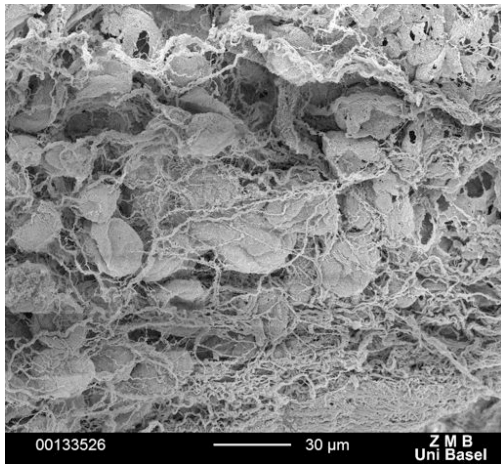
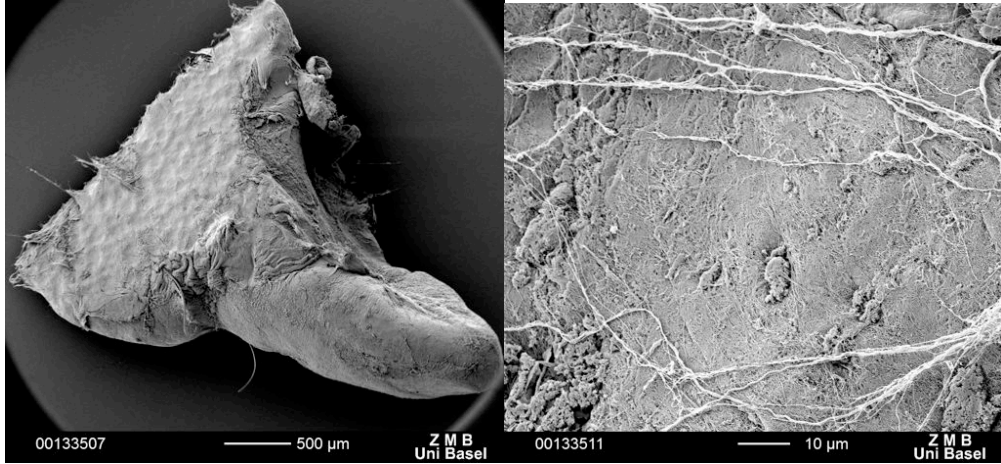


Fig.42 SEM analysis of the matrix obtained with the protocol A at two different magnification

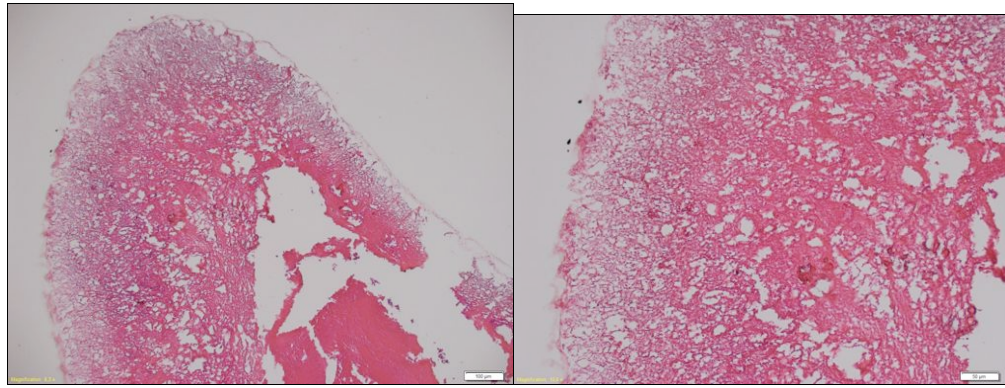


Fig.43 H&E staining of decellularized thymus with the use of the protocol D at 10X and 20X of magnification

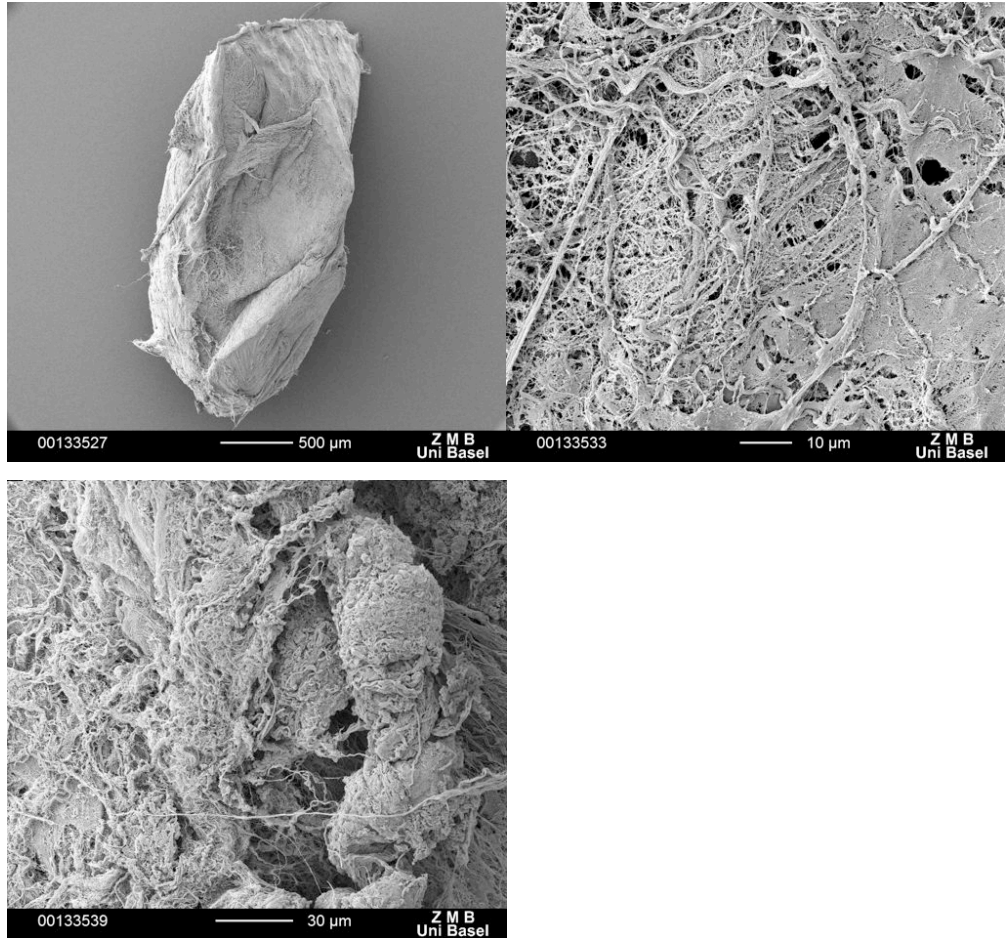


Fig.44 SEM analysis of surface and the inner part of the matrix obtained with the use of the protocol B at two different magnification.

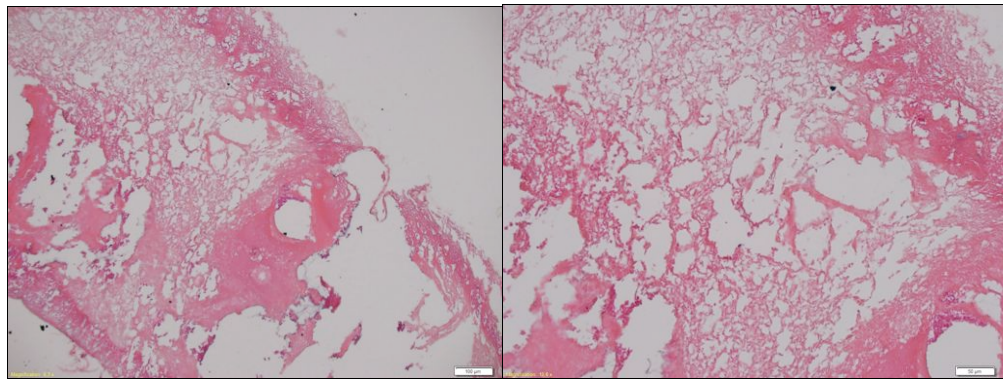


Fig.45 H&E staining of decellularized thymus with the use of the protocol C at 10X and 20X of magnification

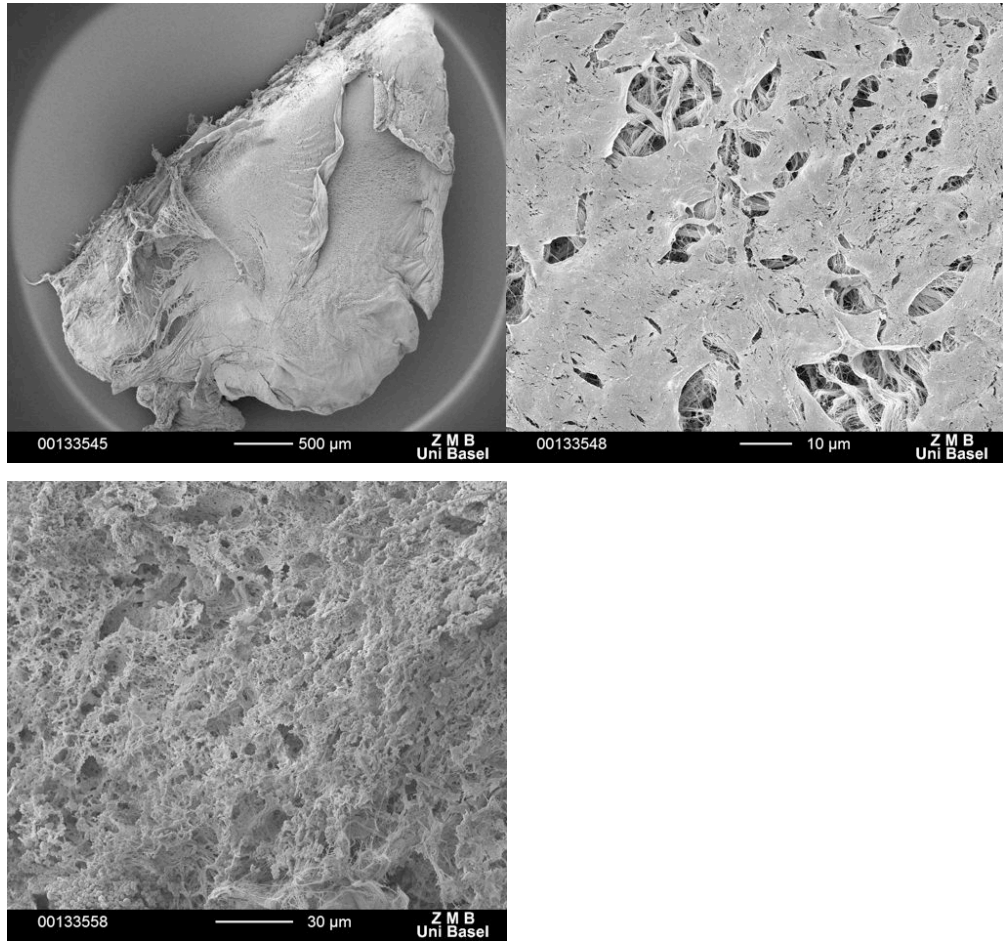


Fig.46 SEM analysis of the surface and the inner part of the matrix obtained with the protocol C at two different magnification

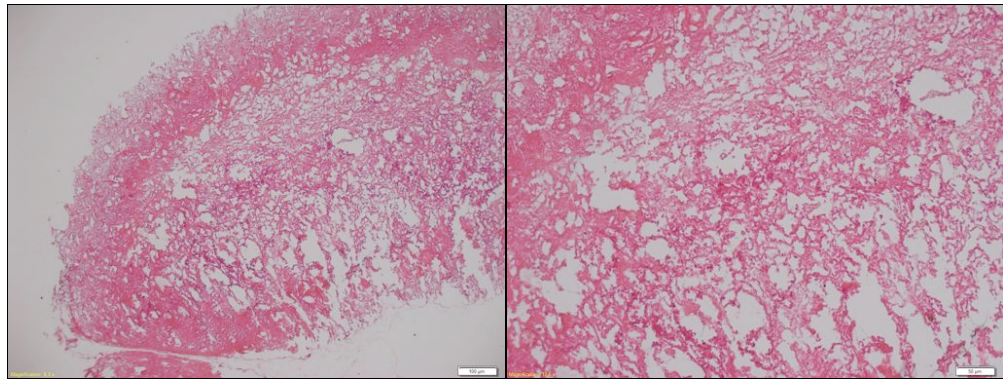


Fig.47 H&E staining of decellularized thymus with the the protocol D at 10X and 20X of magnification

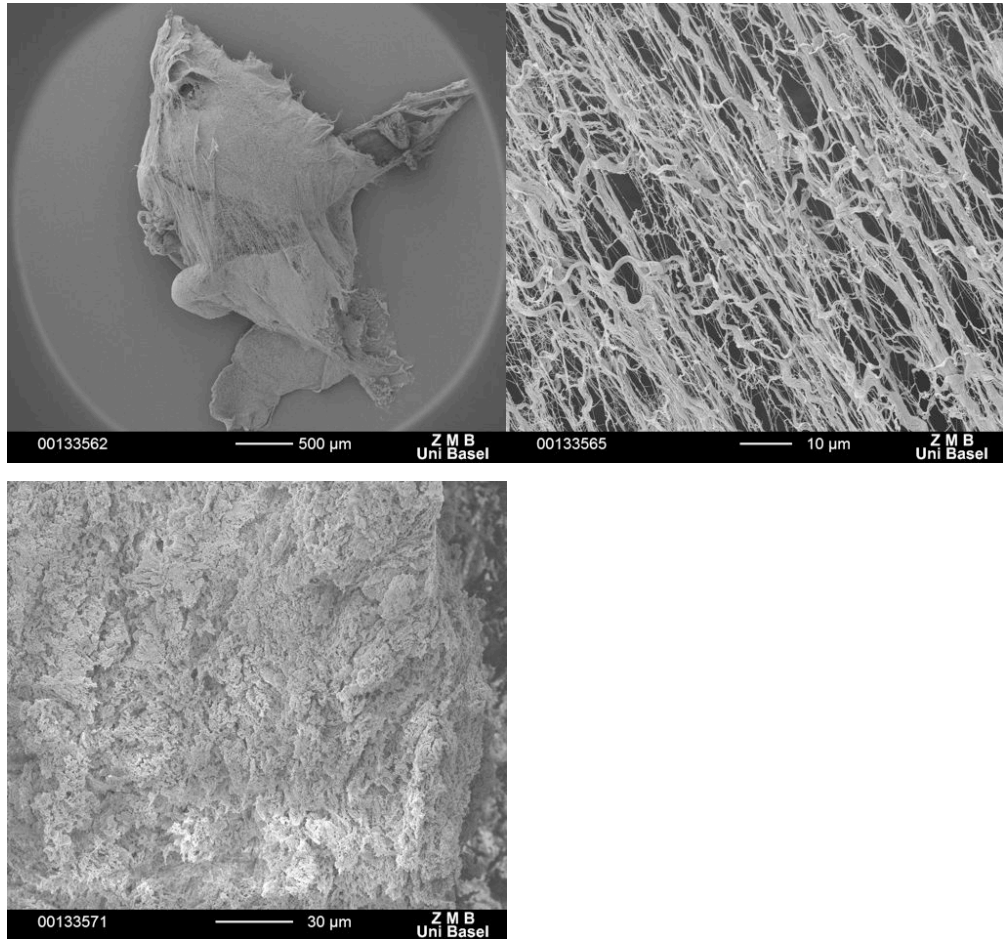


Fig.48 SEM analysis of the surface and the inner part of the matrix obtained with the protocol D at two different magnification.

A DNA quantification was performed to evaluate the remaining cellular material in resulting scaffolds obtained.

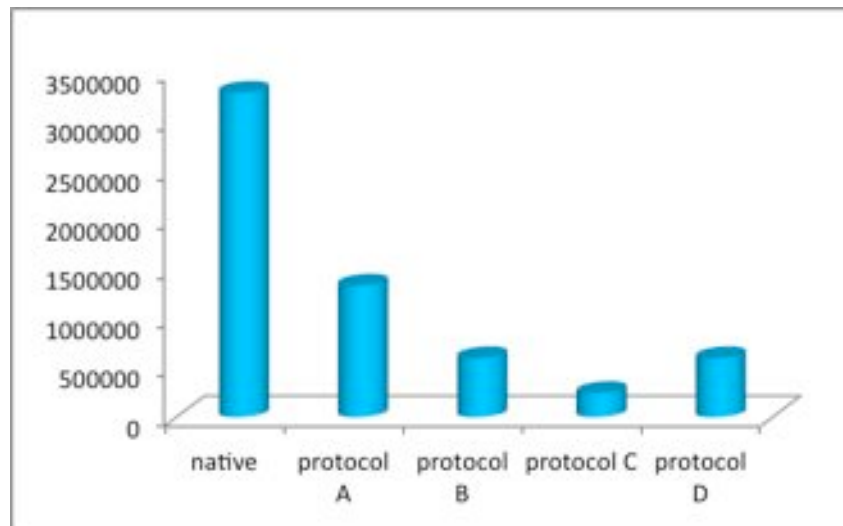


FIG.49 DNA quantification of matrices obtained in absolute value

An immunoistochemistry for the mainly ECM components of the mouse thymus, collagen IV, fibronectin and laminin, was performed to evaluate changes in ECM proteins after the different protocols used. The native mouse thymus was used like positive control.

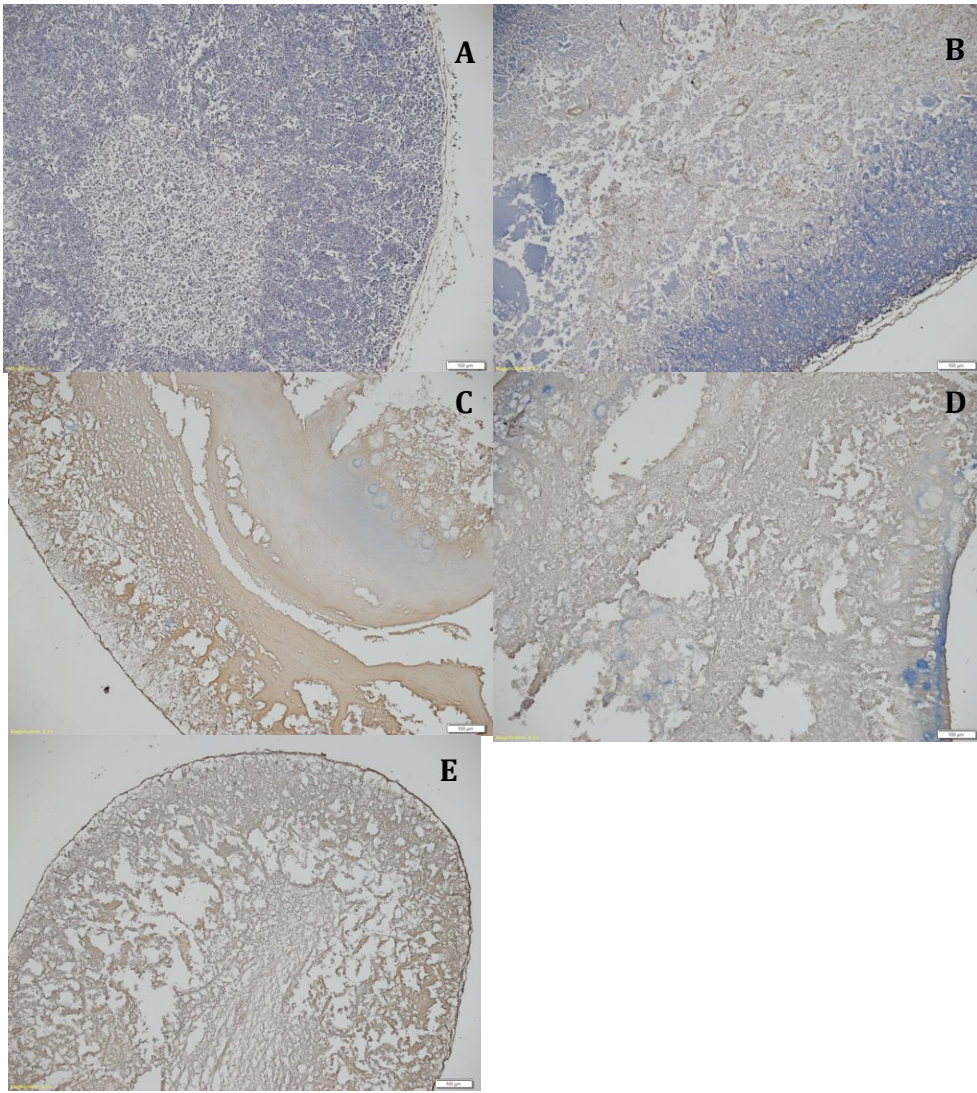


FIG.50 Immunohistochemical staining for collagen IV in native and decellularized thymi. A) native thymus; B) scaffold tissue obtained with the protocol A; C) scaffold tissue obtained with the protocol B; D) scaffold tissue obtained with the protocol C; E) scaffold tissue obtained with the protocol D.

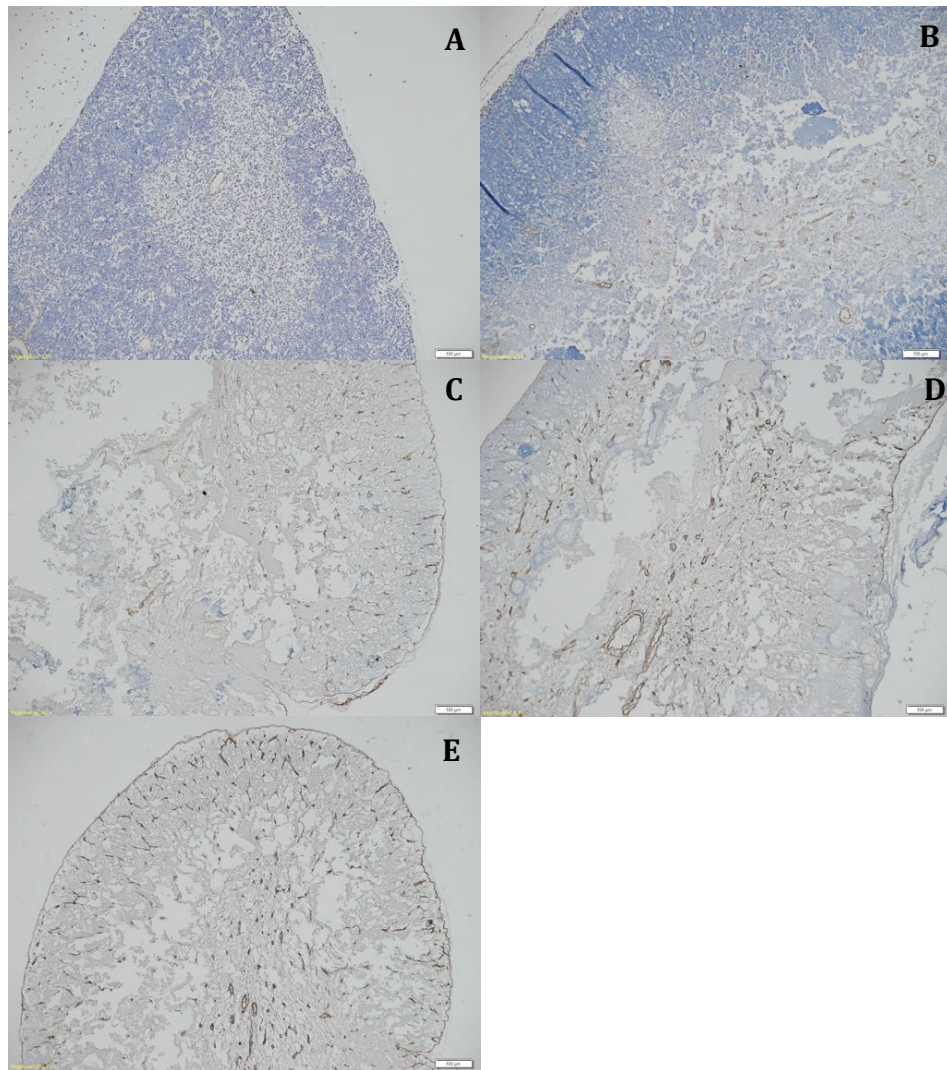


FIG.51 Immunohistochemical staining for fibronectin in native and decellularized thymi. A) native thymus; B) scaffold tissue obtained with the protocol A; C) scaffold tissue obtained with the protocol B; D) scaffold tissue obtained with the protocol C; E) scaffold tissue obtained with the protocol D.

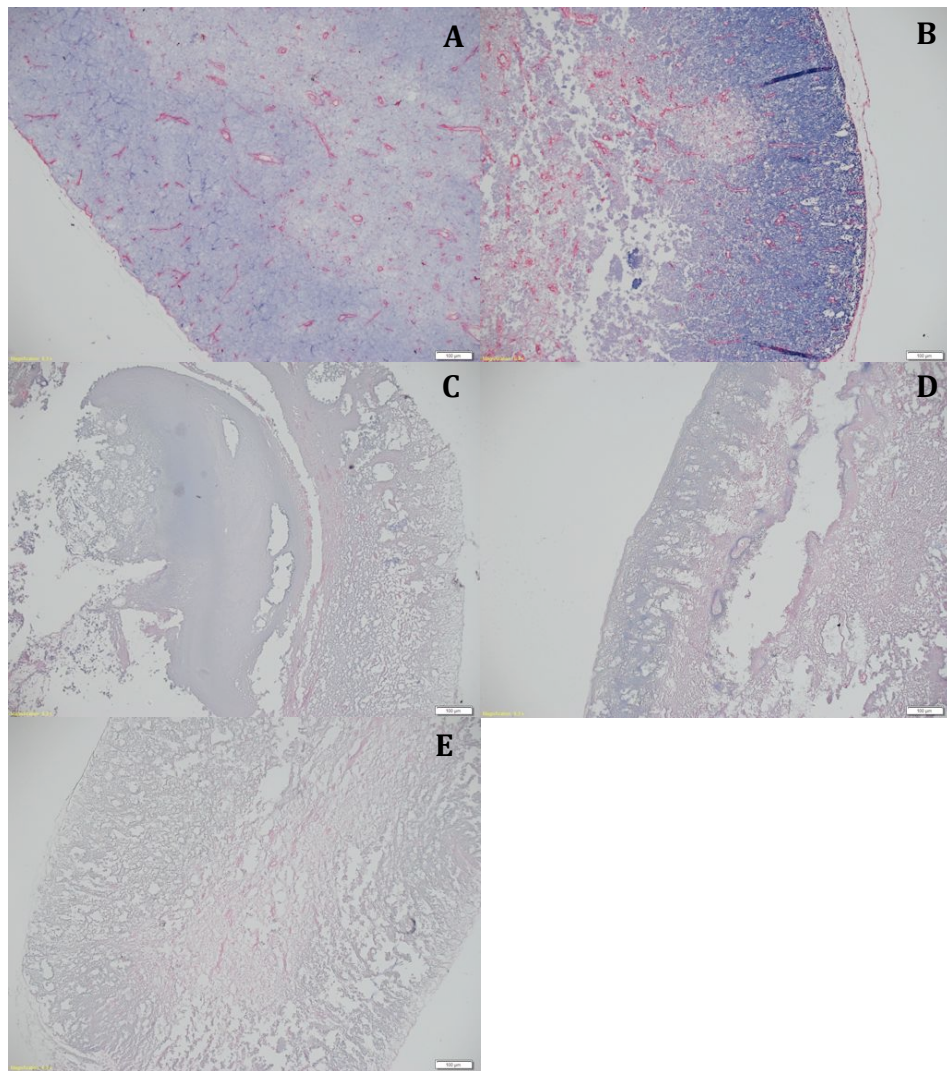


FIG.52 Immunohistochemical staining laminin in native and decellularized thymi. A) native thymus; B) scaffold tissue obtained with the protocol A; C) scaffold tissue obtained with the protocol B; D) scaffold tissue obtained with the protocol C; E) scaffold tissue obtained with the protocol D.

Using these new protocols, a better cleaning and maintenance of the 3D structure of the thymic ECM mouse was achieved.

In particular, using the protocol A, based on Triton X-100, milliQ water and DNase, I observed only a modest decrease in the quantity of cellular contamination, whereas the 3D structure of the matrix was maintained quite well. This was also confirmed by the immunohistochemical analysis, that showed presence of laminin,

collagen IV and fibronectin in distribution consistent with that of the native control tissue.

In contrast, using protocol B based on addition of Deoxycholic Acid, the quantity of DNA decreased in a significant manner, while no changes occurred to the 3D matrix structure. Specifically, using both H&E staining at light microscopic level, and SEM I noticed that the 3D structure of the thymic matrix was reasonably preserved, although some holes formed, possibly due to the removal of resident cells. In addition, ECM proteins were observed by immunocytochemistry in a pattern resembling that of protocol A, but clustered as a result of the absence in resident cells. Collectively, these results suggested that protocol B could provide a good scaffold system for homing and proliferation of seeded TEC.

Using protocol C, in which the Deoxycholic Acid was applied only for 4 hours, no changes in the 3D matrix structure were observed. However, an improvement in the size of the pores occurred, suggesting that the Deoxycholic Acid was able to efficiently remove cells even if used for a short time. In addition, the amount of DNA decreased to a reasonable extent, suggesting a primary decellularizing role for the Deoxycholic Acid. Finally, no relevant changes were found in the amount of ECM proteins.

At variance with previous protocols, using protocol D I found differences in DNA quantity, matrix size, and ECM components. Specifically, the amount of DNA was increased compared to protocol C, a reduction in matrix size occurred, likely depending on the osmotic action of MilliQ water, and the long time of shaking as well, whereas a reduction in fibronectin staining was equally apparent.

In summary, the best protocols proved to be B and C, able to guarantee a very little amount of contaminating DNA, while maintaining the native 3D matrix structure, and protein compositions of the ECM.

4.2 ROLE OF DECELLULARIZED THYMIC MATRICES IN REGULATING THE IN VITRO BEHAVIOUR OF TEC

The decellularized, 3D thymic matrices obtained using the previously described protocol were used as natural, 3D scaffold to study the behaviour of seeded TECs.

Decellularized matrices could influence TEC by releasing different factors into the culture medium, by directing them to their 3D structure or by influencing them through the ECM composition.

Specifically, I started to evaluate the role played by decellularized matrices prepared with the protocol C, which seemed to have the best amount of ECM proteins and low quantity of DNA. To this purpose these matrices were transformed in a sort of “sponge”, as detailed in Material and Methods, and their structure analysed to define the acquired, final geometry. SEM analyses were performed on scaffold obtained and the shape of its surface and their inner parts are showed in figures below.

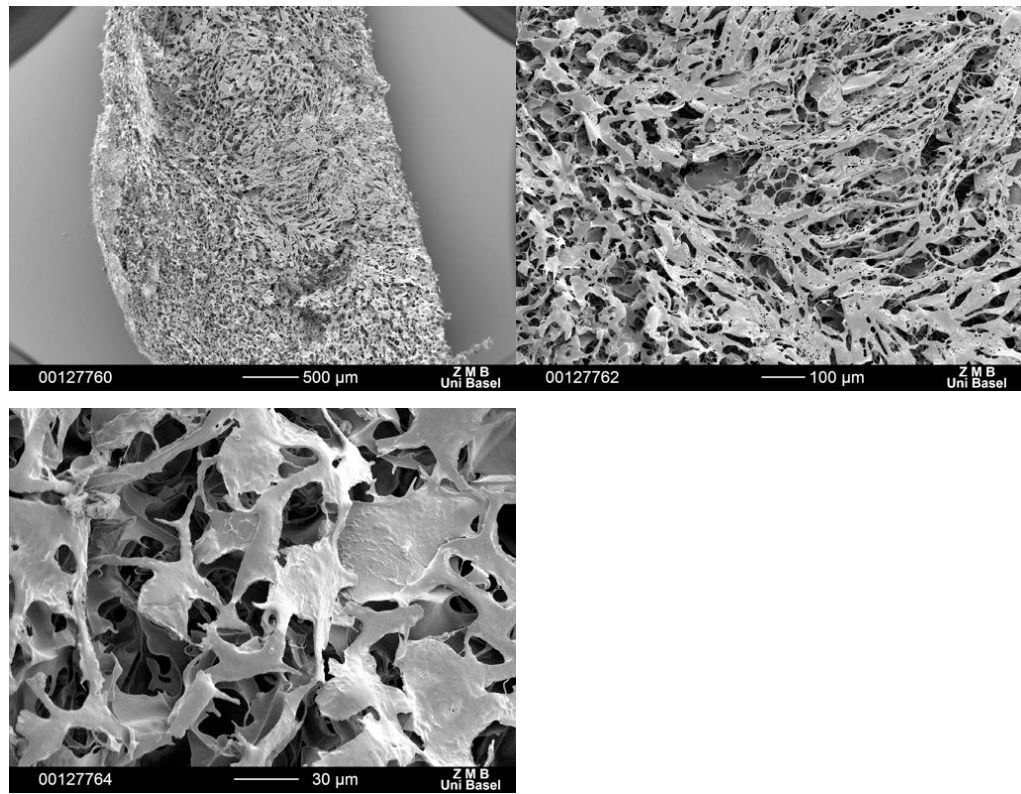


Fig.53 SEM analysis of the surface of the matrix obtained with the protocol C at two different magnification.

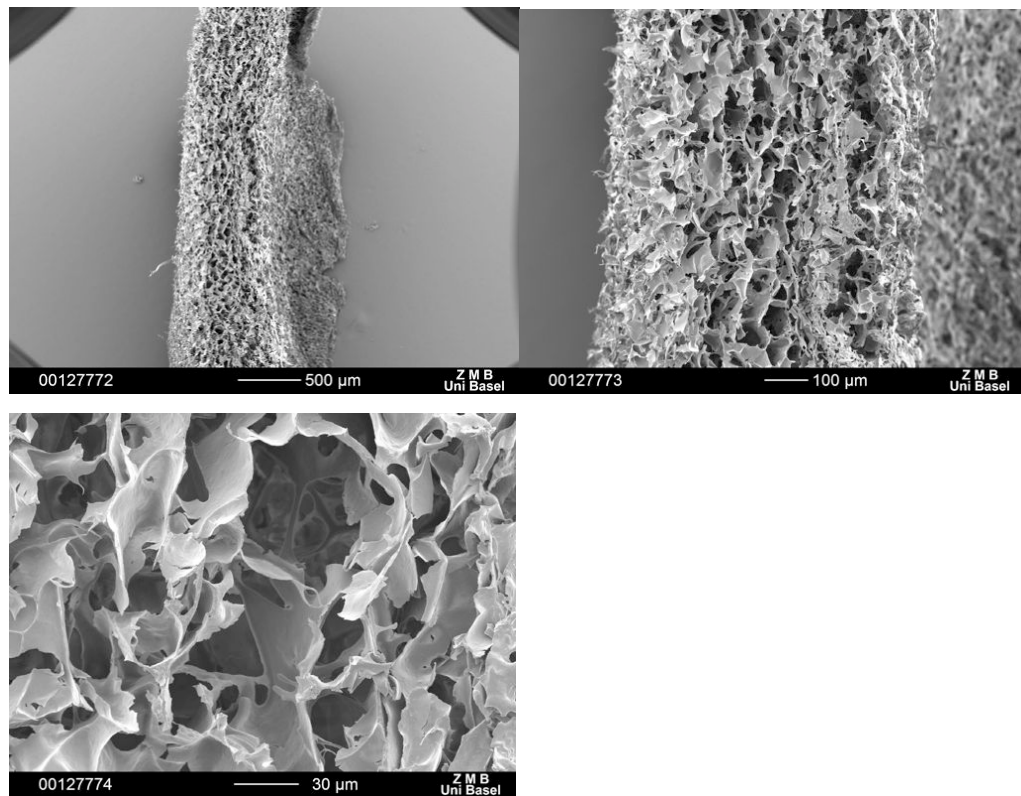


Fig.54 SEM analysis of the inner part of the matrix obtained with the protocol C at two different magnification.

Sem analyses revealed that these “3D scaffolds” had pores big enough, and with a regular distribution to ensure homing and possibly proliferation of eventually seeded TEC.

I, therefore, decided to verify whether the 3D scaffolds made with decellularized matrix might release soluble factors in the culture media able to influence the growth and the differentiation of seeded TECs.

To this aim, scaffolds were used to condition the culture media for 48 hours at 37°C. Media, then were diluted at 5% and filtered through a filter of 0,2µm to select the soluble factors released getting rid of any matrix debris.

At the same time, TECs were seeded on standard 48-well plates, at a density of 50.000 cells/well and conditioned medium was added 24 hours later the seeding, to allow attachment of seeded elements to the bottom of the plastic plate. Subsequently the medium change was done every 48 hours.

Cells were followed day by day taking pictures of them at every medium change having like positive control cells cultured with fresh media.

Pictures, taken every medium change for the positive control, are showed below.

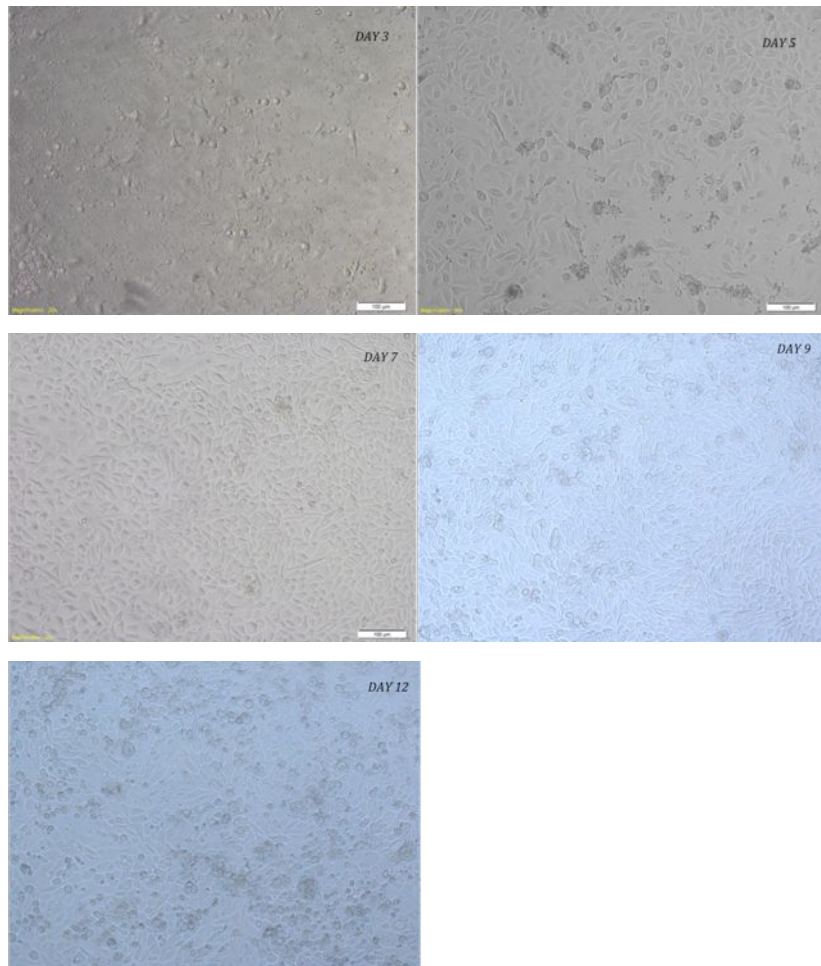


Fig.55 Pictures taken with the light microscope in the control conditon during all the culture at every medium change.

Pictures, taken every medium change for cells cultured with medium conditioned at 5%, are showed in the figure below.

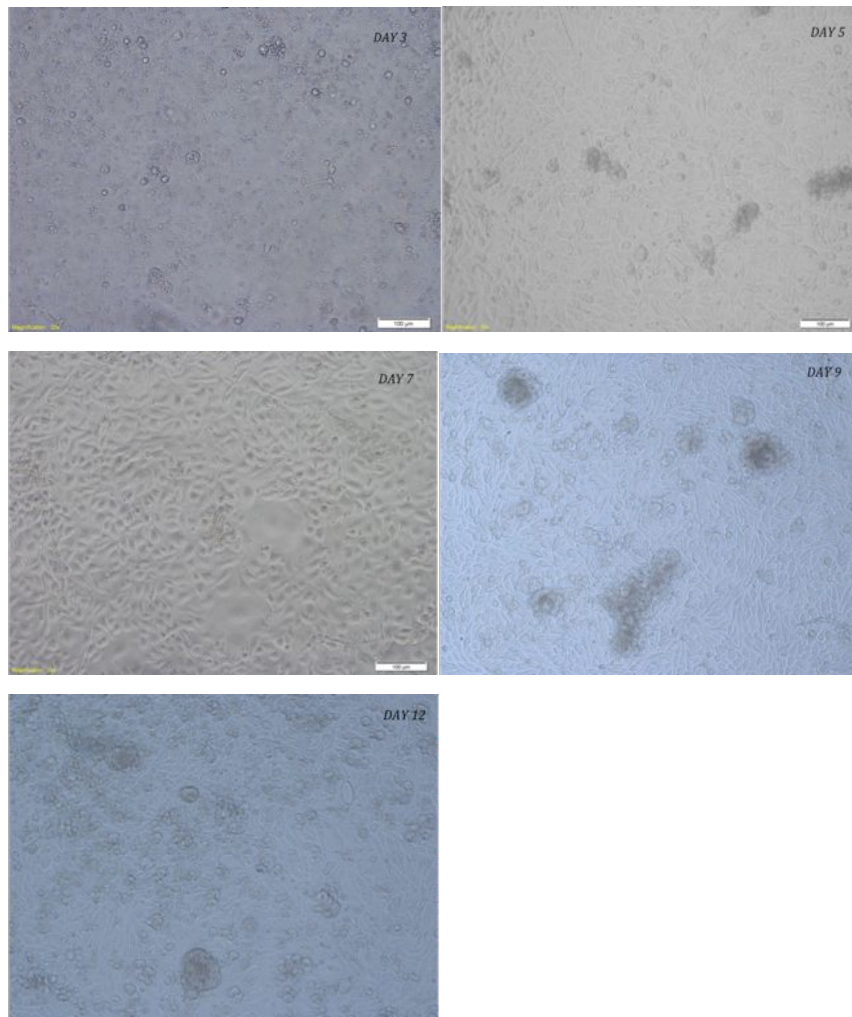


Fig.56 Pictures taken with the light microscope during all the culture, at every medium change, for the cells cultured with medium conditioned with scaffold obtained after disruption, at 5% dilution.

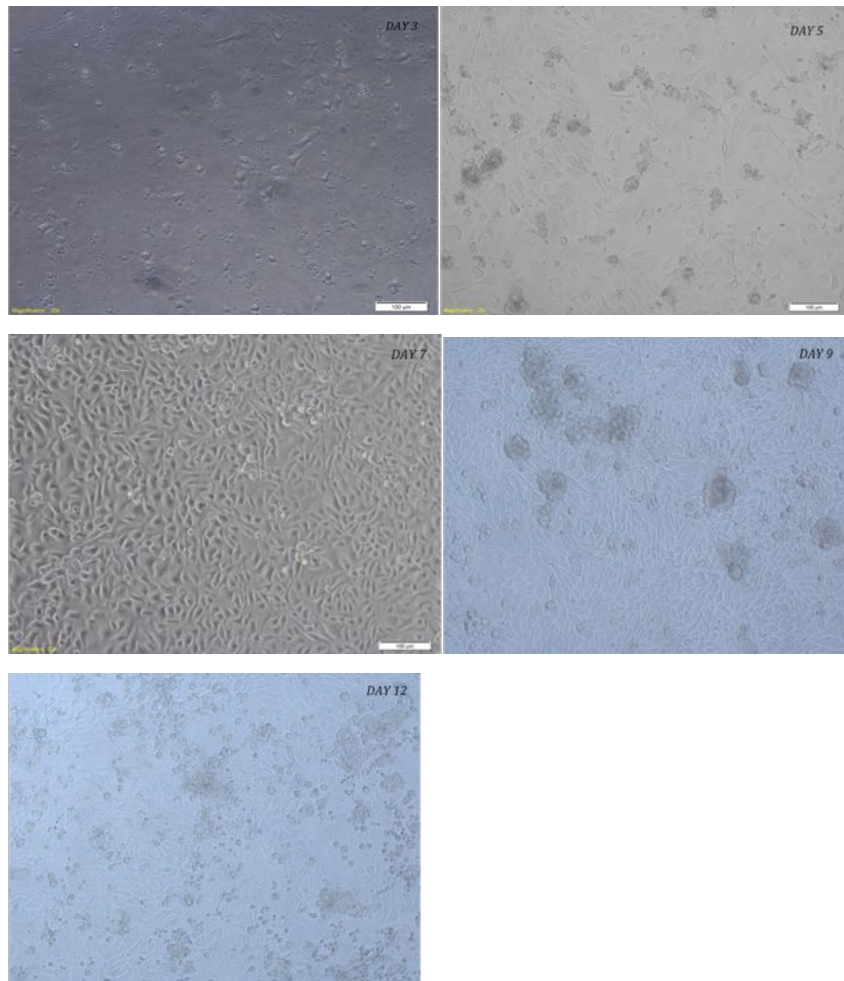


Fig.57 Pictures taken with the light microscope during all the culture, at every medium change, for the cells cultured with medium conditioned by decellularized matrix at 5% dilution.

Following initial seeding of culture cells in all conditions, I found that in the first days they were few, due to the death of differentiated cells, but from day 5 cells started to proliferate reaching confluence and cell clusters at day 9.

Their vitality and markers expression was confirmed by FACS analysis performed at day 12, underlying an expression of MHC II by TEC. FACS data are showed below for the positive control and for different culture conditions.

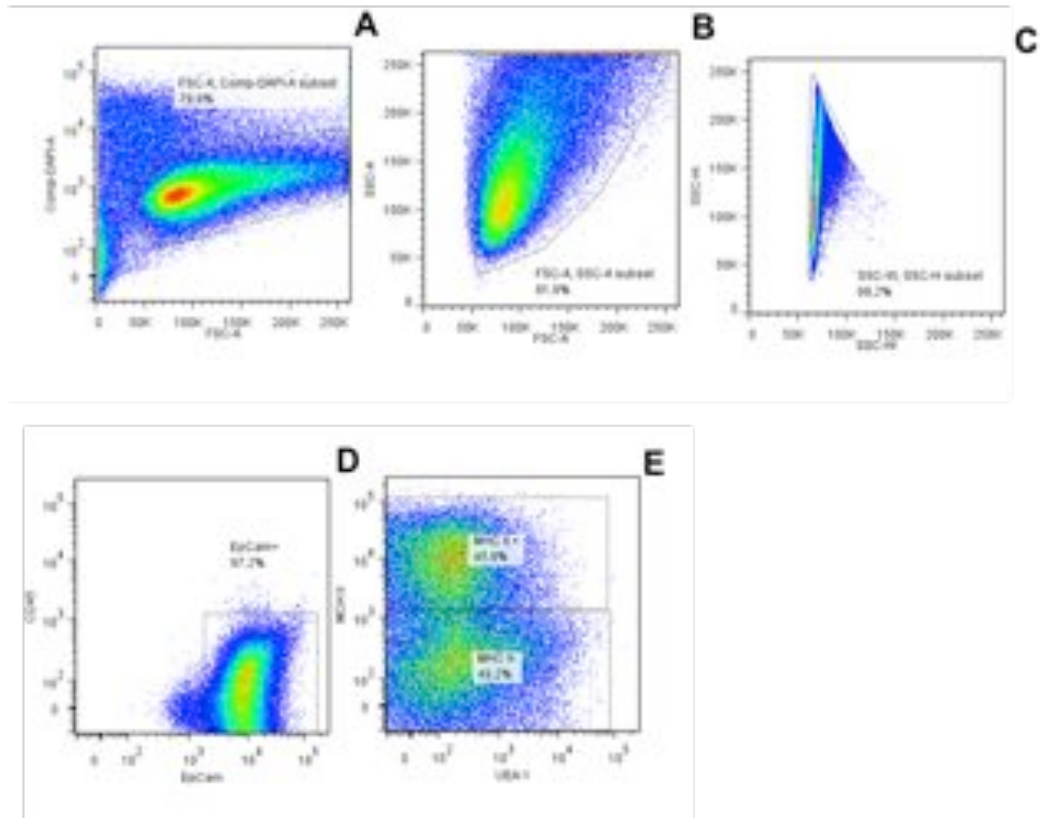


Fig.58 Cell surface marker characterization of the 2D positive control of TEC as determined by flow cytometric analysis. TEC were analyzed for: A) size; B) DAPI staining for the vitality; C) elimination of doublets; D) EpCam staining; E) MHC II staining.

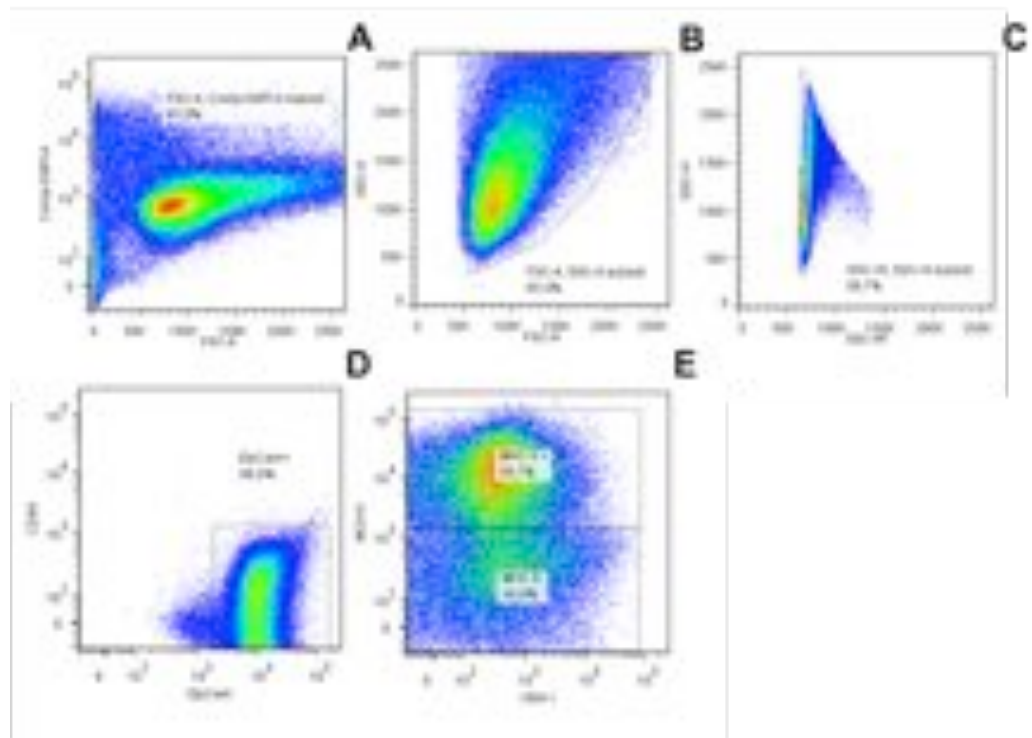


Fig.59 Cell surface marker characterization of TEC, cultured with medium conditioned with scaffold obtained after disruption of decellularized tissue, as determined by flow cytometric analysis. TEC were analyzed for: A) size; B) DAPI staining for the vitality; C) elimination of doublets; D) EpCam staining; E) MHC II staining.

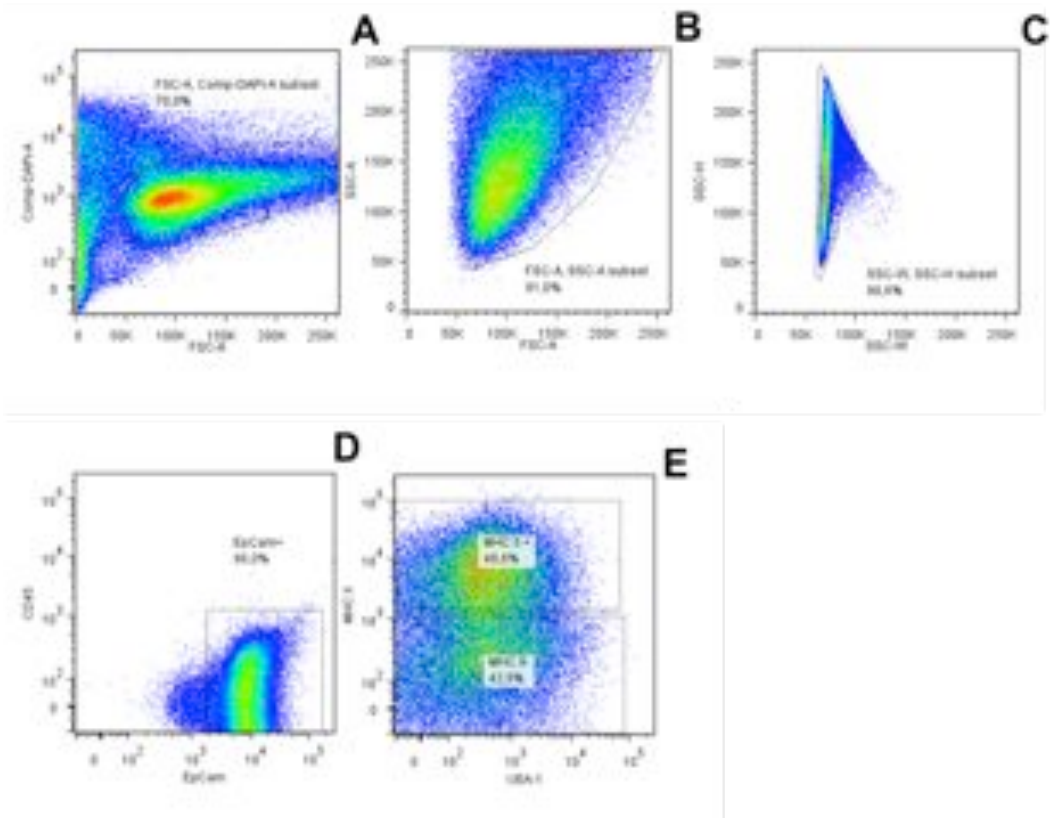


Fig.60 Cell surface marker characterization of TEC, cultured with medium conditioned with decellularized tissue, as determined by flow cytometric analysis. TEC were analyzed for: A) size; B) DAPI staining for the vitality; C) elimination of doublets; D) EpCam staining; E) MHC II staining.

In comparing cell shape, cell number and TECs marker expression, I found that only MHC II antigens resulted slightly higher in the cells treated with the conditioned medium compared to controls, suggesting a favourable effect of matrix products on TECs differentiation state.

In a following step, these culture conditions were applied to cells cultured in fibrin gel. This with the aim to determine whether the changes in the above mentioned parameters could be detected also in cells grown in a 3D environment, known to induce MHC II expression as in vivo conditions.

FACS data are showed below for two different positive controls in two different configuration (2D and 3D) and for different culture conditions.

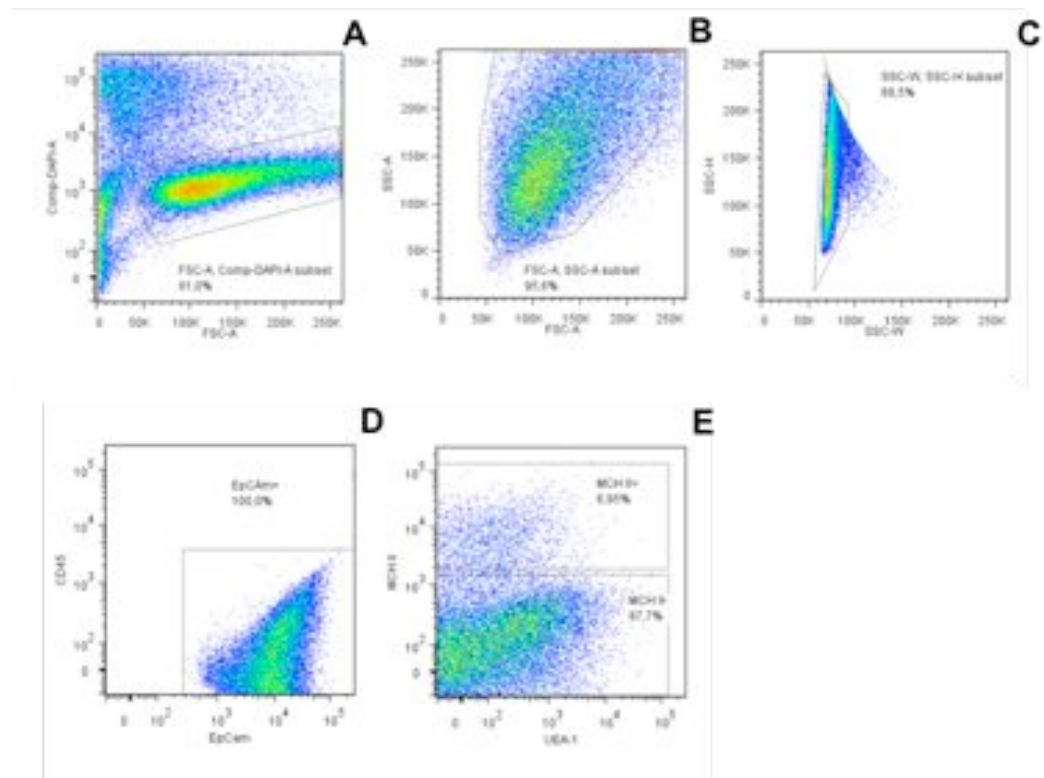


Fig.61 Cell surface marker characterization of 2D positive control of TEC as determined by flow cytometric analysis. TEC were analyzed for: A) size; B) DAPI staining for the vitality; C) elimination of doublets; D) EpCam staining; E) MHC II staining.

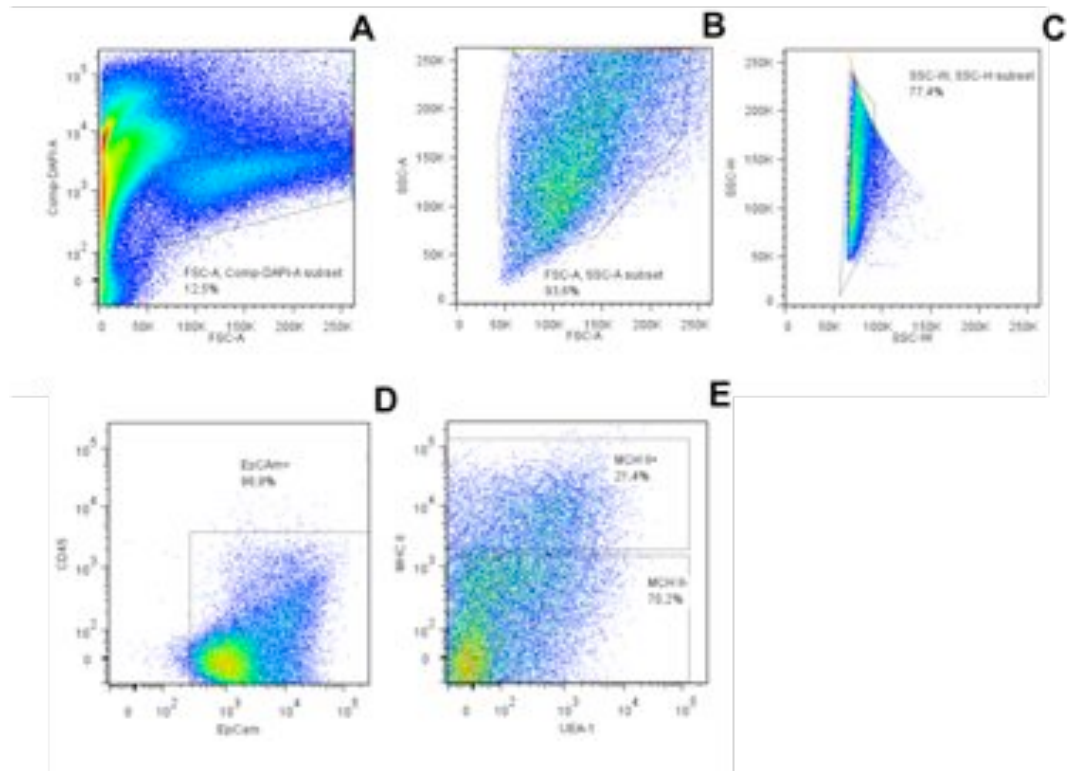


Fig. 62 Cell surface marker characterization of TEC, cultured in 3D fibrin gel, as determined by flow cytometric analysis. TEC were analyzed for: A) size; B) DAPI staining for the vitality; C) elimination of doublets; D) EpCam staining; E) MHC II staining.

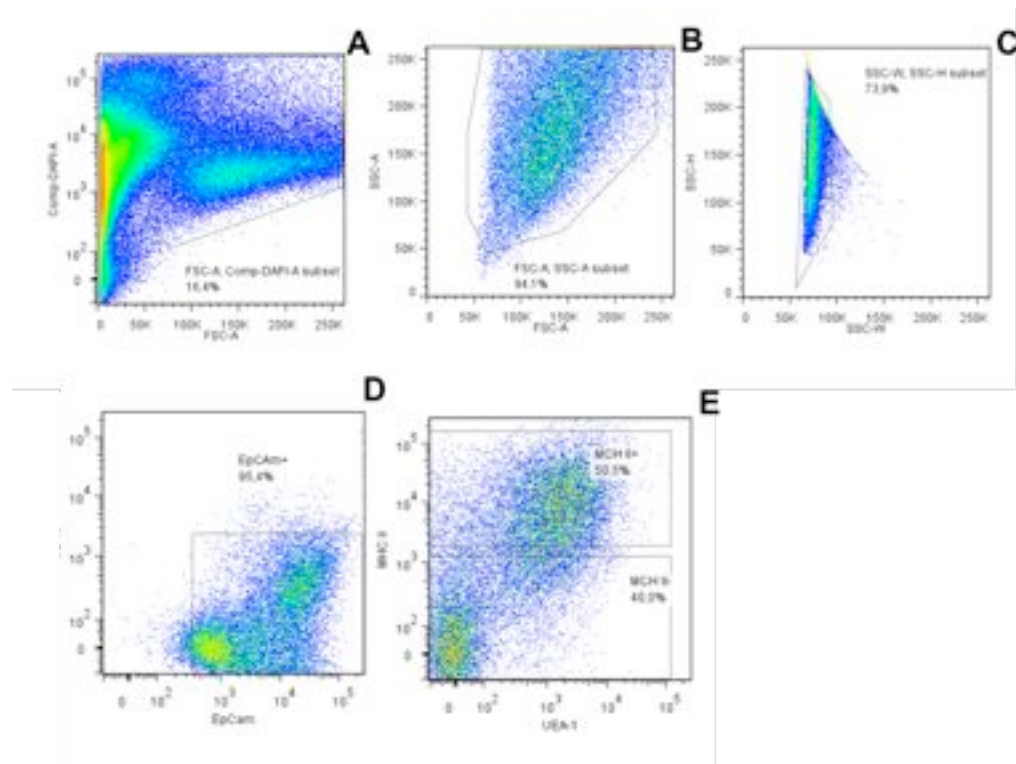


Fig.63 Cell surface marker characterization of TEC, cultured in 3D fibrin gel with medium conditioned with scaffold obtained after disruption of decellularized tissue, as determined by flow cytometric analysis. TEC were analyzed for: A) size; B) DAPI staining for the vitality; C) elimination of doublets; D) EpCam staining; E) MHC II staining.

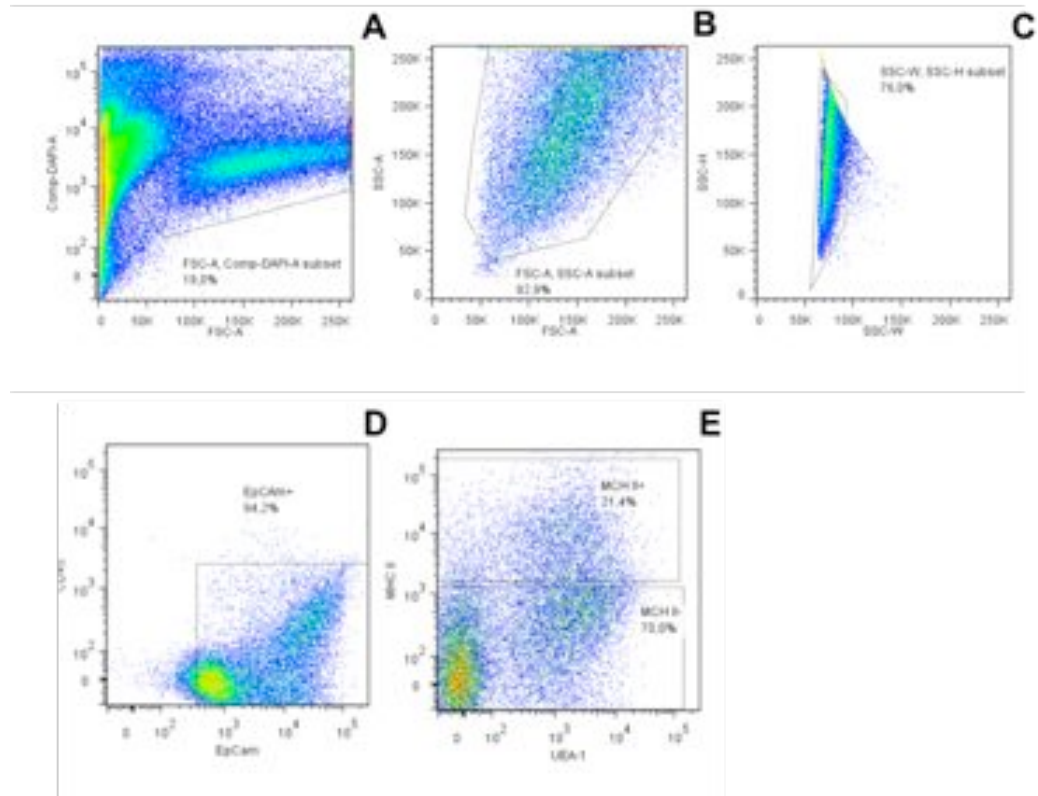


Fig.64 Cell surface marker characterization of TEC, cultured in 3D fibrin gel with medium conditioned with decellularized tissue, as determined by flow cytometric analysis. TEC were analyzed for: A) size; B) DAPI staining for the vitality; C) elimination of doublets; D) EpCam staining; E) MHC II staining.

In preliminary studies still in progress, after 12 days in 3D fibrin culture and conditioned medium, seeded TECs depicted increased expression of MHC II antigens, suggesting a direct stimulatory role of the scaffold products on differentiation parameters for TECs.

Similarly, preliminary studies have also been conducted to assess the role of TEC seeding directly on the decellularized matrix, but limited trapping of the cell suspension by the matrix requires further studies. However, cell viability assays, based on MTT, proved that, at day 3 of culture cells were able to attach and proliferate on the decellularized matrix (fig 65), and that they survived and proliferate up to 10 days in static culture (figure 66).

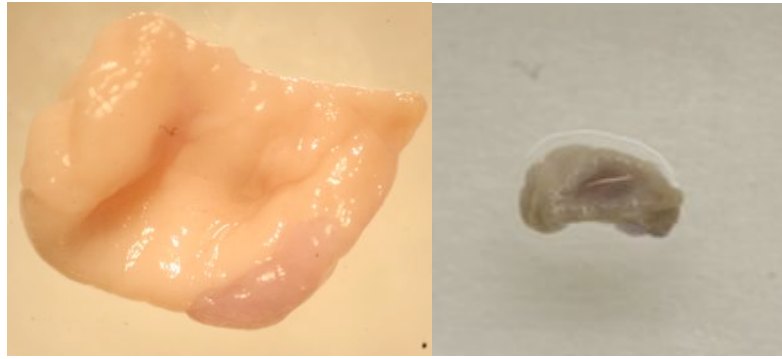


Fig.65 Pictures of the MTT assay after 3 days of culture. The first one taken through the stereomicroscope and the other one with a normal photcamera. Cells alive, that metabolize the MTT, are stained in violet.

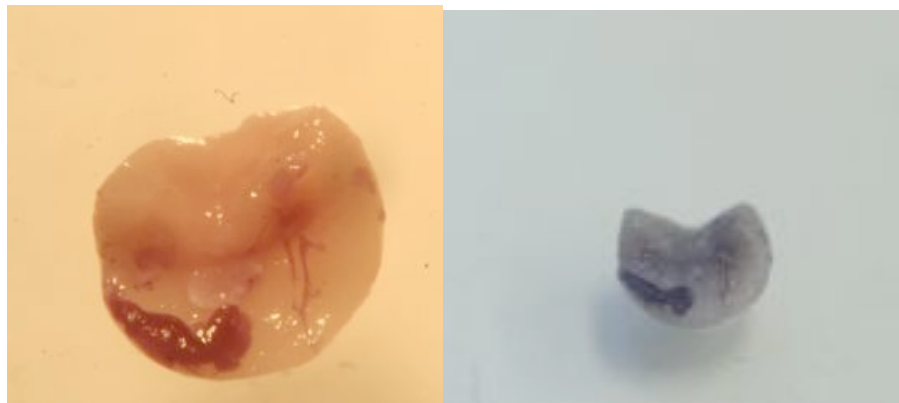


Fig.65 Pictures of the MTT assay after 10 days of culture. The first one taken through the stereomicroscope and the other one with a normal photcamera. Cells alive, that metabolize the MTT, are stained in violet.

These results are very encouraging, suggesting that TECs seeded on native, decellularized matrixes are metabolically active and, likely favourably respond to the 3D geometry of the substrate by preserving their proliferation potential.

5. CONCLUSIONS AND FUTURE PERSPECTIVES

During my PhD tenure at the Tissue Engineering Laboratory of the University of Basel I have investigated the possibility to obtain an efficient protocol for the decellularization of the mouse thymus, and to use it as a scaffold for culturing Thymic Epithelial Cells. Since TEC in normal 2D condition on plastic lose their differentiation state, I investigated a suitable 3D alternative, in particular a 3D scaffold able to support their growth, and maintain their differentiation state.

Due to its anatomy, the thymus is a very difficult organ to decellularize. Indeed, it is served only by small vessels, that cannot be easily used to perform a perfusion-decellularization process. For this reason, I developed an original decellularization process by immersion. Two different protocols satisfied the main characteristics of a decellularized matrix, according to qualitative and quantitative assays. In particular, the quantity of DNA was less than 10% in absolute value, no positive staining for cells was found after the decellularization, and the 3D structure and composition of the ECM were maintained. In addition, I was able to prove that the decellularized matrixes were not cytotoxic for the cells, and were able to increase expression of MHC II antigens with respect to control cells grown in standard conditions.

Further analysis are required to study whether and to which gene level these effects take place, which soluble factors are released by the decellularized matrix in the culture media, and their possible effects on the differentiation state of TECs.

Improvements will be done in seeding efficiency of the cells directly on the matrix, possibly also exploiting appropriate bioreactor conditions, and in the choice of appropriate markers showing the level of differentiation

reached by the seeded TECs.

After a complete characterization of the culture system, these innovative natural scaffolds could be used to improve the standard culture conditions of TEC, to study in vitro the action of different factors on their differentiation genes, and to test the ability of TECs to induce in vitro maturation of seeded T lymphocytes.

In a near future, I also envisage the use of a completely recellularized, thymic matrix as a tool to test in vivo lymphocyte maturation after its implant under the kidney capsule of the athymic mice, and possibly as an innovative therapeutic tool to rescue conditions of immunodepression in specific animal models of immunodeficiency.

6. ACKNOWLEDGMENTS

I would like to thank Prof. Lucio Cocco for having given me the chance to enter and complete this competitive PhD program, including the remarkable opportunity to receive the Marco Polo traineeship fund for foreign research experience.

I would also like to thank Prof. Roberto Toni for his continuous tutorship activity, and for teaching me how a researcher has to be, has to behave, and how to face problems. He introduced me in this big field that is the research, and I will be ever grateful to him for all that he taught me.

I am also grateful to all the people that interacted and worked with me at the Department of SBiBit in Parma (Italy). Everyone of them has contributed to my professional progress.

A particular thanking to Prof. Ivan Martin, Director of the Tissue Engineering Laboratory in Basel, who gave me the opportunity to join for one year his lab and group, where I learnt a lot. He supported me during the difficulties of my research, and find everytime a positive point of view.

Finally, my sincere appreciation to all the exquisite people I met at the Tissue Engineering lab, particularly David Wendt, Elia Piccinini, and Adelaide Asnaghi, who greatly helped for obtaining results in my project.

7. BIBLIOGRAPHY

1. Pearse G. Normal structure, function and histology of the thymus. *AstraZeneca Toxicologic Pathology*, 34:504–514, 2006
2. J Gordon, N.R Manley. Mechanism of thymus organogenesis and morphogenesis. *Development*,138(18):3865-78, 2011 Sep;
3. Palmers, *Frontiers in Immunology* 2013
4. Banks, W.*Applied Veterinary Histology*. Mosby, St. Louis.1993
5. Kuper, C. F., de Heer, E., Van Loveren, H., and Vos, J. G. Immune System. In: *Handbook of Toxicologic Pathology* (W. Haschek, C. Rousseaux, and M. Wallig, eds.), Vol. 2, pp. 585–646. Academic Press, San Diego. 2002
6. van Ewijk W, Brekelmans PJ, Jacobs R, Wisse E. Lymphoid microenvironments in the thymus and lymph node.*Scanning Microsc*.2(4):2129-40.1988
7. De Waal, E. J., Schuurman, H. J., Van Loveren, H., and Vos, J. G. Differential effects of 2,3,7,8-tetrachlorodibenzo-p-dioxin, bis(tri-n-butyltin) oxide and cyclosporine on thymus histophysiology. *Crit Rev Toxicol* 27, 381–430. 1997.
8. Petrie HT Zúñiga-Pflücker JC., Zoned out: functional mapping of stromal signaling microenvironments in the thymus. *Ann Rev Immunol* 25:649-79. 2007
9. Jotereau F, Heuze F, Salomon-Vie V, Gascan H. Cell kinetics in the fetal mouse thymus: precursor cell input, proliferation, and emigration. *J Immunol*. 15;138(4):1026-30.1987
10. Vicente A, Varas A, Sacedón R, Zapata AG. Histogenesis of the epithelial component of rat thymus: an ultrastructural and

- immunohistological analysis. *Anat Rec.*244(4):506-19. 1996
11. Damoiseaux JG, Cautain B, Bernard I, Mas M, van Breda Vriesman PJ, Druet P, Fournié G, Saoudi A. A dominant role for the thymus and MHC genes in determining the peripheral CD4/CD8 T cell ratio in the rat. *J Immunol.* 15;163(6):2983-9. 1999
 12. Pearse G, Histopathology of the thymus. *Toxicol Pathol.* 34(5):515-47.2006
 13. Brelinska R, Thymic epithelial cells in age-dependent involution. *Microsc Res Tech.* 15;62(6):488-500. 2003
 14. De Waal EJ, Rademakers LH. Heterogeneity of epithelial cells in the rat thymus. *Microsc Res Tech.* 1;38(3):227-36. 1997
 15. Boyd RL, Tucek CL, Godfrey DI, Izon DJ, Wilson TJ, Davidson NJ, Bean AG, Ladyman HM, Ritter MA, Hugo P. The thymic microenvironment. *Immunol Today.* 14(9):445-59.1993
 16. Dipasquale B, Tridente G. Immunohistochemical characterization of nurse cells in normal human thymus. *Histochemistry.* 96(6):499-503. 1991
 17. Ushiki T, A scanning electron-microscopic study of the rat thymus with special reference to cell types and migration of lymphocytes into the general circulation., *Cell Tissue Res.* 244(2):285-98.1986
 18. Toussaint-Demyelle D, Scheiff JM, Haumont S. Thymic nurse cells: morphological study during their isolation from murine thymus. *Cell Tissue Res.*;261(1):115-23. 1990
 19. Aguilar LK, Aguilar-Cordova E, Cartwright J Jr, Belmont JW. Thymic nurse cells are sites of thymocyte apoptosis. *J Immunol.*

- 15;152(6):2645-51.1994
20. Kendall MD, Functional anatomy of the thymic microenvironment. *J Anat.* 177:1-29.1991.
 21. Farr AG, Dooley JL, Erickson M. Organization of thymic medullary epithelial heterogeneity: implications for mechanisms of epithelial differentiation. *Immunol Rev.* 189:20-7. 2002
 22. Berrih S, Savino W, Cohen S. Extracellular matrix of the human thymus: immunofluorescence studies on frozen sections and cultured epithelial cells. *J Histochem Cytochem.* 33(7):655-64. 1985
 23. Crisa L, Cirulli V, Ellisman MH, Ishii JK, Elices MJ, Salomon DR. Cell adhesion and migration are regulated at distinct stages of thymic T cell development: the roles of fibronectin, VLA4, and VLA5. *J Exp Med.* 1;184(1):215-28. 1996.
 24. Mizushima H, Koshikawa N, Moriyama K, Takamura H, Nagashima Y, Hirahara F, Miyazaki K. Mizushima H, Koshikawa N, Moriyama K, Takamura H, Nagashima Y, Hirahara F, Miyazaki K. *Horm Res.*50 Suppl 2:7-14.1998
 25. Lannes-Vieira J, Dardenne M, Savino W. Extracellular matrix components of the mouse thymus microenvironment: ontogenetic studies and modulation by glucocorticoid hormones. *J Histochem Cytochem.* 39(11):1539-46.1991.
 26. Savino W, Mendes-da-Cruz DA, Silva JS, Dardenne M, Cotta-de-Almeida V. Intrathymic T-cell migration: a combinatorial interplay of extracellular matrix and chemokines? *Trends Immunol.*;23(6):305-13.2002

27. Savino, W. and Silva-Barbosa, S.D. Laminin/VLA-6 interactions and T-cell function. *Braz. J. Med. Biol. Res.* 29, 1209–1220.1996.
28. Anderson, G. et al. Fibroblast dependency during early thymocyte development maps to the CD25⁺CD44⁺ stage and involves interactions with fibroblast matrix molecules. *Eur. J. Immunol.* 27, 1200–1206. 1997
29. Suniara, R.K. et al. An essential role for thymic mesenchyme in early T-cell development. *J. Exp. Med.* 191, 1051–1056.2000.
30. Crisa, L. et al. Cell adhesion and migration are regulated at distinct stages of thymic T-cell development: the roles of fibronectin, VLA-4 and VLA-5. *J. Exp. Med.* 184, 215–222 .1996
31. Vivinus-Nebot, M. et al. Laminin 5 in the human thymus: control of T-cell proliferation via $\alpha 6\beta 4$ integrins. *J. Cell Biol.* 144, 563–574.1999
32. Kim, M.G. et al. Epithelial-cell-specific laminin-5 is required for survival of early thymocytes. *J. Immunol.* 165, 192–201.2000
33. Savino, W. et al. Role of extracellular-matrix-mediated interactions in the thymus. *Dev. Immunol.* 7, 19–28 .2000
34. Sainte-Marie, G. & Leblond, C. P. Cytologic features and cellular migration in the cortex and medulla of thymus in the young adult rat. *Blood* 23, 275–299 .1964.
35. Cantor, H. & Weissman, I. Development and function of subpopulations of thymocytes and T lymphocytes. *Prog. Allergy* 20, 1–64 .1976.
36. Stutman, O. Intrathymic and extrathymic T cell maturation. *Immunol. Rev.* 42, 138–184 .1978.

37. Bhan, A. K., Reinherz, E. L., Poppema, S., McCluskey, R. T. & Schlossman, S. F. Location of T cell and major histocompatibility complex antigens in the human thymus. *J. Exp. Med.* 152, 771–782 .1980.
38. Petrie, H. T. Cell migration and the control of post-natal T-cell lymphopoiesis in the thymus. *Nature Rev. Immunol.* 3, 859–866 .2003.
39. Gray, D. H. D. et al. Controlling the thymic microenvironment. *Curr. Opin. Immunol.* 17, 137–143.2005.
40. Savino W, Mendes-da-Cruz DA, Silva JS, Dardenne M, Cottade-Almeida V. Intrathymic T-cell migration: a combinatorial interplay of extracellular matrix and chemokines? *Trends Immunol.*;23(6):305-13.2002
41. Owen, J. J. & Ritter, M. A. Tissue interaction in the development of thymus lymphocytes. *J. Exp. Med.* 129, 431–442.1969.
42. Haynes, B. F. & Heinly, C. S. Early human T cell development: analysis of the human thymus at the time of initial entry of hematopoietic stem cells into the fetal thymic microenvironment. *J. Exp. Med.* 181, 1445–1458.1995.
43. Bleul, C. C. & Boehm, T. Chemokines define distinct microenvironments in the developing thymus. *Eur. J. Immunol.* 30, 3371–3379.2000.
44. Liu, C. et al. The role of CCL21 in recruitment of T precursor cells to fetal thymus. *Blood* 105, 31–39.2005.
45. Calderón L, Boehm T. Three chemokine receptors

- cooperatively regulate homing of hematopoietic progenitors to the embryonic mouse thymus. *Proc Natl Acad Sci U S A*. 2011 May 3;108(18):7517-22.
46. Fossa, D. L., Donskoya, E. & Goldschneider, I. The importation of hematogenous precursors by the thymus is a gated phenomenon in normal adult mice. *J. Exp. Med.* 193, 365–374 .2001.
 47. Le Douarin, N. M. & Jotereau, F. V. Tracing of cells of the avian thymus through embryonic life in interspecific chimeras. *J. Exp. Med.* 142, 17–40.1975.
 48. 50 Havran, W. L. & Allison, J. P. Developmentally ordered appearance of thymocytes expressing different T-cell antigen receptors. *Nature* 335, 443–445.1988.
 49. Coltey, M. et al. Analysis of the first two waves of thymus homing stem cells and their T cell progeny in chick–quail chimeras. *J. Exp. Med.* 170, 543–557.1989.
 50. Dunon, D. et al. Ontogeny of the immune system: $\gamma\delta$ and $\alpha\beta$ T cells migrate from thymus to the periphery in alternating waves. *J. Exp. Med.* 186, 977–988.1997.
 51. Ikuta, K. et al. A developmental switch in thymic lymphocyte maturation potential occurs at the level of hematopoietic stem cells. *Cell* 62, 863–874.1990.
 52. Weber-Arden, J., Wilbert, O. M., Kabelitz, D. & Arden, B. $\gamma\delta$ repertoire during thymic ontogeny suggests three novel waves of $\gamma\delta$ TCR expression. *J. Immunol.* 164, 1002–1012 .2000.

53. Pearse, M. et al. A murine early thymocyte developmental sequence is marked by transient expression of the interleukin 2 receptor. *Proc. Natl Acad. Sci. USA* 86, 1614–1618 .1989.
54. Shinkai, Y. et al. RAG-2-deficient mice lack mature lymphocytes owing to inability to initiate V(D)J rearrangement. *Cell* 68, 855–867 1992.
55. Radtke, F. et al. Deficient T cell fate specification in mice with an induced inactivation of Notch1. *Immunity* 10, 547–558 (1999).
56. Zúñiga-Pflücker, J. C. T-cell development made simple. *Nature Rev. Immunol.* 4, 67–72.2004.
57. Peschon, J. J. et al. Early lymphocyte expansion is severely impaired in interleukin 7 receptor-deficient mice. *J. Exp. Med.* 180, 1955–1960 1994.
58. von Freedem-Jeffry, U. et al. Lymphopenia in interleukin (IL)-7 gene-deleted mice identifies IL-7 as a nonredundant cytokine. *J. Exp. Med.* 181, 1519–1526 .1995.
59. Hollander, G. A. et al. Developmental control point in induction of thymic cortex regulated by a subpopulation of prothymocytes. *Nature* 373, 350–353 (1995).
60. van Ewijk, W., Hollander, G., Terhorst, C. & Wang, B. Stepwise development of thymic microenvironments in vivo is regulated by thymocyte subsets. *Development* 127, 1583–1591 (2000).
61. Klug, D. B. et al. Interdependence of cortical thymic epithelial cell differentiation and T-lineage commitment. *Proc. Natl Acad. Sci. USA* 95, 11822–11827 .1998.

62. Klug, D. B., Carter, C., Gimenez-Conti, I. B. & Richie, E. R. Thymocyte-independent and thymocyte-dependent phases of epithelial patterning in the fetal thymus. *J. Immunol.* 169, 2842–2845 .2002.
63. Lind, E. F., Prockop, S. E., Porritt, H. E. & Petrie, H. T. Mapping precursor movement through the postnatal thymus reveals specific microenvironments supporting defined stages of early lymphoid development. *J. Exp. Med.* 194, 127–134 .2001.
64. Plotkin, J., Prockop, S. E., Lepique, A. & Petrie, H. T. Critical role for CXCR4 signaling in progenitor localization and T cell differentiation in the postnatal thymus. *J. Immunol.* 171, 4521–4527 .2003.
65. Misslitz, A. et al. Thymic T cell development and progenitor localization depend on CCR7. *J. Exp. Med.* 200, 481–491 .2004.
66. Benz, C., Heinzl, K. & Bleul, C. C. Homing of immature thymocytes to the subcapsular microenvironment within the thymus is not an absolute requirement for T cell development. *Eur. J. Immunol.* 34, 3652–3663 .2004.
67. Raulet, D. H., Garman, R. D., Saito, H. & Tonegawa, S. Developmental regulation of T-cell receptor gene expression. *Nature* 314, 103–107 .1985.
68. Von Boehmer, H. & Fehling, H. J. Structure and function of the pre-T cell receptor. *Annu. Rev. Immunol.* 15, 433–452.1997.
69. Irving, B. A., Alt, F. W. & Killeen, N. Thymocyte development in the absence of pre-T cell receptor extracellular immunoglobulin domains. *Science* 280, 905–908.1998.

70. Ciofani, M. & Zúñiga-Pflücker, J. C. Notch promotes survival of pre-T cells at the β -selection checkpoint by regulating cellular metabolism. *Nature Immunol.* 6, 881–888 .2005.
71. Takahama, Y., Letterio, J. J., Suzuki, H., Farr, A. G. & Singer, A. Early progression of thymocytes along the CD4/CD8 developmental pathway is regulated by a subset of thymic epithelial cells expressing transforming growth factor β . *J. Exp. Med.* 179, 1495–1506 .1994.
72. Kisielow, P., Teh, H. S., Bluthmann, H. & Von Boehmer, H. Positive selection of antigen-specific T cells in thymus by restricting MHC molecules. *Nature* 335, 730–733 .1988.
73. Jameson, S. C., Hogquist, K. A. & Bevan, M. J. Positive selection of thymocytes. *Annu. Rev. Immunol.* 13, 93–126 .1995.
74. Bousso, P., Bhakta, N. R., Lewis, R. S. & Robey, E. Dynamics of thymocyte-stromal cell interactions visualized by two-photon microscopy. *Science* 296, 1876–1880 .2002.
75. Egerton, M., Scollay, R. & Shortman, K. Kinetics of mature T-cell development in the thymus. *Proc. Natl Acad. Sci. USA* 87, 2579–2582 .1990.
76. Goldrath, A. W. & Bevan, M. J. Selecting and maintaining a diverse T-cell repertoire. *Nature* 402, 255–262.1999.
77. Witt, C. M., Raychaudhuri, S., Schaefer, B., Chakraborty, A. K. & Robey, E. A. Directed migration of positively selected thymocytes visualized in real time. *PLoS Biol.* 3, e160 .2005.
78. Kim, C. H., Pelus, L. M., White, J. R. & Broxmeyer, H. E. Differential chemotactic behavior of developing T cells in response to

- thymic chemokines. *Blood* 91, 4434–4443 .1998.
79. Campbell, J. J., Pan, J. & Butcher, E. C. Cutting edge: developmental switches in chemokine responses during T cell maturation. *J. Immunol.* 163, 2353–2357 .1999.
80. Ueno, T. et al. CCR7 signals are essential for cortex-to-medulla migration of developing thymocytes. *J. Exp. Med.* 200, 493–505 .2004.
81. Egli, P., Schaffner, T., Gerber, H. A., Hess, M. W. & Cottier, H. Accessibility of thymic cortical lymphocytes to particles translocated from the peritoneal cavity to parathymic lymph nodes. *Thymus* 8, 129–139. 1986.
82. Niewenhuis, P. et al. The transcapsular route: a new way for (self-) antigens to by-pass the blood– thymus barrier. *Immunol. Today* 9, 372–375.1988.
83. Burkly, L. et al. Expression of relB is required for the development of thymic medulla and dendritic cells. *Nature* 373, 531–536 .1995.
84. Boehm, T., Scheu, S., Pfeffer, K. & Bleul, C. C. Thymic medullary epithelial cell differentiation, thymocyte emigration, and the control of autoimmunity require lympho-epithelial cross talk via LT β R. *J. Exp. Med.* 198, 757–769 .2003.
85. Kajiura, F. et al. NF- κ B-inducing kinase establishes self-tolerance in a thymic-stroma dependent manner. *J. Immunol.* 172, 2067–2075 .2004.

86. Akiyama, T. et al. Dependence of self-tolerance on TRAF6-directed development of thymic stroma. *Science* 308, 248–251 .2005.
87. Egerton, M., Scollay, R. & Shortman, K. Kinetics of mature T-cell development in the thymus. *Proc. Natl Acad. Sci. USA* 87, 2579–2582.1990.
88. Reichert, R. A., Weissman, I. L. & Butcher, E. C. Phenotypic analysis of thymocytes that express homing receptors for peripheral lymph nodes. *J. Immunol.* 136, 3521–3528.1986.
89. Bendelac, A., Matzinger, P., Seder, R. A., Paul, W. E. & Schwartz, R. H. Activation events during thymic selection. *J. Exp. Med.* 175, 731–742 .1992..
90. Ramsdell, F., Jenkins, M., Dinh, Q. & Fowlkes, B. J. The majority of CD4⁺8⁻ thymocytes are functionally immature. *J. Immunol.* 147, 1779–1785 .1991.
91. Kyewski, B. & Derbinski, J. Self-representation in the thymus: an extended view. *Nature Rev. Immunol.* 4, 688–698 .2004.
92. Zuklys, S. et al. Normal thymic architecture and negative selection are associated with Aire expression, the gene defective in the autoimmune- polyendocrinopathy-candidiasis-ectodermal dystrophy (APECED). *J. Immunol.* 165, 1976–1983.2000.
93. Derbinski, J. et al. Promiscuous gene expression in thymic epithelial cells is regulated at multiple levels. *J. Exp. Med.* 202, 33–45 .2005.
94. Liston, A., Lesage, S., Wilson, J., Peltonen, L. & Goodnow, C. C. Aire regulates negative selection of organ-specific T cells. *Nature*

- Immunol. 4, 350–354 .2003.
95. Gallegos, A. M. & Bevan, M. J. Central tolerance to tissue-specific antigens mediated by direct and indirect antigen presentation. *J. Exp. Med.* 200, 1039–1049.2004.
 96. Anderson, M. S. et al. The cellular mechanism of Aire control of T cell tolerance. *Immunity* 23, 227–239.2005.
 97. Sakaguchi, S. Naturally arising CD4⁺ regulatory T cells for immunologic self-tolerance and negative control of immune responses. *Ann. Rev. Immunol.* 22, 531–562.2004.
 98. Fontenot, J. D. et al. Regulatory T cell lineage specification by the forkhead transcription factor Foxp3. *Immunity* 22, 329–341.2005.
 99. Watanabe, N. et al. Hassall's corpuscles instruct dendritic cells to induce CD4⁺CD25⁺ regulatory T cells in human thymus. *Nature* 436, 1181–1185.2005.
 100. Lieberam, I. & Forster, I. The murine β -chemokine TARC is expressed by subsets of dendritic cells and attracts primed CD4⁺ T cells. *Eur. J. Immunol.* 29, 2684–2694.1999.
 101. Alferink, J. et al. Compartmentalized production of CCL17 in vivo: strong inducibility in peripheral dendritic cells contrasts selective absence from the spleen. *J. Exp. Med.* 197, 585–599.2003.
 102. Chantry, D. et al. Macrophage-derived chemokine is localized to thymic medullary epithelial cells and is a chemoattractant for CD3⁺, CD4⁺, CD8^{low} thymocytes. *Blood* 94, 1890–1898.1999.
 103. Annunziato, F. et al. Macrophage-derived chemokine and EB11-ligand chemokine attract human thymocytes in different stage of development and are produced by distinct subsets of medullary

- epithelial cells: possible implications for negative selection. *J. Immunol.* 165, 238–246 .2000.
104. Rossi, F. M. V. et al. Recruitment of adult thymic progenitors is regulated by P-selectin and its ligand PSGL-1. *Nature Immunol.* 6, 626–634.2005.
105. Chaffin, K. E. & Perlmutter, R. M. A pertussis toxin-sensitive process controls thymocyte emigration. *Eur. J. Immunol.* 21, 2565–2573 .1991.
106. Matloubian, M. et al. Lymphocyte egress from thymus and peripheral lymphoid organs is dependent on S1P receptor 1. *Nature* 427, 355–360.2004.
107. Allende, M. L., Dreier, J. L., Mandala, S. & Proia, R. L. Expression of the sphingosine 1-phosphate receptor, S1P1, on T-cells controls thymic emigration. *J. Biol. Chem.* 279, 15396–15401.2004.
108. Ueno, T. et al. Role for CCR7 ligands in the emigration of newly generated T lymphocytes from the neonatal thymus. *Immunity* 16, 205–218 (2002).
109. Poznansky, M. C. et al. Thymocyte emigration is mediated by active movement away from stroma- derived factors. *J. Clin. Invest.* 109, 1101–1110.2002.
110. Kato, S. Thymic microvascular system. *Microscopy Res. Tech.* 38, 287–299.1997.
111. Ushiki, T. A scanning electron-microscopic study of the rat thymus with special reference to cell types and migration of

- lymphocytes into the general circulation. *Cell Tissue Res.* 244, 285–298 .1986.
112. Centers for Disease Control and Prevention (CDC). Deaths from chronic obstructive pulmonary disease—United States. *MMWR Morb Mortal Wkly Rep* 2008; 57: 1229–32. 2000–2005
113. United States Renal Data System (USRDS). Renal disease data 2009.
114. Heron M, Hoyert DL, Murphy SL, Xu J, Kochanek KD, Tejada-Vera B. Deaths: final data for 2006. *Natl Vital Stat Rep* 57: 1–134. 2009.
115. Shin’oka T, Imai Y, Ikada Y. Transplantation of a tissue-engineered pulmonary artery. *N Engl J Med* 344: 532–33. 2001.
116. Ming He Tissue Engineering 2013
117. Orens JB, Garrity ER Jr. General overview of lung transplantation and review of organ allocation. *Proc Am Thorac Soc* 6: 13–19. 2009.
118. Badilak SF Regenerative medicine and developmental biology: the role of the extracellular matrix. *Anat Rec B New Anat.* 2005 Nov;287(1):36-41. 2005
119. Barkan D, Green JE, Chambers AF. Extracellular matrix:a gatekeeper in the transition from dormancy to metastatic growth. *Eur J Cancer* **46**: 1181–88. 2010.
120. Calve S, Odelberg SJ, Simon HG. A transitional extracellular matrix instructs cell behavior during muscle regeneration. *Dev Biol* **344**: 259–71. 2010.

121. Crapo PM, Gilbert TW, Badylak SF. An overview of tissue and whole organ decellularization processes. *Biomaterials* **32**: 3233–43. 2011.
122. Roomans GM. Tissue engineering and the use of stem/progenitor cells for airway epithelium repair. *Eur Cell Mater* **19**: 284–99. 2010.
123. Takahashi K, Yamanaka S. Induction of pluripotent stem cells from mouse embryonic and adult fibroblast cultures by defined factors. *Cell* **126**: 663–76. 2006.
124. Uygun BE, Soto-Gutierrez A, Yagi H, et al. Organ reengineering through development of a transplantable recellularized liver graft using decellularized liver matrix. *Nat Med* **16**: 814–20. 2010.
125. Soto-Gutierrez A, Zhang L, Medberry C, et al. A whole-organ regenerative medicine approach for liver replacement. *Tissue Eng Part C Methods* **17**: 677–86. 2011.
126. Ott HC, Matthiesen TS, Goh SK, et al. Perfusion-decellularized matrix: using nature's platform to engineer a bioartificial heart. *Nat Med* **14**: 213–21. 2008.
127. Ott HC, Clippinger B, Conrad C, et al. Regeneration and orthotopic transplantation of a bioartificial lung. *Nat Med* **16**: 927–33. 2010.
128. Petersen TH, Calle EA, Zhao L, et al. Tissue-engineered lungs for in vivo implantation. *Science* **329**: 538–41. 2010.
129. Cortiella J, Niles J, Cantu A, et al. Influence of acellular natural lung matrix on murine embryonic stem cell differentiation and tissue formation. *Tissue Eng Part A* 2010; **16**: 2565–80.

130. Daly AB, Wallis JM, Borg ZD, et al. Initial binding and recellularization of decellularized mouse lung scaffolds with bone marrow-derived mesenchymal stromal cells. *Tissue Eng Part A*; **18**: 1–16. 2012.
131. Macchiarini P, Jungebluth P, Go T, et al. Clinical transplantation of a tissue-engineered airway. *Lancet*; **372**: 2023–30. 2008.
132. Badylak SF, Hoppo T, Nieponice A, Gilbert TW, Davison JM, Jobe BA. Esophageal preservation in five male patients after endoscopic inner-layer circumferential resection in the setting of superficial cancer: a regenerative medicine approach with a biologic scaffold. *Tissue Eng Part A*; **17**: 1643–50. 2011.
133. Mase VJ Jr, Hsu JR, Wolf SE, et al. Clinical application of an acellular biologic scaffold for surgical repair of a large, traumatic quadriceps femoris muscle defect. *Orthopedics* **33**: 511. 2010.
134. Chen F, Yoo JJ, Atala A. Acellular collagen matrix as a possible “off the shelf” biomaterial for urethral repair. *Urology* **54**: 407–10. 1999.
135. Dahl SL, Koh J, Prabhakar V, Niklason LE. Decellularized native and engineered arterial scaffolds for transplantation. *Cell Transplant* **12**: 659–66. 2003.
136. Badylak SF. The extracellular matrix as a biologic scaffold material. *Biomaterials* **28**: 3587–93. 2007.
137. Barkan D, Green JE, Chambers AF. Extracellular matrix: a gatekeeper in the transition from dormancy to metastatic growth. *Eur J Cancer* **46**: 1181–88. 2010.

138. Gilbert, T.W., et al. Degradation and remodeling of small intestinal submucosa in canine Achilles tendon repair. *J Bone Joint Surg Am* 89, 621, 2007.
139. Badylak, S., et al. Resorbable bioscaffold for esophageal repair in a dog model. *J Pediatr Surg* 35, 1097, 2000.
140. Ritchey, M.L., and Ribbeck, M. Successful use of tunica vaginalis grafts for treatment of severe penile chordee in children. *J Urol* 170(4 Pt 2), 1574, discussion 1576, 2003.
141. Bissel MJ, Aggeler J. Dynamic reciprocity: how do extracellular matrix and hormones direct gene expression? *Prog Clin Biol Res*;249:251-62. 1987.
142. schwarzabuer 1999
143. Sechler JL, Corbett SA, Wenk MB, Schwarzbauer JE. Modulation of cell-extracellular matrix interactions. *Ann N Y Acad Sci.* 1998 Oct 23;857:143-54
144. Hynes RO. Targeted mutations in cell adhesion genes: what have we learned from them? *Dev Biol.* 15;180(2):402-12. 1996
145. Kleman JP, Hartmann DJ, Ramirez F, van der Rest M. The human rhabdomyosarcoma cell line A204 lays down a highly insoluble matrix composed mainly of alpha 1 type-XI and alpha 2 type-V collagen chains. *Eur J Biochem.* 15;210(1):329-35.1992.
146. Miyamoto S *et al* Fibronectin and integrins in cell adhesion, signaling, and morphogenesis *Ann. NY Acad. Sci.* **857** 119–29. 1998
147. Allman AJ, Mcpherson TB, Badylak SF, Merrill LC, Kallakury B, Sheehan C, Raeder RH, Metzger DW: Xenogeneic extracellular

- matrix grafts elicit a TH2-restricted immune response. *Transplantation* 71: 1631–1640, 2001
148. Timpl P. Macromolecular organization of basement membranes. *Curr Opin Cell Biol.* 8(5):618-24. 1996
149. Timpl R, Brown JC. Supramolecular assembly of basement membranes. *Bioessays.* 18(2):123-32. 1996
150. Ponce ML, Nomizu M, Delgado MC, Kuratomi Y, Hoffman MP, Powell S, Yamada Y, Kleinman HK, Malinda KM. Identification of endothelial cell binding sites on the laminin gamma 1 chain. *Circ Res.* 2;84(6):688-94. 1999
151. Werb Z, Vu TH, Rinkenberger JL, Coussens LM. Matrix-degrading proteases and angiogenesis during development and tumor formation. *APMIS.* 107(1):11-8. 1999
152. Li S, Harrison D, Carbonetto S, Fassler R, Smyth N, Edgar D, Yurchenco PD. Matrix assembly, regulation, and survival functions of laminin and its receptors in embryonic stem cell differentiation. *J Cell Biol.* 24;157(7):1279-90. 2002
153. Badylak, S.F., et al. The use of xenogeneic small intestinal submucosa as a biomaterial for Achilles tendon repair in a dog model. *J Biomed Mater Res* 29, 977, 1995.
154. Boruch, A.V., et al. Constructive remodeling of biologic scaffolds is dependent on early exposure to physiologic bladder filling in a canine partial cystectomy model. *J Surg Res* 161, 217, 2010.
155. Badylak, S.F., et al. Biologic scaffolds for constructive tissue remodeling. *Biomaterials* 32, 316, 2011.
156. Voytik-Harbin SL, Brightman AO, Kraine MR, Waisner B,

- Badylak SF. Identification of extractable growth factors from small intestinal submucosa. *J Cell Biochem* 67(4):478–91. 1997.
157. Hodde J, Record R, Tullius B, Badylak S. Fibronectin peptides mediate HMEC adhesion to porcine-derived extracellular matrix. *Biomaterials* 23:1841–8. 2002.
158. Hodde JP, Record RD, Liang HA, Badylak SF. Vascular endothelial growth factor in porcine-derived extracellular matrix. *Endothelium*;8(1):11–24. 2001.
159. Hodde JP, Record RD, Tullius RS, Badylak SF. Retention of endothelial cell adherence to porcine-derived extracellular matrix after disinfection and sterilization. *Tissue Eng*;8(2):225–34. 2002.
160. McDevitt CA, Wildey GM, Cutrone RM. Transforming growth factor-beta1 in a sterilized tissue derived from the pig small intestine submucosa. *J Biomed Mater Res*;67A(2):637–40. 2003
161. Hodde J, Hiles M. Bioactive FGF-2 in sterilized extracellular matrix. *Wounds*;13:195. 2001.
162. Zantop T, Gilbert TW, Yoder MC, Badylak SF. Extracellular matrix scaffolds attract bone marrow derived cells in a mouse model of achilles tendon reconstruction. *J Orthop Res*;24(6):1299–309. 2006.
163. Badylak SF, Park K, McCabe G, Yoder M. Marrow-deprived cells populate scaffolds composed of xenogeneic extracellular matrix. *Exp Hematol*;29:1310–8. 2001.
164. Nakayama KH, Batchelder CA, Lee CI, Tarantal AF. Decellularized rhesus monkey kidney as a three-dimensional scaffold for renal tissue engineering. *Tissue Eng Part A*; **16**: 2207–16. 2010.

165. Murry CE, Keller G. Differentiation of embryonic stem cells to clinically relevant populations: lessons from embryonic development. *Cell*; **132**: 661–80. 2008.
166. Tottey S, Corselli M, Jeffries EM, Londono R, Peault B, Badylak SF. Extracellular matrix degradation products and low-oxygen conditions enhance the regenerative potential of perivascular stem cells. *Tissue Eng Part A*; **17**: 37–44. 2011.
167. Agrawal V, Tottey S, Johnson SA, Freund JM, Siu BF, Badylak SF. Recruitment of progenitor cells by an ECM cryptic peptide in a mouse model of digit amputation. *Tissue Eng Part A* **17**: 2435–43. 2011.
168. Valentin JE, Stewart-Akers AM, Gilbert TW, Badylak SF. Macrophage participation in the degradation and remodeling of extracellular matrix scaffolds. *Tissue Eng Part A* **15**: 1687–94. 2009.
169. Petersen TH, Calle EA, Zhao L, et al. Tissue-engineered lungs for in vivo implantation. *Science*; **329**: 538–41. 2010.
170. Sellaro TL, Ranade A, Faulk DM, et al. Maintenance of human hepatocyte function in vitro by liver-derived extracellular matrix gels. *Tissue Eng Part A*; **16**: 1075–82. 2010.
171. Nelson CM, Bissell MJ. Modeling dynamic reciprocity: engineering three-dimensional culture models of breast architecture, function, and neoplastic transformation. *Semin Cancer Biol* **15**: 342–52. 2005.
172. BadylakSF, TaylorD and UygunK. Whole-organ tissue engineering: decellularization and recellularization of three-

- dimensional matrix scaffolds *Annu. Rev. Biomed. Eng.* **13** 27–53
2011
173. Gilbert TW, Wognum S, Joyce EM, Freytes DO, Sacks MS, Badylak SF. Collagen fiber alignment and biaxial mechanical behavior of porcine urinary bladder derived extracellular matrix. *Biomaterials* 29(36):4775e82. 2008.
174. Hodde JP, Hiles M. Virus safety of a porcine-derived medical device: evaluation of a viral inactivation method. *Biotechnol Bioeng* 79(2):211e6. 2002.
175. Dong X, Wei X, Yi W, Gu C, Kang X, Liu Y, et al. RGD-modified acellular bovine pericardium as a bioprosthetic scaffold for tissue engineering. *J Mater Sci Mater Med*; 2009.
176. Prasertsung I, Kanokpanont S, Bunaprasert T, Thanakit V, Damrongsakkul S. Development of acellular dermis from porcine skin using periodic pressurized technique. *J Biomed Mater Res B Appl Biomater* 85(1):210e9. 2008.
177. Reing JE, Brown BN, Daly KA, Freund JM, Gilbert TW, Hsiong SX, et al. The effects of processing methods upon mechanical and biologic properties of porcine dermal extracellular matrix scaffolds. *Biomaterials* 31 (33):8626e33. 2010.
178. Gorschewsky O, Puetz A, Riechert K, Klakow A, Becker R. Quantitative analysis of biochemical characteristics of bone-patellar tendon-bone allografts. *Biomed Mater Eng*;15(6):403e11. 2005.
179. Cox B, Emili A. Tissue subcellular fractionation and protein extraction for use in mass-spectrometry-based proteomics. *Nat Protoc*;1(4):1872e8. 2006.

180. Xu CC, Chan RW, Tirunagari N. A biodegradable, acellular xenogeneic scaffold for regeneration of the vocal fold lamina propria. *Tissue Eng*; 13(3):551e66. 2007.
181. Giusti S, Bogetti ME, Bonafina A, Fiszer de Plazas S. An improved method to obtain a soluble nuclear fraction from embryonic brain tissue. *Neurochem Res*;34(11):2022e9. 2009.
182. Alhamdani MS, Schroder C, Werner J, Giese N, Bauer A, Hoheisel JD. Single-step procedure for the isolation of proteins at near-native conditions from mammalian tissue for proteomic analysis on antibody microarrays. *J Proteome Res*;9(2):963e71. 2010.
183. Patel N, Solanki E, Picciani R, Cavett V, Caldwell-Busby JA, Bhattacharya SK. Strategies to recover proteins from ocular tissues for proteomics. *Proteomics*;8(5):1055e70. 2008.
184. Elder BD, Kim DH, Athanasiou KA. Developing an articular cartilage decellularization process toward facet joint cartilage replacement. *Neurosurgery*;66(4):722e7. 2010.
185. Du L, Wu X, Pang K, Yang Y. Histological evaluation and biomechanical characterisation of an acellular porcine cornea scaffold. *Br J Ophthalmol*; 95(3):410-4.2010.
186. Nakayama KH, Batchelder CA, Lee CI, Tarantal AF. Decellularized rhesus monkey kidney as a three-dimensional scaffold for renal tissue engineering. *Tissue Eng Part A*;16(7):2207e16. 2010
187. Alhamdani MS, Schroder C, Werner J, Giese N, Bauer A, Hoheisel JD. Single- step procedure for the isolation of proteins at near-native conditions from mammalian tissue for proteomic analysis on antibody microarrays. *J Proteome Res*;9(2):963e71. 2010.

188. Patel N, Solanki E, Picciani R, Cavett V, Caldwell-Busby JA, Bhattacharya SK. Strategies to recover proteins from ocular tissues for proteomics. *Proteomics*;8(5):1055e70. 2008.
189. Rieder E, Kasimir MT, Silberhumer G, Seebacher G, Wolner E, Simon P, et al. Decellularization protocols of porcine heart valves differ importantly in efficiency of cell removal and susceptibility of the matrix to recellularization with human vascular cells. *J Thorac Cardiovasc Surg*;127(2):399e405. 2004.
190. Cebotari S, Tudorache I, Jaekel T, Hilfiker A, Dorfman S, Ternes W, et al. Detergent decellularization of heart valves for tissue engineering: toxicological effects of residual detergents on human endothelial cells. *Artif Organs*;34(3):206e10. 2010.
191. Meyer SR, Chiu B, Churchill TA, Zhu L, Lakey JR, Ross DB. Comparison of aortic valve allograft decellularization techniques in the rat. *J Biomed Mater Res A*;79(2):254e62. 2006.
192. Lumpkins SB, Pierre N, McFetridge PS. A mechanical evaluation of three decellularization methods in the design of a xenogeneic scaffold for tissue engineering the temporomandibular joint disc. *Acta Biomater*;4 (4):808e16. 2008.
193. Yang B, Zhang Y, Zhou L, Sun Z, Zheng J, Chen Y, et al. Development of a porcine bladder acellular matrix with well-preserved extracellular bioactive factors for tissue engineering. *Tissue Eng Part C Methods*;16 (5):1201e11. 2010.
194. Ott HC, Clippinger B, Conrad C, Schuetz C, Pomerantseva I, Ikonomou L, et al. Regeneration and orthotopic transplantation of a bioartificial lung. *Nat Med*;16(8):927e33. 2010

195. Kasimir MT, Rieder E, Seebacher G, Silberhumer G, Wolner E, Weigel G, et al. Comparison of different decellularization procedures of porcine heart valves. *Int J Artif Organs*;26(5):421e7. 2003.
196. Deeken CR, White AK, Bachman SL, Ramshaw BJ, Cleveland DS, Loy TS, et al. Method of preparing a decellularized porcine tendon using tributyl phosphate. *J Biomed Mater Res B Appl Biomater*;96(2):199e206. 2010.
197. Gui L, Chan SA, Breuer CK, Niklason LE. Novel utilization of serum in tissue decellularization. *Tissue Eng Part C Methods*;16(2):173e84. 2010.
198. Hudson TW, Liu SY, Schmidt CE. Engineering an improved acellular nerve graft via optimized chemical processing. *Tissue Eng*;10(9e10): 1346e58. 2004.
199. Cebotari S, Tudorache I, Jaekel T, Hilfiker A, Dorfman S, Ternes W, et al. Detergent decellularization of heart valves for tissue engineering: toxicological effects of residual detergents on human endothelial cells. *Artif Organs*;34(3):206e10. 2010.
200. Feil G, Christ-Adler M, Maurer S, Corvin S, Rennekampff HO, Krug J, et al. Investigations of urothelial cells seeded on commercially available small intestine submucosa. *Eur Urol*;50(6):1330e7. 2006.
201. Flynn LE. The use of decellularized adipose tissue to provide an inductive microenvironment for the adipogenic differentiation of human adipose-derived stem cells. *Biomaterials* 2010;31(17):4715e24.
202. Brown BN, Freund JM, Li H, Rubin PJ, Reing JE, Jeffries EM, et al. Comparison of three methods for the derivation of a biologic

- scaffold composed of adipose tissue extracellular matrix. *Tissue Eng Part C Methods*; 17(4):411-212010.
203. Jamur MC, Oliver C. Cell fixatives for immunostaining. *Methods Mol Biol*;588:55e61. 2010.
204. Gorschewsky O, Klakow A, Riechert K, Pitzl M, Becker R. Clinical comparison of the Tutoplast allograft and autologous patellar tendon (bone-patellar tendon-bone) for the reconstruction of the anterior cruciate ligament: 2- and 6-year results. *Am J Sports Med*;33(8):1202e9. 2005.
205. Cole Jr MB. Alteration of cartilage matrix morphology with histological processing. *J Microsc*;133(Pt 2):129e40. 1984.
206. Funamoto S, Nam K, Kimura T, Murakoshi A, Hashimoto Y, Niwaya K, et al. The use of high-hydrostatic pressure treatment to decellularize blood vessels. *Biomaterials*;31(13):3590e5. 2010.
207. Grauss RW, Hazekamp MG, Oppenhuizen F, van Munsteren CJ, Gittenberger- de Groot AC, DeRuiter MC. Histological evaluation of decellularised porcine aortic valves: matrix changes due to different decellularisation methods. *Eur J Cardiothorac Surg*;27(4):566e71. 2005.
208. Yang M, Chen CZ, Wang XN, Zhu YB, Gu YJ. Favorable effects of the detergent and enzyme extraction method for preparing decellularized bovine peri- cardium scaffold for tissue engineered heart valves. *J Biomed Mater Res B Appl Biomater*;91(1):354e61. 2009.
209. Schenke-Layland K, Vasilevski O, Opitz F, Konig K, Riemann I, Halbhuber KJ, et al. Impact of decellularization of xenogeneic tissue

- on extracellular matrix integrity for tissue engineering of heart valves. *J Struct Biol*;143(3): 201e8. 2003.
210. Chen RN, Ho HO, Tsai YT, Sheu MT. Process development of an acellular dermal matrix (ADM) for biomedical applications. *Biomaterials*; 25(13):2679e86. 2004.
211. Hopkinson A, Shanmuganathan VA, Gray T, Yeung AM, Lowe J, James DK, et al. Optimization of amniotic membrane (AM) denuding for tissue engineering. *Tissue Eng Part C Methods*;14(4):371e81. 2008.
212. Xu H, Wan H, Sandor M, Qi S, Ervin F, Harper JR, et al. Host response to human acellular dermal matrix transplantation in a primate model of abdominal wall repair. *Tissue Eng Part A* 2008;14(12):2009e19.
213. Daly KA, Stewart-Akers AM, Hara H, Ezzelarab M, Long C, Cordero K, et al. Effect of the alphaGal epitope on the response to small intestinal submucosa extracellular matrix in a nonhuman primate model. *Tissue Eng Part A*;15(12):3877e88. 2009.
214. Klebe RJ. Isolation of a collagen-dependent cell attachment factor. *Nature*;250(463):248e51. 1974.
215. Gailit J, Ruoslahti E. Regulation of the fibronectin receptor affinity by divalent cations. *J Biol Chem*;263(26):12927e32. 1988.
216. Maurer P, Hohenester E. Structural and functional aspects of calcium binding in extracellular matrix proteins. *Matrix Biol*;15(8e9):569e80. 1997.
217. Lehr EJ, Rayat GR, Chiu B, Churchill T, McGann LE, Coe JY, et al. Decellularization reduces immunogenicity of sheep pulmonary artery vascular patches. *J Thorac Cardiovasc Surg*; 2010.

218. Wicha MS, Lowrie G, Kohn E, Bagavandoss P, Mahn T. Extracellular matrix promotes mammary epithelial growth and differentiation in vitro. *Proc Natl Acad Sci U S A*;79(10):3213e7. 1982.
219. Gulati AK. Evaluation of acellular and cellular nerve grafts in repair of rat peripheral nerve. *J Neurosurg*;68(1):117e23. 1988.
220. Cartmell JS, Dunn MG. Effect of chemical treatments on tendon cellularity and mechanical properties. *J Biomed Mater Res* 2000;49(1):134e40.
221. Nagata S, Hanayama R, Kawane K. Autoimmunity and the clearance of dead cells. *Cell*;140(5):619e30. 2010.
222. Ott, H.C., et al. Perfusion-decellularized matrix: using nature's platform to engineer a bioartificial heart. *Nat Med* 14, 213, 2008.
223. Price, A.P., et al. Development of a decellularized lung bio-reactor system for bioengineering the lung: the matrix re-loaded. *Tissue Eng Part A* 16, 2581, 2010.
224. Song, J.J., Kim, S.S., Liu, Z., Madsen, J.C., Mathisen, D.J., Vacanti, J.P., and Ott, H.C. Enhanced in vivo function of bioartificial lungs in rats. *Ann Thorac Surg* 92, 998, 2011.
225. Shupe, T., et al. Method for the decellularization of intact rat liver. *Organogenesis* 6, 134, 2010.
226. De Kock, J., Ceelen, L., De Spiegelaere, W., Casteleyn, C., Claes, P., Vanhaecke, T., and Rogiers, V. Simple and quick method for whole-liver decellularization: a novel in vitro three-dimensional bio-engineering tool? *Arch Toxicol* 85, 607, 2011.

227. Barakat, O., Abbasi, S., Rodriguez, G., Rios, J., Wood, R.P., Ozaki, C., Holley, L.S., and Gauthier, P.K. Use of decellularized porcine liver for engineering humanized liver organ. *J Surg Res* 173, e11, 2012.
228. Baptista, P.M., et al. Whole organ decellularization - a tool for bioscaffold fabrication and organ bioengineering. *Conf Proc IEEE Eng Med Biol Soc* 2009, 6526, 2009.
229. Liu, C.X., et al. [Preparation of whole-kidney acellular matrix in rats by perfusion]. *Nan Fang Yi Ke Da Xue Xue Bao* 29, 979, 2009.
230. Ross, E.A., et al. Embryonic stem cells proliferate and differentiate when seeded into kidney scaffolds. *J Am Soc Nephrol* 20, 2338, 2009.
231. Song J, Guyette JP, Gilpin SE, Gonzalez G, Joseph P Vacanti JP & Ott HC. Regeneration and experimental orthotopic transplantation of a bioengineered kidney. *Nature Medicine* 19; 646. 2013
232. Totonelli G, Maghsoudlou P, Garriboli M, Riegler J, Orlando G, Burns AJ, Sebire NJ, Smith VV, Fishman JM, Ghionzoli M, Turmaine M, Birchall MA, Atala A, Soker S, Lythgoe MF, Seifalian A, Pierro A, Eaton S, De Coppi P. A rat decellularized small bowel scaffold that preserves villus-crypt architecture for intestinal regeneration. *Biomaterials*. Apr;33(12):3401-10. 2012
233. Strusi V., Zini N., Dallatana D., Mastrogiacomo S., Parrilli A., Giardino R., Lippi G., Spaletta G., Bassoli E., Gatto A., Iafisco M, Sandri M., Tampieri A., Toni R. Endocrine bioengineering: reconstruction of a bioartificial thyroid lobe using its three-

- dimensional (3D) stromal/ vascular matrix as a scaffold. *End. Abst.* 29, P1586, 2012.
234. Barnes, D.W., and Sato, G.H. (1980b) Serum-free culture: A unifying approach. *Cell*, 22:649–655.
235. Röpke C. Thymic epithelial cell culture. *Microsc Res Tech.* 1;38(3):276-86.1997
236. Andersen, A., Pedersen, H., Bendtzen, K., and Röpke, C. Effects of growth factors on cytokine production in serum-free cultures of human thymic epithelial cells. *Scand. J. Immunol.*, 38:233–238. 1993
237. Ropke, C., and Elbroend, J. Human thymic epithelial cells in serum-free culture: Nature and effects on thymocyte cell lines. *Dev.Immunol.*, 2:111–121. 1992
238. Eshel, I., Savion, N., and Shoham, J. Analysis of thymic stromal cell populations grown in vitro on extracellular matrix in defined medium. II. Cytokine activities in murine thymic epithelial and mesenchymal cell culture supernatants. *J. Immunol.*, 144:1563–1570. 1990
239. Ehmann UK, Shiurba RA, Peterson WD Jr. Long-term proliferation of mouse thymic epithelial cells in culture. *In Vitro Cell Dev Biol.* 22(12):738-48.1986
240. Schreiber, L., Eshel, I., Meilin, A., Sharabi, Y., and Shoham, J. Analysis of thymic stromal cell populations grown in vitro on extracellular matrix in defined medium. III. Growth conditions of human thymic epithelial cells and immunomodulatory activities in their culture supernatant. *Immunology*, 74:621–629. 1991

241. Gill J, Malin M, Holländer GA, Boyd R. Generation of a complete thymic microenvironment by MTS24(+) thymic epithelial cells. *Nat Immunol.* 2002 Jul;3(7):635-42.
242. Pinto S, Schmidt K, Egle S, Stark HJ, Boukamp P, Kyewski B. An organotypic coculture model supporting proliferation and differentiation of medullary thymic epithelial cells and promiscuous gene expression. *J Immunol.* 1;190(3):1085-93.2013
243. Nunes-Cabaço H, Sousa AE. Repairing thymic function. *Curr Opin Organ Transplant.*18(3):363-8.2013
244. E Piccinini, C Berkemeier, G Hollander, T Barthlott, I Martin*,D Wendt . A 3D Scaffold-Based Model To Culture Functional Thymic Epithelial Cells. *Termis* 2011

